



TWO-DIMENSIONAL LIQUID CHROMATOGRAPHY PRINCIPLES, PRACTICAL IMPLEMENTATION AND APPLICATIONS

Primer



Agilent Technologies

TWO-DIMENSIONAL LIQUID CHROMATOGRAPHY PRINCIPLES, PRACTICAL IMPLEMENTATION AND APPLICATIONS

Primer

Peter W. Carr and Dwight R. Stoll



Agilent Technologies

This information is subject to change without notice.

© Agilent Technologies, Inc., 2015

Printed in Germany, May 15, 2015

5991-2359EN

CONTENTS

Foreword by Professor Oliver Schmitz	VI
Foreword by Pat Sandra and Koen Sandra	VII
Preface and Acknowledgment	X
About the Authors	XI
Introduction	XV
Symbols	XVI
Abbreviations	XVIII

1 Introduction to Two-Dimensional Liquid Chromatography 1

1.1 What is two-dimensional liquid chromatography?	1
1.2 Nomenclature of two-dimensional separations	5
1.3 Some historical perspective on 2D-LC	6
1.4 Fields of application of 2D-LC	6
1.5 Types of two-dimensional liquid phase separations	7
1.6 Implementations of 2D-LC	9
1.7 Generation of the 2D-LC chromatogram	12

2 Principles of 2D-LC 15

2.1 Introduction	15
2.2 Peak capacity and related concepts	16
2.3 Basics of gradient elution liquid chromatography and 2D-LC	20
2.4 Fundamentals of peak capacity in LCxLC	36
2.5 Comparison of 1D gradient elution and online LCxLC	51
2.6 Summary	53

3 Practical Implementation of 2D-LC 54

3.1 Setting up a LCxLC system	54
3.2 Heart-cutting 2D-LC Methods	85

4 Method Development in LCxLC	88
4.1 Possible combinations of separation modes	88
4.2 Choosing stationary phases in RPxRP	91
4.3 Optimizing performance through use of separation space or shifted gradients	98
4.4 Managing the trade-off between performance, robustness, and operating cost	100
4.5 Method development case studies	101
 5 Data Analysis in LCxLC	 107
5.1 Introduction	107
5.2 Baseline detection	108
5.3 Determination of noise level	110
5.4 Data smoothing and filtering	110
5.5 Peak detection	110
5.6 Peak area measurement	112
5.7 Merging ² D daughter peaks from the same ¹ D parent peak	112
5.8 Total peak size	114
5.9 Comparison of quantitative performance of 1D-LC and LCxLC	114

6 Applications of LCxLC	116
6.1 Natural products and herbal extracts – Analysis of taxanes	116
6.2 Natural product profiling – Analysis of citrus oil extracts	119
6.3 Biopharmaceuticals – Analysis of monoclonal antibodies	121
6.4 Chemicals – Determination of homolog technical detergents	124
6.5 Pharmaceuticals – Determination of impurities	125
6.6 Food testing – Polyphenols in beverages	126
6.7 Food testing – Quality control of virgin olive oil	127
6.8 Food testing – Analysis of beer	129
6.9 Summary of application methodologies	131
 7 The Future of 2D-LC	 143
7.1 The future	143
7.2 Theoretical factors influencing the comparison of 1D and 2D-LC	145
7.3 Practical factors influencing the comparison of 1D and 2D-LC	148
7.4 Progress in instrumentation for 2D-LC	149
7.5 Other challenges and opportunities for 2D-LC	149
 References	 153

FOREWORD BY PROFESSOR OLIVER SCHMITZ



Oliver J. Schmitz

Professor for Applied Analytical Chemistry, Faculty of Chemistry, University of Duisburg-Essen, Germany

Two opposing trends in the instrumental analysis of small organic molecules (up to 2,000 Da) are currently observed. First, very fast analysis methods without or with only minor sample preparation have to develop to realize the analysis of ever increasing number of samples. Promising developments here are, for example, immunoassays and ambient desorption ionization methods such as DART, DESI, ASAP, and so on. Second, the requirements on sensitivity and separation power for many samples are becoming greater, which lead to increasingly sophisticated analytical platforms. Powerful analytical methods for such samples are, in addition to the classic one-dimensional chromatography, multidimensional chromatographic methods such as heart-cut (also multiple heart-cut) and comprehensive two-dimensional liquid chromatography. The most important detector for the analysis of complex samples with such methods are various mass analyzers (for example, triple quadrupole MS for ultrasensitive target analysis and high resolution MS such as qTOF-MS or IMS-qTOF-MS for nontarget approaches).

The beginning of comprehensive two-dimensional liquid chromatography (LCxLC) can be defined on two papers that are 12 years apart. In 1978 Erni and Frei described the two-dimensional separation of a Senna-glycoside extract by GPC in the first and RPLC in the second dimension. The analysis time was 10 hours in the first dimension and, with two 1.8-mL sample loops, a total of seven 1.5-mL fractions were collected and transferred to the second dimension. The long accumulation time and the resulting mixing within the sample loops led to a reduced first-dimension separation. But the technique for real comprehensive two-dimensional liquid chromatography was developed in this work.

Then, in 1990, Bushey and Jorgenson showed the first truly comprehensive two-dimensional liquid chromatography separation of a protein sample with a microbore cation-exchange column in the first and a size exclusion column in the second dimension. This publication initiated the interest in LCxLC, and, in recent years, because of commercially available systems, a significant increase in publications is to be found.

The authors of this primer are two of the leading scientists in the field of multidimensional liquid chromatography and it is an excellent entry for novices. I am sure that multidimensional liquid chromatography has, particularly for polar substances and those not analyzable by GC, great potential, for example in the field of metabolomics, nontarget analysis, and polymer analysis.

FOREWORD BY PAT SANDRA AND KOEN SANDRA



Professor Pat Sandra

Emeritus Professor,
Ghent University, Belgium



Koen Sandra

Manager Life Sciences,
RIC, Kortrijk, Belgium

"...but the two-dimensional chromatogram is especially convenient, in that it shows at a glance information that can be gained otherwise only as the result of numerous experiments". This sentence taken from a seventy year old publication of A.J.P. Martin and coworkers (*Biochem J.*, **1944**, *38*, 224) illustrates not only that 2D chromatographic separations are not new but above all shows that the early chromatographers were already aware of the potential inherent in these separations. Indeed, it has now been demonstrated numerous times that a substantial gain in resolution can be obtained upon adding an extra separation dimension. *At a glance* definitely did not mean *fast* as the developing time for the amino acids from wool hydrolysate on Whatman no 1 paper was 3 days in one direction and 27 hours in the second direction.

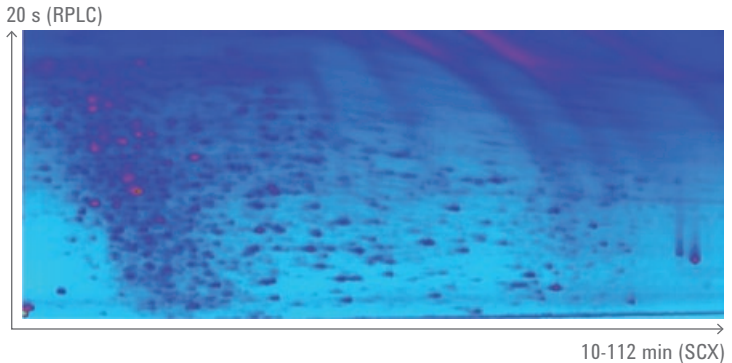
Over the years, the principle of 2D in space has been intensively applied in 2D-TLC and 2D-gel electrophoresis and has even evolved to workhorse technology in several disciplines. 2D in time was much more challenging to develop and most research activities were noted in the beginning of the 21st century. The reason is that new instrumental developments were needed to take full advantage of the claimed features of 2D chromatographic separations. Comprehensive GC or GCxGC is nowadays considered a mature technique and intensively applied for the profiling of mixtures of extreme complexity, for example, petroleum samples. The faster development of GCxGC and its commercialization compared to LCxLC is primarily due to the nature of the mobile phase – a gas – that is moreover applied in both dimensions.

Around a decade ago, tremendous improvements were made in LC column technology and instrumentation. The introduction of sub-2- μm particles and superficially porous particles in combination with LC instrumentation that could operate at pressures of 1000 bar and higher, opened new possibilities in terms of speed and resolution. This not only offered high peak capacities in one-dimensional LC but was also of utmost importance in the development of two-dimensional LC. On the one hand, these developments could be applied in 2D-LC instrumentation but, on the other hand, it soon became clear that the high peak capacities now available in 1D-LC were still insufficient to resolve samples of high complexity. Presently, the analysis of such mixtures is performed with high resolution 1D-LC combined with contemporary mass spectrometers

offering high resolution, MS/MS and ion mobility capabilities. However, even with the most powerful MS instruments, the higher the resolution at the front-end, the better are the data. On the other hand, high resolution and peak capacity are increasingly needed in QA/QC laboratories in which such mass spectrometers are not established tools.

2D-LC embraces different two-dimensional techniques as explained in the primer but LCxLC is definitely the most impressive one. High orthogonality (optimum occupancy of the 2D-space) is obtained by combining the different modes of LC (RPLC, NPLC, HILIC, IEC, SEC, SFC). Most often RPLC is placed in the second dimension because of the availability of high quality RPLC columns and the compatibility with MS. The selected combination depends on the application which is clearly described in this primer. We should mention here that for many applications, the combination RPLCxRPLC is surprisingly powerful. The partial correlation is no harm to obtain excellent separations as illustrated in this primer for the analysis of taxanes. RPLCxRPLC is very robust because of the solvent compatibility (remember GCxGC!) and can form the basis for the development of robust generic methods, for example, in pharmaceutical analysis!

Writing a foreword with two authors is not that common – definitely not when they belong to the same family. One of us (PS) has been active in 2D-LC since more than ten years and has promoted the technique at several symposia. The younger one (KS) is working in life sciences and is typically confronted with demanding separations. He was very skeptical about LCxLC and was not willing to implement methods that are performed on home-made *academic* prototypes. The availability of commercial instrumentation changed that situation completely and he is now a strong protagonist of 2D-LC even for use in a QA/QC environment with UV detection. A typical plot of an *E. coli* lysate tryptic digest with SCXxRPLC-UV is shown in the figure below. It is exciting that all LC practitioners are now able to obtain similar results in a highly reproducible way.



Separation of the tryptic digest of *E. coli* by SCXxRPLC
on the Agilent 1290 Infinity 2D-LC solution.

We are sure 2D-LC will serve us all in the near future. This primer is an excellent entry for neophytes in 2D-LC and will furthermore inspire more experienced scientists in the field. The booklet also provides the reader with several applications on which method development for other complex mixtures can be based. We can only congratulate Pete and Dwight for a very good job.

PREFACE AND ACKNOWLEDGMENT

Jens Trafkowski

Product Manager for
2D-LC Solutions at
Agilent Technologies,
Walldbronn, Germany

At Agilent Technologies we are deeply honored to have been able to work with Peter Carr and Dwight Stoll on development of this publication. As two of the leading scientists in the field of multidimensional separations, who could have been better qualified to author a primer about two-dimensional liquid chromatography?

Their combined experience spans decades of research and development in pursuit of higher performance in terms of chromatographic resolution, selectivity and sensitivity. At the same time they have laid down the theoretical background, empirically deriving fundamental equations. This work is presented in this primer, which provides an indispensable reference for anyone interested in the field of two-dimensional liquid chromatography and its application.

We greatly appreciate the collaboration with the authors and are convinced that the interested reader will gain considerable understanding about the theory and practical application of this rapidly evolving technique.

One chapter in this primer is dedicated to applications of 2D-LC, presenting data and results from fields such as biopharmaceuticals, foods and natural products. Further applications can be accessed through the Agilent Application Finder at:

www.agilent.com/chem/application-finder

ABOUT THE AUTHORS

Peter W. Carr received his B.S. in Chemistry (1965) from the Polytechnic Institute of Brooklyn where he worked with Professor Louis Meites and a Ph.D. in Analytical Chemistry at Pennsylvania State University (1969) under the guidance of Professor Joseph Jordan. Prior to joining the faculty at the University of Georgia in 1969, he was a research assistant and associate at Brookhaven National Laboratory during the summers of 1965 and 1966 and a postdoctoral associate with David Glick at Stanford University Medical School (1968). From 1969 until 1977 he was first an Assistant Professor and then Associate Professor of Chemistry at the University of Georgia (Athens).

In 1977, Professor Carr joined the faculty at the University of Minnesota where he became Professor of Chemistry in 1981. He has been a consultant to Leeds and Northrup, Hewlett-Packard, the 3M Company and Agilent Technologies, and was the founder and first President of ZirChrom Separations Inc. of Anoka Minnesota. In 1986, he became an Associate Director of the Institute for Advanced Studies in Biological Process Technology at the University of Minnesota. He has been President of the Symposium on Analytical Chemistry in the Environment (1976), founder and first President of the Minnesota Chromatography Forum, and Chairman of the Subdivision of Chromatography and Separation Science of the Analytical Chemistry Division of the American Chemical Society (1988-1989). Professor Carr has served on the Editorial Advisory Boards of Analytical Chemistry, Talanta, the Microchemical Journal, LC/GC, Journal of Chromatography, Chromatographia and Separation Science and Technology. In addition, he has participated in numerous advisory committees of the National Science Foundation and American Chemical Society, and has organized a number of symposia for National American Chemical Society meetings. Professor Carr was the Program Chair of HPLC 94, the Eighteenth International Symposium on Column Liquid Chromatography which was held in Minneapolis, MN on May 8–13, 1994. He has received the Leroy Sheldon Palmer Award of the Minnesota Chromatography Forum and the Merit Award of the Chicago Chromatography Discussion Group. He has also been the recipient of the Benedetti-Pichler Award from the American Microchemical Society in 1990, the Eastern Analytical Symposium, Inc. Award in Separation Science in 1993, the Stephen Dal Nogare Award of the Delaware Valley Chromatography Forum in 1996, the 1996 ACS Award in Chromatography sponsored by SUPELCO, Inc., the ISCO Award in 1997

and the Award in Separation Science of the Eastern Analytical Symposium in 2000. He was inducted into the Academy of Distinguished Teachers, University of Minnesota in 2002. He was awarded the Pittsburgh Conference Award in Analytical Chemistry in 2004. He is the 2009 recipient of the American Chemical Society Award in Analytical Chemistry. He is the 2010 winner of the Martin Medal of the Chromatographic Society and the Horvath Medal of the Connecticut Separation Science Society and of the Hungarian Separation Science Society. He is the 2013 winner of the LCGC Lifetime Achievement Award. He received the ACS Division of Analytical Chemistry's Award for Excellence in Education in 2013.

Professor Carr and his 100 former graduate students and postdoctoral associates have published over 400 papers in a variety of areas of analytical chemistry including: electrochemistry, ion selective electrodes, thermochemistry, immobilized enzymes, and chromatography. He holds 21 U.S. patents in areas related to chemical analysis and chromatography. He and his student L. D. Bowers have jointly authored a monograph entitled *Immobilized Enzymes in Analytical Chemistry and Clinical Chemistry*. Most recently, his research interests have focused on the development of high speed comprehensive two-dimensional liquid chromatography. Additional areas of study include affinity chromatography, bio-separations, the theory of nonlinear chromatography, and the development of chemically and thermally stable supports for high performance liquid chromatography (HPLC) and most recently ultra-fast and comprehensive two dimensional HPLC.

Professor Carr has focused a great deal of his professional life on teaching primarily at the upper division undergraduate and graduate levels. He for many years was the instructor in a unique undergraduate course on analytical chemistry for honors students and chemistry majors. This course was the third quarter of the general chemistry curriculum. During that era (1982-1985) he suggested the development of a computer-aided instructional facility for the department and formed a committee with Professor John Evans and Kent Mann to get it funded and hire staff. The facility is one of the most vibrant parts of the undergraduate teaching effort to this day.

Subsequently for many years Professor Carr taught the senior year course in instrumental analysis. One of his significant contributions to that course was the institution of a final project in which each student either originates or is

assigned a problem in chemical analysis and through a detailed literature study comes up with a solution. This is written up and developed into a poster that is viewed by the entire class. The student solutions are then built into part of the final written exam. The unique aspect of this project, which counts as one of the three mid-semester exams, is its evaluation by a panel of three professional analytical chemists including managers of local environmental consulting labs, analytical labs at 3M and other industrial labs. In essence each student undergoes a set of three mini-oral exams. These scientist and managers have many years' experience hiring bachelor level chemists and are able to offer very insightful and practical feedback. This practice has been continued by Professor Carr's successors.

At the graduate level Professor Carr has taught courses on chemical equilibria, statistics in analytical chemistry, thermal analysis, bio-analytical chemistry, the analytical uses of immobilized enzymes and enzyme electrodes. However, for many years he has taught a very fundamental course on separation science which is taken primarily by analytical chemistry graduate students but also chemical engineers, pharmaceutical scientists, environmental engineers and many biological scientists. It emphasized the thermodynamics of phase equilibria, the intermolecular interactions responsible for chemical separations and the principles of diffusion and mass transfer involved in transport and dispersion. He also taught a very mathematical lab/lecture course on electronic instrumentation which became known as *boot camp for analytical grad students*.

Dwight Stoll did his undergraduate work at Minnesota State University, Mankato, receiving B.S. degrees in plant biology and biochemistry in 1999 and 2001. Upon graduation in 1999 he took a job in industry as a research technician with ZirChrom Separations, Inc. At ZirChrom he quickly learned about the liquid chromatography market, and in fact became quite interested in the role of separation science in the development of new analytical methodologies for use in other disciplines such as biology. In 2000 he shored up his chemistry background at the University of Minnesota before enrolling in the graduate program in chemistry there in 2001. At the University of Minnesota he studied with Professor Peter Carr, and worked on the development of fast, comprehensive two-dimensional liquid chromatography, using the principles of high temperature and ultra-fast gradient elution liquid chromatography to improve the overall speed

of two-dimensional separations. Before receiving the Ph.D. in analytical chemistry in 2007, he took a nine-month break from graduate studies to teach as an adjunct faculty member at St. Olaf College where he taught analytical and general chemistry. Following graduate in 2007, he spent nine months working as a postdoc with Dr. Christine Wendt in the Lung Health Center at the University of Minnesota, where he began analyzing the low molecular weight constituents of human lung lavage fluid using liquid chromatography coupled with mass spectrometry.

In the fall of 2008, Dwight accepted a faculty position as Assistant Professor in the chemistry department at Gustavus Adolphus College, where he mainly teaches quantitative and instrumental analysis courses, in addition to directing a vibrant research program involving mainly undergraduate students. In 2014 he was promoted to Associate Professor at Gustavus. His active research projects include the development of rapid multidimensional liquid chromatography for both targeted and untargeted analysis in samples of moderate to high complexity. Active research projects in his laboratory touch upon most aspects of multidimensional separation methodologies, including optimization of isocratic and gradient elution HPLC, characterization of selectivity in reversed-phase HPLC, and instrument development.

Dwight is the author or co-author of 40 peer-reviewed publications and one book chapter in the area of separation science, and is a named co-inventor on two patents. He has authored or co-authored over 80 presentations at local, national, and international meetings, and has instructed short courses in two-dimensional liquid chromatography: HPLC2013 (Amsterdam); Pittcon 2104 (Chicago, IL). In 2009 he was the winner of the John B. Phillips Award for contributions to multidimensional gas chromatography, and in 2011 he was the recipient of LCGC's Emerging Leader in Chromatography Award. In 2012 he was elected to the editorial advisory board of LCGC Magazine, the leading trade publication for the separation science community. In 2014 he was named to The Analytical Scientist's list of *Top 40 Under 40* analytical scientists, and in 2015 he received the American Chemical Society Division of Analytical Chemistry Award for Young Investigators in Separation Science.

INTRODUCTION

The origins of modern two-dimensional liquid chromatography (2D-LC) can be traced to the late 1970's and early 1980's when proof-of-principle experiments along with much conceptual and theoretical work clearly made the case that 2D-LC offered more potential resolving power compared to conventional one-dimensional liquid chromatography (1D-LC). In the 1990's 2D-LC played a key role in the separation of complex and difficult-to-separate materials encountered in the fields of proteomics and polymer chemistry. However, these improved separations typically came at the cost of long analysis times (for example, several hours to days) and thus 2D-LC was really a niche technique limited to a small fraction of all liquid phase separations.

Over the past ten years there have been significant changes in the capabilities of instrument components for liquid chromatography, so that now high resolution 2D-LC separations can be carried out in less than an hour. This, along with increasing awareness of the performance limits associated with modern 1D-LC, and the continually increasing need to separate samples of greater complexity, in less time, and with better detection limits is fueling a great deal of current research and development in 2D-LC.

Historically most users of 2D-LC have had to assemble their own instruments using existing and suboptimal components of 1D-LC systems. This too has changed, and today we find that commercial instruments configured for 2D-LC work can be purchased from several LC manufacturers. While this has removed some of the instrument development burden from users of 2D-LC, there still remain a large number of experimental variables that needed to be decided upon as a part of 2D-LC method development. In this Primer we first establish the fundamental principles of how 2D-LC works and why it has more separation potential than conventional 1D-LC. We then go on to describe a number of practical factors that must be considered during method development, and provide guidelines and development tools wherever possible. Finally, we briefly address the topic of data analysis, which is a critical component of any 2D-LC workflow, and give examples from various fields of applications where 2D-LC has been shown to be useful, and sometimes indispensable.

SYMBOLS

Symbols	
a	saturation factor
B	van Deemter fitting coefficient
b	gradient slope
β	average peak broadening factor
C	van Deemter fitting coefficient
D_m	diffusion coefficient of analyte in eluent
d_p	column particle size (diameter)
$\Delta\phi$	range in gradient composition
ϵ_e	interstitial porosity
ϵ_i	intraparticle porosity
F	eluent flow rate
f_{cov}	fractional coverage metric
$G(p)^\alpha$	oncolumn zone compression factor
k	solute retention factor
k_0	solute retention factor at initial eluent composition (ϕ_0)
k_e	solute retention factor at time solute leaves column
k_w	solute retention factor in pure water ($\phi = 0$)
L	column length
λ	¹ D efficiency factor
m	number of chemical components in mixture
N	column plate number
n_c	peak capacity
$n_{c,2D}$	peak capacity of two-dimensional separation
$n_{c,2D}^*$	corrected peak capacity of two-dimensional separation
$n'_{c,2D}$	effective peak capacity of two-dimensional separation
η	eluent viscosity
$n_{c,max}$	limiting peak capacity
σ	peak standard deviation
P	system pressure
P_{max}	maximum system pressure
p	average number of observed peaks
ϕ	column permeability

Symbols

ϕ_{fin}	final mobile phase composition
ϕ_0	initial mobile phase composition
S	slope of log solute retention factor against eluent composition
T	column temperature
t_d	gradient delay time
t_c	gradient elution cycle time
t_g	time for composition to change linearly from initial to final value (ϕ_{fin})
t_0	column dead time
t_R	retention time
t_{re-eq}	re-equilibration time
T	crossover time
u_e	interstitial eluent velocity
V_d	gradient delay volume
V_m	column dead volume
V_σ	system delay volume
\bar{W}	average 4σ width

ABBREVIATIONS

Abbreviations	
¹ D	first dimension (column or separation)*
² D	second dimension (column or separation)*
1D-LC	one-dimensional liquid chromatography
2D-LC	two-dimensional liquid chromatography
CE	capillary electrophoresis
GC	gas chromatography
GCxGC	comprehensive two-dimensional gas chromatography
HILIC	hydrophilic interaction liquid chromatography
HPLC	high performance liquid chromatography
id	inside diameter
IEX	ion exchange chromatography
LCxCE	comprehensive two-dimensional liquid chromatography / capillary electrophoresis
LCxGC	comprehensive two-dimensional liquid chromatography / gas chromatography
LCxLC	comprehensive two-dimensional liquid chromatography
LCxSFC	comprehensive two-dimensional liquid chromatography / supercritical fluid chromatography
LC-LC	comprehensive two-dimensional liquid chromatography
mLC-LC	multiple heart-cutting two-dimensional liquid chromatography
sLCxLC	selective comprehensive two-dimensional liquid chromatography
RPLC	reversed-phase liquid chromatography
RPxRP	comprehensive two-dimensional reversed-phase liquid chromatography
SEC	size exclusion chromatography
SFC	supercritical fluid chromatography

* The index digits 1 and 2 are used with other symbols to indicate first or second dimension. For example, ¹*n*_c represents first-dimension peak capacity; ²*F* represents second-dimension eluent flow rate.

INTRODUCTION TO TWO-DIMENSIONAL LIQUID CHROMATOGRAPHY

1

This first chapter aims to introduce you to the basic motivations for deploying two-dimensional liquid chromatography (2D-LC), and illustrate its power relative to one-dimensional methods. Further, some of the history of 2D-LC is presented along with a description of where the technique is best applied to the spectrum of chemical analysis problems. It is also necessary to familiarize you with some important new nomenclature and symbols specific to two-dimensional separation techniques to facilitate reading later chapters. Last we will describe both forms of two-dimensional separations (comprehensive versus heart cutting) and different ways in which they can be implemented (online versus offline, stop-and-go). It is admitted up front that this Primer is solely concerned with two-dimensional separations in time and not at all with two-dimensional separations in space, such as those encountered in thin layer chromatography and slab-gel electrophoresis.

1.1

What is two-dimensional liquid chromatography?

Two-dimensional liquid chromatography is a significant addition to the family of LC techniques, which includes one-dimensional isocratic and gradient elution LC. When used properly multidimensional separations can offer great improvements in resolving power over conventional one-dimensional liquid chromatography (1D-LC). Figure 1.1 shows the relation of a 2D-LC system to a 1D-LC system. A conventional separation is carried out on the first dimension (¹D) column. This can be either an isocratic or a gradient elution separation. Aliquots of the effluent from the ¹D column are then passed into a second-dimension (²D) column that must have very different separation selectivity compared to the ¹D column, if it is to have any real impact on the overall chromatographic resolution of the sample. In a very real sense *the ²D separation column and its accompanying detector act as a chemically selective analysis system acting on the effluent from the ¹D column*. Given that the selectivity of the second column is different from the first there is an increase in the probability that peaks that are totally or partially overlapping neighbors on the ¹D column will separate on the ²D column. As long as there is no (or minimal) remixing of compounds separated by the ¹D column during the sampling process, the resolving power of the second dimension does not merely add to that of the first-dimension but actually multiplies that of the first dimension.

We will delve into why and how this happens in Chapter 2 “Principles of 2D-LC”. Thus, under *ideal* circumstances (no remixing and uncorrelated selectivity) the resolving power of a 2D separation is much greater than of a 1D separation.

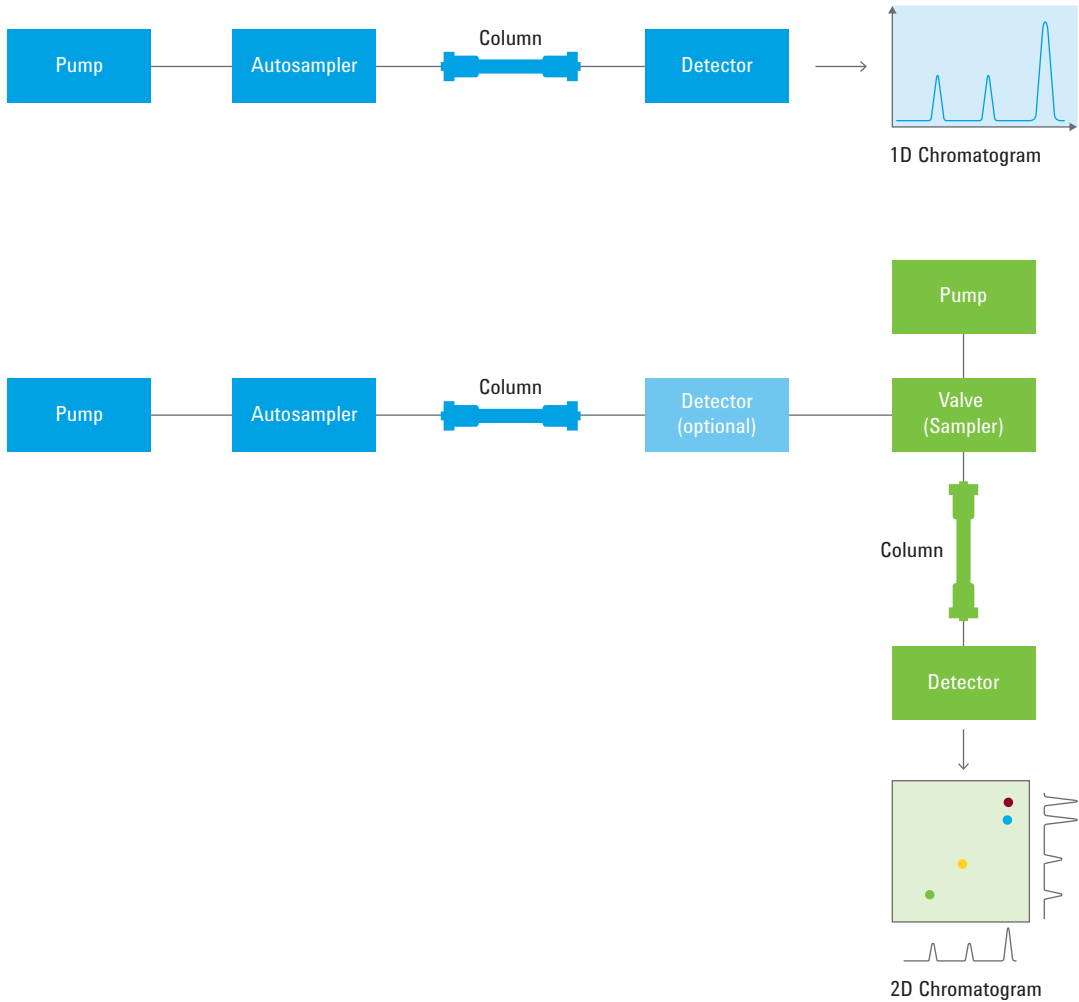


Figure 1.1 Relation of a 2D-LC system to a 1D-LC system – the conventional detector of a 1D-LC can be regarded as a ***chemically selective detector*** comprised of a second chromatograph and a conventional detector.

Two-dimensional LC can be segmented into two major types that have significant differences. In *comprehensive* two-dimensional liquid chromatography (denoted as LCxLC) a continuous stream of effluent from the ¹D column is transferred to the ²D column. In contrast in *heart-cutting* chromatography (LC-LC), only judiciously selected portions of the ¹D effluent are transferred to the ²D column. Between these two chief categories several subcategories have been described, including *selective* two-dimensional chromatography (sLCxLC) and *multiple heart-cutting* 2D-LC (mLC-LC).

The tremendous power of LCxLC is well illustrated by the chromatogram shown in Figure 1.2. Here we see that a complex biological sample has been separated into several hundred components in only 30 minutes. It is currently well beyond the ability of any conventional 1D-LC method to produce such high resolving power in such a short period of time regardless of how small the particles used in the column are or how high is the operating pressure of the instrument.

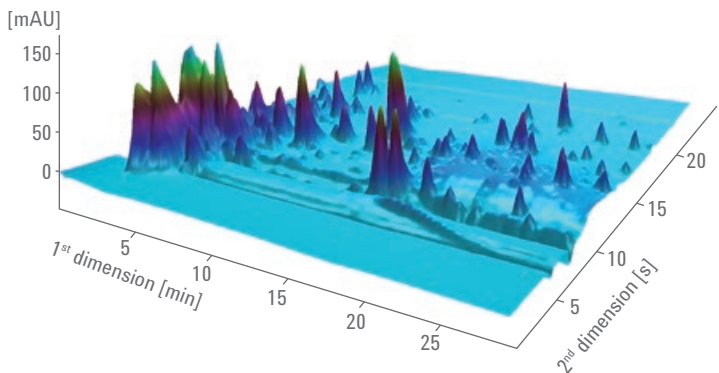


Figure 1.2 A typical comprehensive 2D-LC chromatogram showing the separation of a complex biological sample.

The real power of 2D-LC is that it is a mechanism for greatly increasing the resolving power without greatly increasing analysis time. Two analytically important examples of this enhancement in the power of 2D-LC relative to 1D-LC are shown in Figure 1.3 and Figure 1.4.

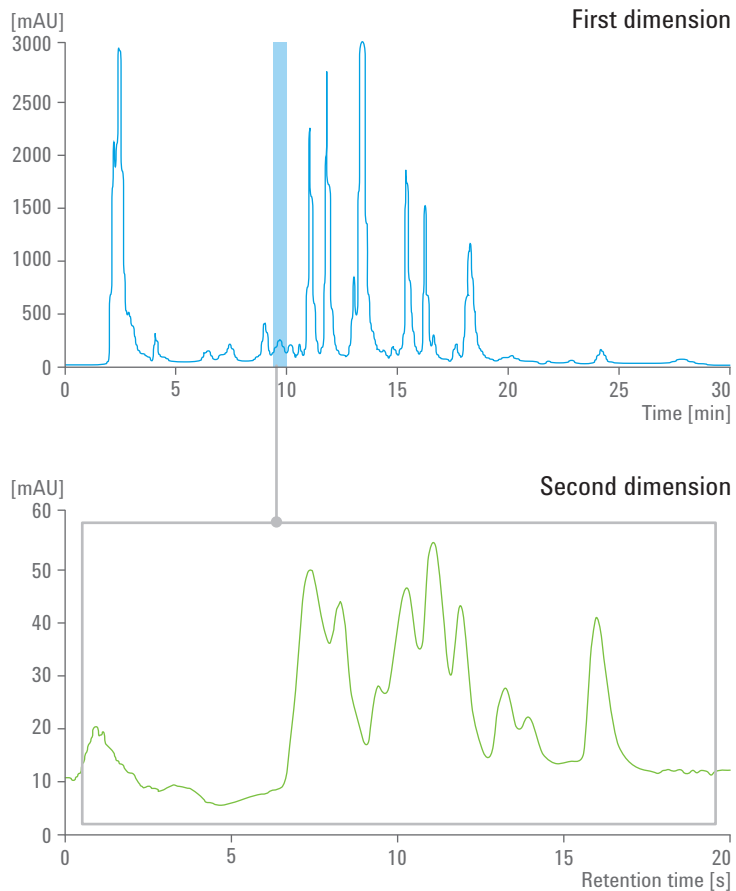


Figure 1.3 The peak in the blue stripe taken from the ¹D of an online LCxLC chromatogram is injected into the ²D column. What appears to be a single peak is actually a set of at least nine components. The sample was a maize seed extract separated with the following ¹D conditions: 2.1 x 50 mm Discovery HS-F5, 5 μ m; A: 20 mM phosphate, 20 mM sodium perchlorate, pH 5.7; B: Acetonitrile; Gradient program 5 %B to 70 %B over 23 min.; 40 °C; 0.1 mL/min; 10 μ L injection.; 220 nm detector wavelength. ²D conditions: 2.1 x 50 mm ZirChrom-CARB, 3 μ m; A: 20 mM perchloric acid in water; B: Acetonitrile; Gradient, 0 to 74 %B in 17.4 s; 110 °C, 34 μ L injection, 220 nm detector. Adapted from Reference 2.

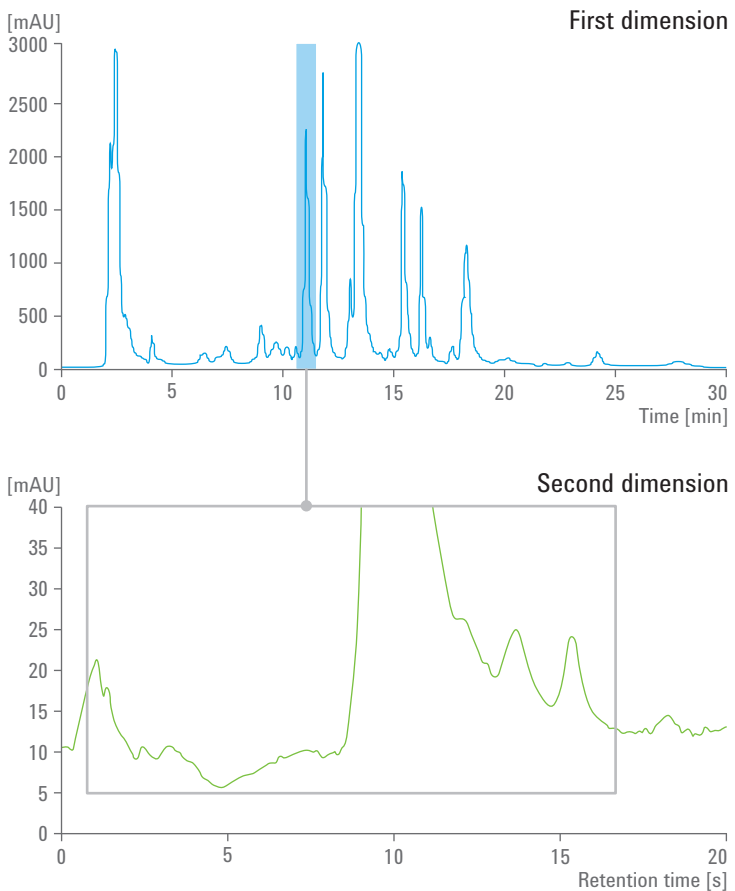


Figure 1.4 The peak in the blue stripe taken from the ^1D of an online LCxLC chromatogram was injected into the ^2D column. This illustrates the fact that the increased resolving power of LCxLC allows you to see small peaks in the tail of a large peak and greatly relieve the ionization suppression problem endemic in electrospray ionization mass spectrometry. All conditions are as in Figure 1.3; Adapted from Reference 2.

1.2 Nomenclature of two-dimensional separations

In this Primer we will use the standardized notation proposed by Schoenmakers *et al.* in 2012³. In their terminology 1D and 2D mean one-dimensional and two-dimensional whereas ^1D and ^2D stand for the first and second dimension respectively. The terms listed in Table 1.1 and in the Abbreviations list will be used extensively in this and subsequent chapters. We advise you to take some time to become familiar with this new vocabulary.

Abbreviation	Description
¹ D	first dimension (column or separation)
² D	second dimension (column or separation)
1D-LC	one-dimensional liquid chromatography
2D-LC	two-dimensional liquid chromatography
LCxLC	comprehensive two-dimensional liquid chromatography
LC-LC	heart-cutting two-dimensional liquid chromatography
mLC-LC	multiple heart-cutting two-dimensional liquid chromatography
sLCxLC	selective two-dimensional liquid chromatography

Table 1.1 Nomenclature of two-dimensional separations.

1.3 Some historical perspective on 2D-LC

In fact 2D liquid phase separations have been around for quite some time. One very nice example was presented by Anthony Synge, who along with Archer Martin co-invented liquid partition chromatography. In his Nobel Prize acceptance speech⁴, he showed a two-dimensional paper chromatographic separation of 19 amino acids extracted from potato⁵. However, the first truly instrumental form of 2D-LC was not developed until 1978⁶. Nonetheless it was not until the work of Bushey and Jorgenson⁷ in 1990 on the comprehensive 2D-LC separation of a 14-component mixture of proteins using a combination of size exclusion chromatography (SEC) and ion exchange chromatography (IEX) that interest in the technique really began to blossom. In that work SEC was used as the second dimension; each SEC chromatogram took six minutes and 59 ²D chromatograms were required to cover the entire first-dimension IEX separation. In contrast in Figure 1.3 each ²D gradient separation was completed in 21 seconds and 90 chromatograms were collected in just over 30 minutes. A much higher resolving power was achieved in no small measure due to the use of high speed separations in the second dimension.

1.4 Fields of application of 2D-LC

A search of the literature (as of 2013) indicated that over 3600 papers mentioned two-dimensional liquid chromatography somewhere in their abstracts. As an example of activity in the field, in the year 2012 over 80 papers were directly concerned with 2D-LC. In this same period about 300 papers mentioned 2D-LC in the abstract. A large majority of 2D-LC papers are concerned with the analysis of proteins and peptides; next in frequency is pharmaceutical analysis followed closely by the analysis and characterization of polymers by 2D-LC. The analysis of foods comes fourth closely behind polymer analysis with environmental analysis in last place.

1.4.1

The spectrum of analytical problems

To a person with a hammer every problem is a nail that needs pounding. A question that naturally arises is; what kinds of problems are best addressed using 2D-LC? Thus far the vast majority of its applications are found in dealing with very complex naturally occurring mixtures (biological cells, blood, urine, environmental samples, and so on) and in the complex mixtures that inherently arise in dealing with synthetic polymers, especially copolymers. A second area of considerable interest is in the search for *biomarkers* for various biological conditions. More specifically 2D-LC is used in proteomics and metabolomics in which patterns of changes in the concentrations of proteins and small molecules are used as indicators of the early-onset of disease states. When used in combination with mass spectrometry, 2D-LC provides a huge amount of qualitative and quantitative data that are ripe for mining. A third area of application, which seems to us is vastly underdeveloped, is as a *universal* analyzer, which due to its high resolving power will require no or a minimal amount of method development to quantify a few components in relative simple mixtures such as those having fewer than 20 components.

However, it should be clear that the utility of 2D-LC and especially the range of analytical problems that it will be used to address will be dominated by how fast the technique can be done. Thus a great deal of recent work has been focused on improving the speed of 2D-LC, and we will return to this issue in Chapter 2 "Principles of 2D-LC". In Section 1.3 "Some historical perspective on 2D-LC" we compared the time it took Bushey and Jorgenson to generate a 2D separation (about 6 hours) to that used by Stoll (about 30 minutes). There is little question that analysis time has a major influence on the range of problems that an analytical method can be applied to.

1.5

Types of two-dimensional liquid phase separations

1.5.1

Modes of 2D chromatographic separation

In brief, we are concerned here only with 2D-LC; however, it is evident that we could do LC in one of the dimensions and supercritical fluid chromatography (LCxSFC), capillary electrophoresis (LCxCE), or gas chromatography (LCxGC) in the second separation dimension. Comprehensive 2D-GC (GCxGC) is a more mature two-dimensional separation technique and many of the fundamental ideas that will be introduced in later chapters were strongly influenced by earlier GCxGC work. Certainly those already familiar with GCxGC have an excellent *head start* in coming up to speed with online LCxLC. Combining LC with a distinctly different mode actually makes a lot of sense, as will become evident in Chapter 2 "Principles of 2D-LC". The great difficulty comes in *interfacing* LC with the other separation modes; however, these alternative combinations of modes have all achieved a

degree of success but not without solving some significant compatibility problems. If you are interested, we would refer you to papers describing the coupling of LC with GC⁸, LC coupled with SFC⁹, and LC coupled with CE¹⁰.

1.5.2 Various combinations of LC types

The most common combinations of modes of LC that have been described in the literature are summarized in Table 1.2.

First Dimension	Second Dimension
Reversed Phase*	Reversed Phase
Ion Exchange	Reversed Phase
Size Exclusion	Reversed Phase
Normal Phase	Reversed Phase
HILIC	Reversed Phase
Argentation LC	Reversed Phase
Critical Condition LC	Reversed Phase
Critical Condition LC	SEC
Ion Exchange	SEC

Table 1.2 Common combinations of LC modes (* with different separation selectivity).

Some of these combinations are difficult to implement because of the incompatibility of the mobile phases used in the two dimensions due to solvent immiscibility or other considerations; others are straightforward, for example, the pairing of ion exchange and reversed phase. However, the positive aspect of combining, for example, normal phase and reversed phase chromatography, is that their selectivities are likely to be much more different than what might be achieved by using two (hopefully) quite different reversed phases. A more detailed comparison of the types of LC used in pairs in 2D-LC will be described in Chapter 4 “Method Development in LCxLC”.

1.6 Implementations of 2D-LC

There are various ways that 2D-LC can be performed and there are two different classes of ways in which the technology can be implemented. Here we give brief descriptions of each type. If you are interested in more detail about each type, please refer to a recent comprehensive review article¹¹.

1.6.1

Classification based on
number of peaks analyzed

1.6.1.1

Heart-cutting 2D-LC

The purpose of heart-cutting 2D-LC is quite different from comprehensive chromatography. In heart-cutting chromatography one or a few peaks are specifically targeted and a fraction of a given peak is collected and injected onto a second column. You could capture the entire peak in a single fraction or select an aliquot near the front, the middle or at the end of the peak as desired (see Figure 1.5). Heart-cutting 2D-LC is quite useful for not too complex samples that contain compounds with very similar retention behavior. The system and method setup is usually less complex and operating costs are lower compared to comprehensive 2D-LC. Depending on the analysis time in the second dimension, it is also possible to sample multiple peaks from the first dimension for further separation in the second dimension. To sample more peaks from the first dimension without risking temporary overlap of the second-dimension analysis a multiple heart-cutting (mLC-LC) setup with more than one sampling loop might be advised.

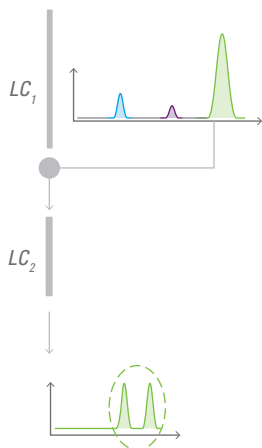


Figure 1.5 Conceptual representation of the heart-cutting implementation of 2D-LC.

1.6.1.2

Comprehensive 2D-LC

In this form of the method every peak that elutes from the '1D column is fully sampled. Although the entire '1D separation is sampled, it is not necessary to transfer the entire effluent from the first to the second column. For example, you could continuously split a portion of the flow coming from the '1D column, sending some percentage of it to waste and the rest to the sampling valve (see Figure 1.1 and Figure 1.2). This form of 2D-LC is known as comprehensive chromatography and is conventionally denoted as LC_xLC^3 .

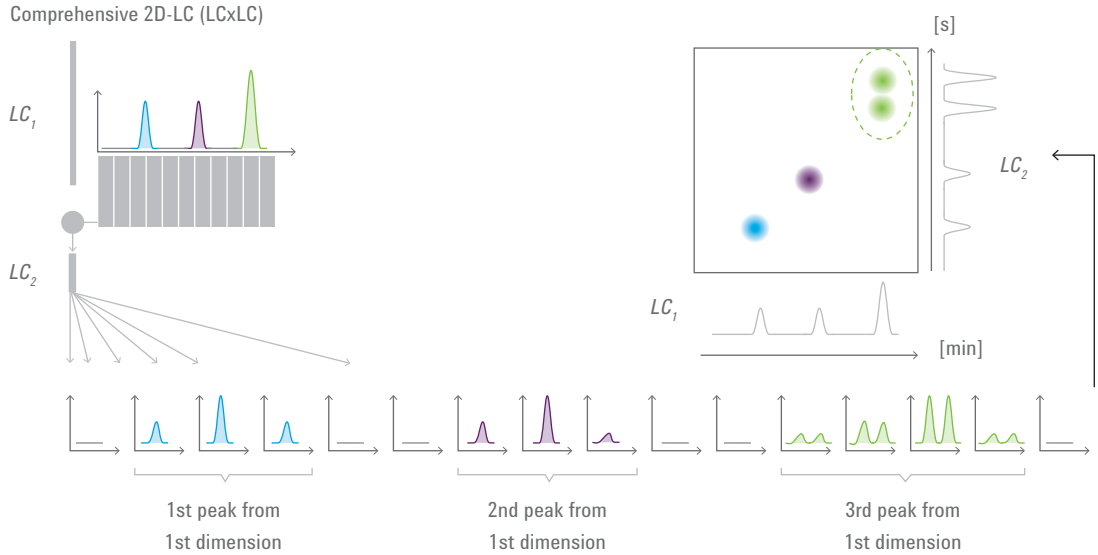


Figure 1.6 Conceptual representation of the comprehensive implementation of 2D-LC.

1.6.2 Classification based on temporal implementation

1.6.2.1 Online 2D-LC

In online 2D-LC the effluent from the ^1D column is injected into the ^2D column immediately after it is collected (see Figure 1.1). This form of 2D-LC is definitely the fastest and can be fully-automated and requires no operator intervention at least until all the data has been acquired. It is possible to analyze multiple samples when an autosampler is used in the first dimension. Its chief limitation is that its theoretical maximum resolving power is not as high as in the much slower offline mode of 2D-LC. However, the total resolving power per unit run time is usually better than with offline LCxLC. As we will describe in more detail in Chapter 2 “Principles of 2D-LC”, the ^2D analysis time for each fraction of ^1D effluent must be equal to the sampling time in online LCxLC because the fraction is immediately transferred from one column to the other. In order for the total 2D-LC analysis time to be kept reasonable this means that the samples must be collected frequently and each ^2D separation executed on a fast time scale. This in turn significantly limits the resolving power of each ^2D separation.

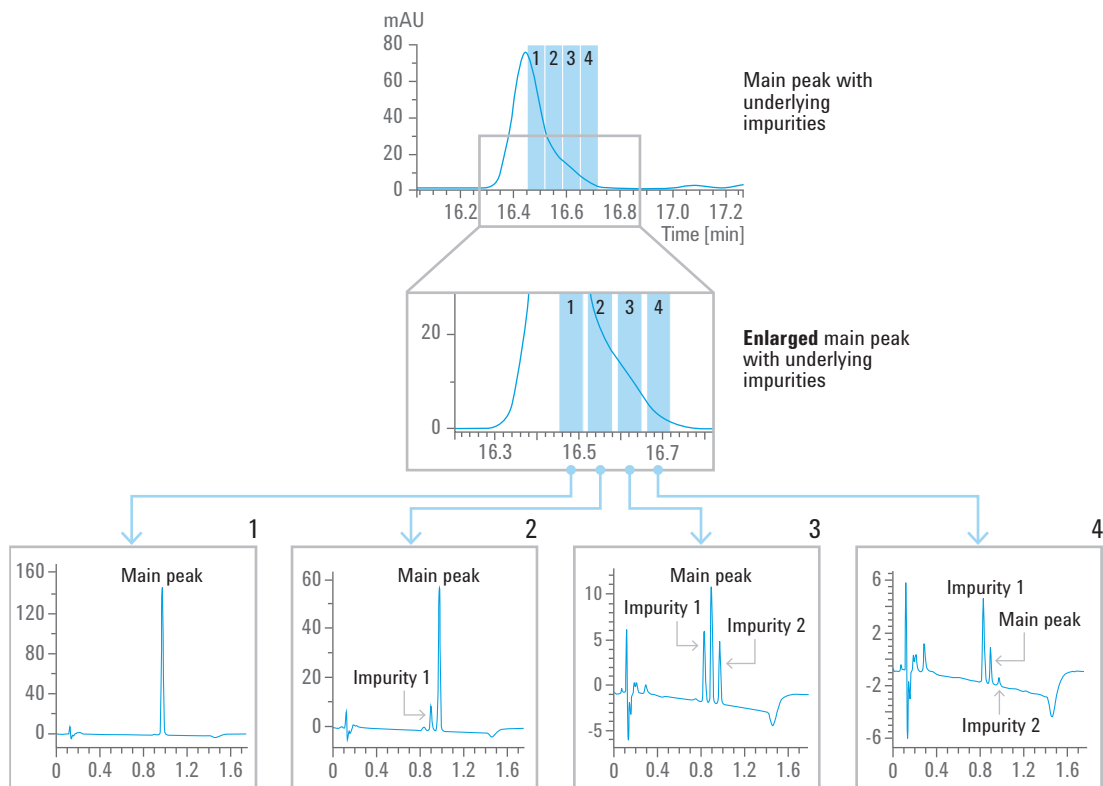


Figure 1.7 Example of multiple heart-cutting 2D-LC used to obtain information about changes in the composition of a ${}^1\text{D}$ peak across half of its width. The upper panel shows the full ${}^1\text{D}$ peak, the middle one a detailed view of the main ${}^1\text{D}$ peak and where four fractions of the peak were collected for subsequent separation by the ${}^2\text{D}$ column. The 4 chromatograms, that reveal a significant impurity peak was obscured by the large ${}^1\text{D}$ peak, are shown below.

1.6.2.2 Offline 2D-LC

In the offline form of 2D-LC fractions of the ${}^1\text{D}$ effluent are collected and stored before they are subjected to the ${}^2\text{D}$ separation. Naturally this results in a longer overall analysis time than in online chromatography; however, the ${}^2\text{D}$ analysis time no longer needs to be equal to the sample collection time, and usually is much greater. Consequently it is possible to achieve higher resolving power in the second dimension and thus an overall increase in the resolving power of the two-dimensional methodology. Offline 2D-LC is frequently used when some form of mass spectrometry is employed as the detector. It must be understood that in contrast to *stop-and-go* 2D-LC, in offline 2D-LC the ${}^1\text{D}$ separation is run continuously. The storage of samples until they are subjected to the ${}^2\text{D}$ separation may entail losses of some trace species in the collection

vessel as well as the possibility of contamination or decomposition, or both. In some cases the eluent is partially or totally removed. It is a much more tedious method than online LCxLC and frequently requires considerable operator attention. As such the required manual steps make it error-prone.

1.6.2.3

Stop-and-go 2D-LC

In the stop-and-go implementation the ^1D and ^2D separations are run alternately. Thus we run the ^1D separation for a while, collect the effluent, then stop the ^1D separation and carry out the ^2D separation of the collected ^1D effluent. The MudPIT – multidimensional protein identification technology – approach¹³ is a form of stop-and-go chromatography. Since the sample can continue to diffuse along the axis of the ^1D column even though the flow has stopped, there is some diminution in the ^1D resolving power¹⁴. Thus in general the stop-and-go methodology is a compromise both in resolving power and analysis time as compared to online and offline chromatography. When the sample involves the analysis of larger molecules with lower diffusion coefficients it turns out that stop-and-go does not cost much in terms of resolving power in the first dimension. Because it allows the second dimension to be run on a longer timescale the overall resolving power is pretty good and the increased analysis time in the second dimension facilitates combining the approach with mass spectrometry. However, it is unavoidable that the more time you spend doing each ^2D separation the longer is the overall analysis time. There is no question that online LCxLC is generally the fastest way to go.

1.7

Generation of the 2D-LC chromatogram

Some thought will indicate that in doing LCxLC what you wind up with is simply a series of ^2D chromatograms acquired throughout the duration of the ^1D separation. These data are recorded as a two-dimensional column matrix; one column of the matrix being the total time from the start of the first ^2D chromatogram and the second being corresponding signal intensity output by the detector at that time. The entire data string is parsed into a series of N ^2D chromatograms, where N is the number of fractions of ^1D effluent transferred to the ^2D column for further separation. Figure 1.8 should make this clear, where it is shown that the 3D plot shown must be constructed from this series of ^2D chromatograms. The data are compiled into a matrix such that the first column is ^2D time, and the subsequent columns are the detector intensities at each ^1D sampling time. However, some explanation is needed as to how the data are manipulated to generate the three-dimensional picture, that is, the chromatogram, such as that shown in Figure 1.2. This was very nicely explained graphically (see Figure 1.8) by Adahchour *et al.*¹⁵. Consider the large ^1D peak which contains three poorly resolved

chemical components eluting in the order 1 (green), 2 (yellow) and 3 (pink). First, samples are taken at equal time intervals across the fused ^1D peak. This is often referred to as the modulation or sampling process in which the ^1D peak is segmented. Second, the single ^1D chromatogram is transformed into a series of fast ^2D chromatograms each of which has several peaks. Examination of the figure shows the green, yellow and pink peaks growing in with increasing ^1D , and then attenuating. Third, the series of ^2D chromatograms are visualized by rearrangement of the data matrix into contour, color, and the 3D type of plot shown in Figure 1.2. Additional types of plots that are also useful include apex plots in which only the position of the peak apex is plotted against the apex time on both dimensions and bubble plots in which a circle (centered on the peak apex) whose area is proportional to the peak size is drawn.

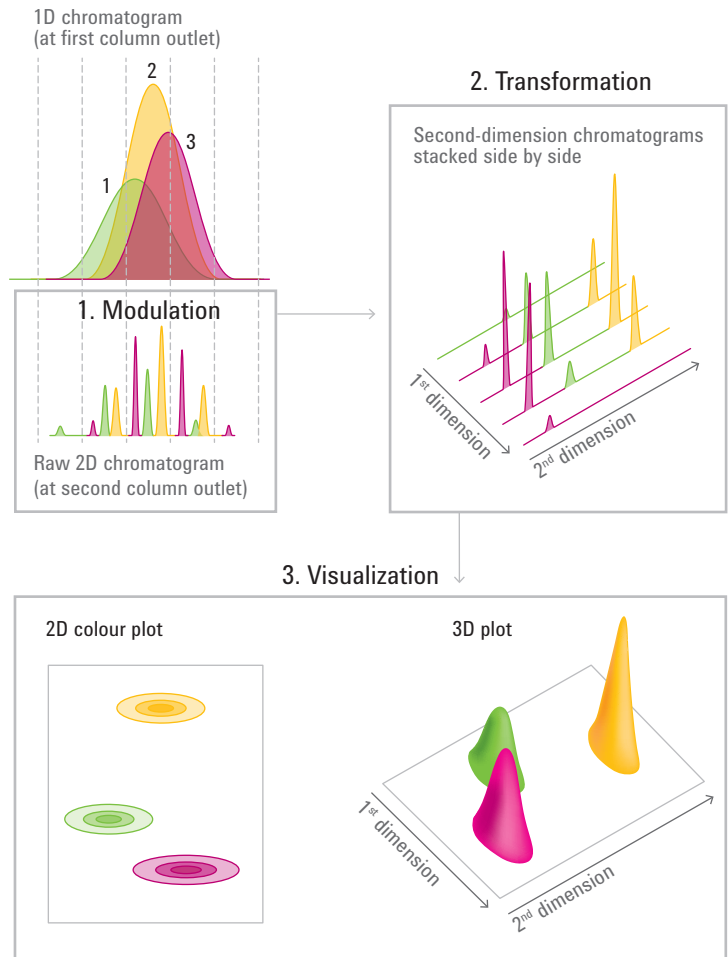


Figure 1.8 Assembly of the collection of ^2D chromatograms into a composite $^2\text{D-LC}$ chromatogram. In part 1, the green, yellow and pink peaks which comprise an unresolved composite peak are shown being *modulated* or sampled into a series of ^2D chromatograms. In part 2, these are transformed so that the series can be better seen and the individual yellow, green and pink peaks grow in and then fade out as the ^1D composite peak is passed over. In part 3, three different visualizations of the ^2D chromatogram are shown including a colored contour plot, a simple contour plot and a 3D plot.

INTRODUCTION TO TWO-DIMENSIONAL PRINCIPLES OF 2D-LC

2

2.1

Introduction

In the "Introduction" at the beginning of this primer, we indicated that the work was addressed to those who have had considerable prior experience in one-dimensional liquid chromatography. There are several concepts that are vital to understand multidimensional chromatography. These include the concept of peak capacity, as well as the basic aspects of gradient elution chromatography. These are so prevalent in multidimensional chromatography that we feel even some of you who have had significant experience in one-dimensional chromatography may not be sufficiently familiar with these ideas. Thus before getting into the principles of two-dimensional liquid chromatography we are going to review these ideas. If you are already familiar with these concepts, Section 2.2 "Peak capacity and related concepts" and Section 2.3 "Basics of gradient elution liquid chromatography and 2D-LC" might well be skipped but they are quite vital to those of you who are not familiar with these concepts; you are strongly advised to study these sections. In Section 2.2 we introduce the peak capacity concept and in Section 2.3 we review the basics of retention, peak width and peak capacity in 1D gradient elution chromatography, emphasizing their role in reversed phase chromatography. At the end of Section 2.3 we go into some detail about how peak capacity can be optimized in 1D gradient elution by choice of particle size, column length, and eluent velocity as well as system pressure and column temperature. We also describe the reasons why gradient elution plays such an important role in LCxLC.

The heart of this chapter lies in Section 2.4 "Fundamentals of peak capacity in LCxLC". The chief advantage of 2D versus 1D methods, namely the *product rule*, is introduced. The product rule tells us that under *ideal* conditions the peak capacity of a 2D separation is equal to the product of the ¹D and ²D peak capacities. The two fundamental problems of 2D-LC namely the *spatial coverage* issue (also called the orthogonality issue) and the *undersampling* issue (also called the remixing issue) are described and the correction factors that should be applied to the ideal peak capacity leading to the real or *effective peak capacity* are developed. Once the effective peak capacity is in hand we then consider how to optimize the peak capacity of an online LCxLC separation. This is examined primarily from the perspective of the ¹D sampling time, which in online LCxLC is

equal to the time allotted to do each ²D separation. We show theoretically and experimentally that optimum sampling times and thus ²D cycle times are quite short – typically between 12 and 20 seconds. It is thereby possible to obtain effective peak capacities of over 1000 in analysis times of only 30 minutes.

2.2

Peak capacity and related concepts

We will shortly introduce you to the concept of the product rule in two-dimensional chromatography. The product rule is formulated in terms of a measure of the resolving power of each of the two dimensions. It is most convenient to choose peak capacity (denoted n_c) as the measure of resolving power. Peak capacity is defined as *the largest number of peaks that can be fit into the separation window* taken as the time difference between the last eluting peak and the first eluting peak. It should be clear that the largest number of peaks that fit will be obtained when all of the peaks are equally well resolved. That is, some space is wasted if all the peaks are not equally resolved. Clearly peak capacity is a theoretical or hypothetical quantity, as in reality peaks never elute such that they are equally resolved. Usually the requisite resolution (R_s) is assumed to be 1.0. This corresponds to a separation of precisely four peak standard deviations (4σ) between adjacent peak maxima.

In Figure 2.1 we show two chromatograms to illustrate the peak capacity concept. Chromatogram A shows the peak capacity obtained under *isocratic* conditions. We assume that the first peak elutes at the dead volume. Whereas using the same column, with the same flow rate, at the same temperature and holding the plate count constant chromatogram B shows the anticipated gradient elution chromatogram. Here we assume that all of the peaks have about the same width; this is commonly the case in gradient chromatography (see Section 2.3.2 “Peak width in gradient elution”). It is evident that more peaks can be fit into a gradient chromatogram than in an isocratic chromatogram. This is a major reason why in two-dimensional liquid chromatography we do gradient elution in one or both of the dimensions of the separation. In fact, there are many reasons for using gradient elution and we will go into this in more detail in Chapter 3 “Practical Implementation of 2D-LC” that is focused on instrumentation.

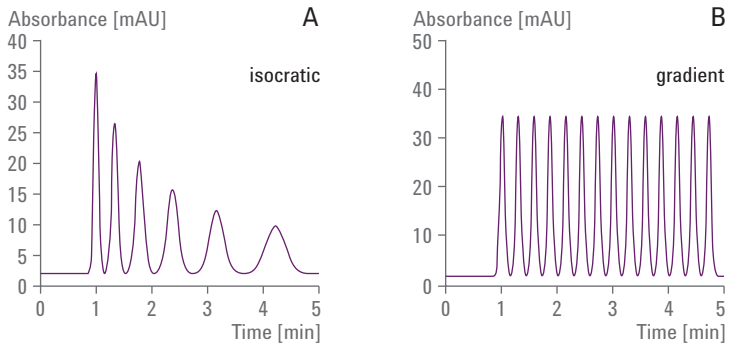


Figure 2.1 Comparison of isocratic (A) and gradient elution (B) peak capacities. Both columns have the same plate count, and resolution of all peaks is taken as 1.5. All peaks have the same area and first peak comes out at the column dead time.

Because the peaks are all assumed to have equal widths the equation for the peak capacity in gradient elution is especially simple, see Equation 2.1.

$$n_c = 1 + \frac{t_{R,\text{last}} - t_{R,\text{first}}}{4R_s\sigma} = 1 + \frac{t_{R,\text{last}} - t_{R,\text{first}}}{\bar{W}}$$

Equation 2.1 Peak capacity in gradient elution.

Generally we take R_s equal to 1 and when all the peaks do not have the same width we use the average 4σ width (\bar{W}) giving the form of the right hand side of Equation 2.1. In theoretical treatments of peak capacity where peak height is allowed to vary or various methods of peak deconvolution, or multivariate curve resolution techniques are used, R_s is taken as the average value needed to resolve a pair of fused peaks into two maxima. However, in most experimental work R_s is taken as unity.

In much practical work the initial and final eluent compositions are chosen so that the first peak elutes at or shortly after the column dead time (t_0) and the last peak at the time that the final gradient strength reaches the end of the column ($t_D + t_0 + t_g$). Given that the second term in Equation 2.1 is generally a lot larger than the first we can estimate the peak capacity as shown in Equation 2.2.

$$n_c \approx \frac{t_g}{\bar{W}}$$

Equation 2.2 Estimation of gradient peak capacity.

This equation is very useful. If we assume a 30-minute gradient and a typical peak width (4σ) of 20 seconds, for example, we quickly estimate a best-case peak capacity of about 90.

A real problem with the peak capacity concept is that it is a *hypothetical* concept. In real samples the peaks are not regularly spaced, rather they are randomly spaced. Further, peaks do not all have the same height. It is well known that two adjacent peaks of the same height and the same width will show a valley, albeit an infinitesimal one, between two maxima at a resolution of exactly 0.5. However, peaks of unequal height require higher values of the resolution and the more dissimilar the two peaks are in height the greater is the required minimum resolution.

To understand the consequences of the hypothetical nature of the peak capacity, Davis and Giddings¹⁶ developed their statistical theory of peak overlap for 1D chromatography, although it has now been extended to multidimensional chromatography. They allowed the relative retention times of a series of peaks to vary according to a Poisson distribution. In a one-dimensional separation they found that the *average number* of observed peaks (p) could be related to the number of chemical components (m) in the mixture and to the peak capacity (n_c) by Equation 2.3

$$p = m \times \exp\left(-\frac{m}{n_c}\right)$$

Equation 2.3 Relationship of average number of observed peaks to number of components and peak capacity.

The ratio m/n_c is quite important and occurs repeatedly; it is called, for good reason, the *saturation factor* and is given the symbol α . A low α means that only a few peaks are occupying the separation space. That is, the peak saturation is low. *We should anticipate an easy separation in this case.* Another way to look at this is that at lower α the probability of peak overlap is lower than at higher α . Clearly it is not the absolute number of components that makes a separation difficult but the number of components relative to the resolving power of the separation space as measured by the peak capacity. In gradient elution 1D chromatography it is known that the peak capacity is quantitatively related to the *average resolution* of all the peaks regardless of their relative retentions. The same concept should also apply at least qualitatively to higher dimension separations.

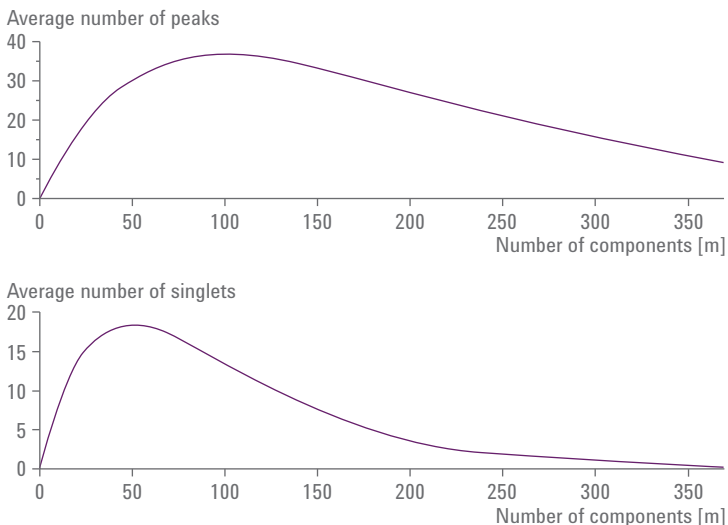


Figure 2.2 The upper graph shows a plot of average number of peaks versus number of components at a peak capacity of 100, whereby the maximum is at 37 percent. The lower graph shows a plot of average number of *singlets* versus the number of components with peak capacity of 100, whereby the maximum is at 18 percent. The need for high peak capacities to analyze natural mixtures containing a large number of components, for example, in proteomics, metabolomics, and environmental samples, has been the chief driving force for interest in 2D-LC.

One of the most important consequences of the Davis-Giddings theory is that the number of peaks (p), when plotted against the number of analyte components, goes through a maximum when p is equal to $0.37 \cdot n_c$ (see Figure 2.2). Thus if a large number of samples having 100 components were analyzed with a system having a 1D peak capacity of 100, a value that is reasonably easy to obtain in a well-designed 30-minute gradient elution separation, *on average* we would see only 37 peaks when no attempt is made to optimize the separation selectivity. However, these are only 37 peaks. The peaks might be singlets, doublets or peaks containing even a higher number of sample constituents. A more important question is; how many pure peaks (peaks comprised of only a single component) we will see *on average*? Again theory predicts (see Figure 2.2) that the number of singlet peaks (s) will be $0.18 \cdot n_c$. That is, of the 37 peaks seen when a mixture of 100 components is analyzed on a column having a peak capacity of 100 only 18 of the peaks will be singlets and 19 of the 37 peaks will be doublets or higher order multiplets. Given that only singlet peaks can be analyzed by simple means (that is, with univariate detectors and not diode array detectors or mass spectrometers) and not employing any mathematical curve resolution methods, it is evident that we need very high peak capacity to minimize the need for extensive method

development. Figure 2.2 is especially telling in that once m exceeds $0.5n_c$ the number of singlet peaks drops steeply. More detailed analysis of the problem shows that when $\alpha=1$ the probability that any component is well separated from both neighboring peaks is only 13.5 percent and that to make it 99 percent probable that a given component is well separated from both neighbors we need $n_c \geq 200m$. Clearly without method development to adjust band spacing we need huge peak capacities to resolve even moderately complex mixtures, as illustrated in Figure 2.3.

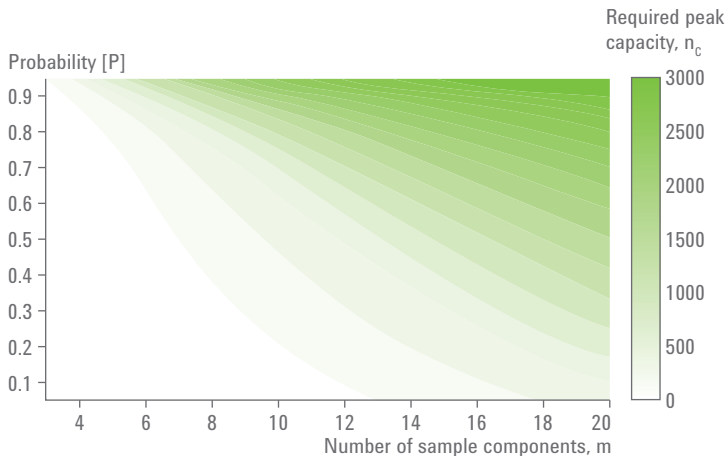


Figure 2.3 Illustration of the required peak capacity n_c to get all peaks of an unknown mixture separated with a certain probability P , if the mixture contains m components (calculated using Equation 9 from Reference 17).

2.3 Basics of gradient elution liquid chromatography and 2D-LC

As should be clear from the preceding section the issue of peak capacity is very important in 2D-LC. The peak capacity that can be generated in a gradient elution separation can be significantly greater than in an isocratic separation given a reasonable minimum amount of time. There are actually a number of other reasons why it can be very beneficial to use gradient elution in either the first or second dimension of a 2D separation and there are a number of reasons why it is either difficult to use gradient elution or preferable to use isocratic elution. These issues require a somewhat detailed understanding of the instrumentation and we will delve into them at much greater length in Chapter 3 “Practical Implementation of 2D-LC” as it is vital to understand them to do high quality LC_xLC work. However, just to raise an issue of very deep concern, the major operational difference between gradient and isocratic elution is that in gradient elution chromatography both the instrument and the column must be re-equilibrated to the initial eluent composition at the end of

each separation. This has a huge impact on how we do the ^{2D} chromatography, nonetheless in many instances we have found it vastly preferable to do gradient elution chromatography in the second dimension even though it is much easier to do isocratic elution on a fast time scale. There are only a few reasons for not using gradient elution in the first dimension. Thus we believe it is essential that some basic aspects of gradient elution be clearly understood before we introduce the principles of 2D-LC.

2.3.1

Retention time in gradient elution

In isocratic chromatography the mobile phase composition is held constant throughout the separation. The solute retention time (t_R) is simply related to the column dead time (t_0) and the solute retention factor (k) as shown in Equation 2.4.

$$t_R = t_0(1 + k)$$

Equation 2.4 Relationship of solute retention time to column dead time and solute retention factor.

In contrast, in gradient elution chromatography the mobile phase strength is deliberately varied from an initially *weak* eluent composition to a *stronger* one. More often than not a simple linear gradient is used. This means that the eluent strength or composition is varied as a linear function of time. Certainly the bulk of the theoretical literature on gradient elution is concerned with linear gradients. The monograph by Snyder and Dolan on gradient elution should be consulted for a much more detailed treatment than can be provided here¹⁸. Obviously the instantaneous retention factor of the solute is no longer a constant as it is in isocratic chromatography but decreases approximately exponentially throughout the separation. According to the linear solvent strength theory (LSST) of gradient elution for reversed phase chromatography the relationship between retention time, instrumental variables and solute parameters is shown in Equation 2.5.

$$t_R = t_0 + t_D + \frac{t_0}{b} \cdot \ln \left(b \cdot \left(k_0 - \frac{t_D}{t_0} \right) + 1 \right)$$

Equation 2.5 Relationship between retention time, instrumental variables and solute parameters.

There are a number of important terms in Equation 2.5; they are all defined in Table 2.1 along with some auxiliary terms.

Symbol	Definition	Dimensions	Secondary relationship
t_R sometimes $t_{R,g}$	Retention time	time	
t_0	Column dead time	time	$t_0 = V_m/F$
V_m	Column dead volume	volume	
F	Eluent flow rate	volume/time	
t_D	Gradient delay time	time	$t_D = V_D/F$
V_D	Gradient delay volume	volume	
S	Slope of log solute retention factor against eluent composition	dimensionless	
k_w	Solute retention factor in pure water ($\phi = 0$)	dimensionless	
k_0	Solute retention factor at initial eluent composition (ϕ_0)	dimensionless	$k_0 = k_w \exp(-S\phi_0)$
t_g	Time for composition to change linearly from its initial to final value (ϕ_{fin})	time	
$\Delta\phi$	Range in gradient composition	dimensionless	$\Delta\phi = \phi_{fin} - \phi_0$
b	Gradient slope	dimensionless	$b = S \Delta\phi t_0 / t_g$

Table 2.1 Summary of symbols and terms used in the discussion of gradient elution liquid chromatography.

The most important thing we learn from this equation is that retention time is now related to the logarithm of initial retention factor (k_0) whereas in isocratic chromatography the relationship is linear (see Figure 2.4). This results because the solute retention factor is decreasing throughout the gradient run. Thus in gradient work a much wider range in solute retention can be handled in a given separation time, which is set by the dead time and the most strongly retained solute, than in isocratic work. We also point out that the equation contains a *delay time* (t_0). This is needed to account for the time it takes the mobile phase composition changes to propagate through the gradient mixer and get to the column inlet. Gradient systems are constructed such that the sample does not pass through the gradient mixer. If it did it would be subjected to a huge amount of unnecessary extracolumn peak broadening. The impact of the gradient delay can be compensated by deliberately starting the solvent gradient before the sample injection is made. This is called a delayed injection. The concept of the gradient delay is extremely important in the second dimension of 2D-LC systems, and it will be discussed more in Chapter 3 “Practical Implementation of 2D-LC”.

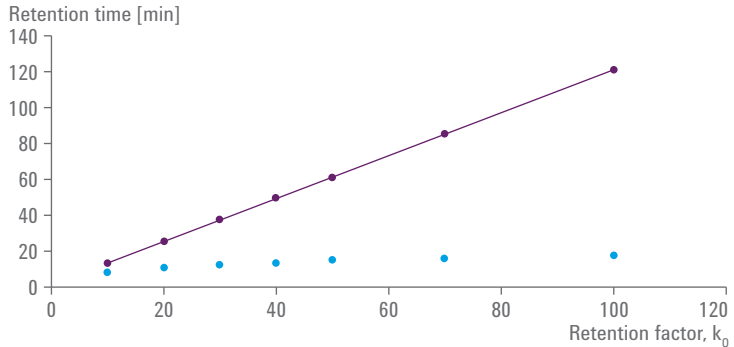


Figure 2.4 Plot of retention time versus retention factor. Isocratic results in purple filled circles and purple solid line. Gradient (non-linear) results shown as filled blue circle. Conditions: $F = 1 \text{ mL/min}$; $V_m = 1.2 \text{ mL}$; $V_D = 0.5 \text{ mL}$; $t_g = 30 \text{ min.}$; $S = 12$; k_0 or $k = 10, 20, 30, 40, 50, 70, 100$.

By analogy to how retention factor is measured in isocratic chromatography (see Equation 2.4) it is possible to define what we call here an *apparent* or operational *retention factor* for gradient elution as given by Equation 2.6.

$$k_g \equiv \frac{t_{R,g} - t_0}{t_0}$$

Equation 2.6 Apparent or operational retention factor.

Assuming that the delay time is zero or that we are using a properly delayed injection leads to the logarithmic relationship between the gradient retention factor (k_g) and the initial retention factor of the solute (k_0).

2.3.2 Peak width in gradient elution

The relationships between peak width, operational variables, and solute properties are also important considerations when working with gradient elution. In fact it is really the relationship between peak width and retention that makes the peak capacity of gradient elution so much better than that of isocratic elution. The equation for peak standard deviation in isocratic chromatography is shown in Equation 2.7.

$$\sigma_{iso} = \frac{t_0}{\sqrt{N}} (1 + k)$$

Equation 2.7 Calculation of peak standard deviation in isocratic chromatography.

The corresponding equation that applies in gradient elution is shown in Equation 2.8.

$$\sigma_{grad} = \frac{t_0}{\sqrt{N}} G(p)(1 + k_e)$$

Equation 2.8 Calculation of peak standard deviation in gradient elution.

The various terms in these equations are defined in Table 2.2. Clearly the two equations are closely related. The gradient compression factor, $G(p)$, accounts for the fact that the upstream side of the solute zone travels through the column in a stronger eluent than the downstream side.

In a very slow gradient (slow increase in composition) elution becomes isocratic and $G(p)$ will approach a value of unity; in a fast gradient the largest effect we could see would be a halving of the peak width; however, diffusion will oppose this effect so that in a very fast gradient $G(p)$ only approaches a limit of 0.58 as it descends from unity. On-column compression of the solute tail is a real *but not* big effect. Do not confuse this process with the sample focusing effect of gradient elution that can occur at the column inlet, which is often of great importance in the second dimension.

Symbol	Definition	Units	Secondary relationships
σ	Peak standard deviation	time	
t_0	Column dead time	time	See Table 2.1
N	Column plate number	dimensionless	$N = (t_R/\sigma)^2$
k	Retention factor	dimensionless	
$G(p)^*$	On-column zone compression factor	dimensionless	$G = \sqrt{\frac{1 + p + \frac{p^2}{3}}{(1 + p)^2}}$
p		dimensionless	$p = k_0 b / (1 + k_0)$
k_e	Retention factor at the time the solute leaves the column	dimensionless	$k_e = \frac{k_0}{bk_0 + 1}$

Table 2.2 Symbols and terms required for discussing peak width in gradient elution liquid chromatography. Terms not defined here are defined in Table 2.1 (* $0.58 < G(p) < 1.0$).

The real difference between isocratic and gradient LC lies in the meanings of k and k_e . The term k_e is the solute's retention factor that applies as the solute exits the column. According to the equation given in Table 2.2 this term depends on k_0 and b . Both terms depend on the solute but for solutes

of roughly the same molecular mass, k_o varies a great deal more than does b . In fact when k_o is big, as it frequently is, k_e takes on the limiting value of $1/b$ as shown in Equation 2.9.

$$k_e \approx \frac{1}{b} = \frac{t_g}{S\Delta\phi t_o}$$

Equation 2.9 Limiting value of solute retention factor.

Thus Equation 2.8 can be written as shown in Equation 2.10.

$$\sigma_{grad} = \frac{t_o}{\sqrt{N}} G(p) \left(\frac{t_g + S\Delta\phi t_o}{S\Delta\phi t_o} \right)$$

Equation 2.10 Peak standard deviation with limiting value of solute retention factor.

Plots of σ_{grad} versus k_o and S using the exact equation for k_e are shown in Figure 2.5. The most important point this plot teaches is that when k_o is bigger than about 20 all peaks having about the same S value have approximately the same peak width. Small molecules like benzene have S values of about six. The peptides resulting from the digestion of proteins with trypsin have S values in the range of 20 to 40.

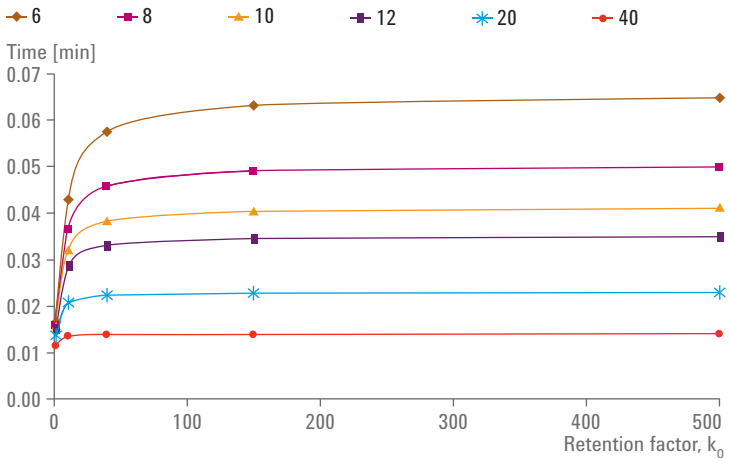


Figure 2.5 Plot of peak σ_{grad} value (minutes) versus initial retention factor (k_o) for gradient elution chromatography. The solute S factor is shown in the legend. Other conditions are: $t_0 = 0.5$ min, $t_D = 0$ min, $t_g = 15$ min, $N = 3,000$, $\Delta\phi = 0.75$. The b values corresponding to the S values are 0.20, 0.27, 0.33, 0.40, 0.67, and 1.33. The most important point this plot teaches is that when k_o is bigger than about 20 all peaks having about the same S value have approximately the same peak width.

Choosing a value of S typical of a low molecular weight drug, such as 12, we can simulate a gradient elution separation to produce a chromatogram like that shown in Figure 2.6. All peaks have the same area. It is clear that the peak widths increase somewhat as retention increases but soon become almost constant as indicated by the near constancy of the peak heights. This is quite different from what we see in isocratic chromatography where the peak width, assuming all peaks have the same plate number, increases with retention. This is a vital feature of gradient chromatography. It leads directly to its improved peak capacity relative to isocratic chromatography.

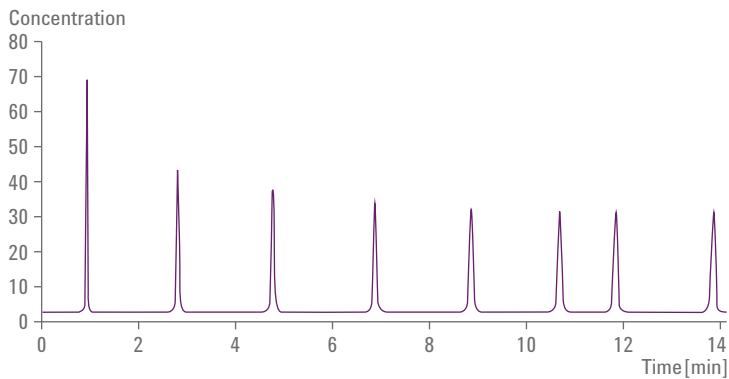


Figure 2.6 Chromatogram generated using Equations 2.5 and 2.8. The k_0 values were taken as 1, 10, 40, 150, 500, 1500, 3000 and 10,000. All other conditions are as in Figure 2.5 with $S = 12$.

2.3.3 Peak capacity of gradient elution

For simplicity we assume that the initial eluent composition is adjusted so that the first peak elutes shortly after t_0 and that the final composition can be adjusted so that the last peak elutes at $t_g + t_0$. Thus the numerator in Equation 2.1 will be at its maximum. We will assume that the approximate form of Equation 2.9 can be used so k_0 is sufficiently large that k_e is accurately given by $1/b$, as shown in Equation 2.11.

$$n_c = 1 + \frac{\sqrt{N}}{4G(p)} \frac{S\Delta\phi t_g}{t_g + S\Delta\phi t_0} \approx \frac{\sqrt{N}}{4} \frac{S\Delta\phi t_g}{t_g + S\Delta\phi t_0}$$

Equation 2.11 Calculation of peak capacity using approximate form of Equation 2.9.

We can use Equation 2.11 for a single peak (usually the last peak) or the average value over all peaks. It must be understood that this estimate is sometimes only approximate. It usually appears with $G(p)$ estimated as 1.0. That is, the beneficial effect of on-column zone compression is usually ignored. Clearly the peak capacity depends on several instrument and column parameters (t_0 and t_g). It depends on the solute dependent parameter (S). Of course, S also varies with the chemical nature of the stationary and mobile phases. There is a strong tendency to think of $\Delta\phi$ as primarily an instrumental variable. In our view this is incorrect. In order to make the first solute elute near t_0 and the last near $t_0 + t_g$ both ϕ_0 and ϕ_{fin} must be adjusted. Their values depend on the properties of the solute set, specifically the k_0 values of the least and most retained solutes.

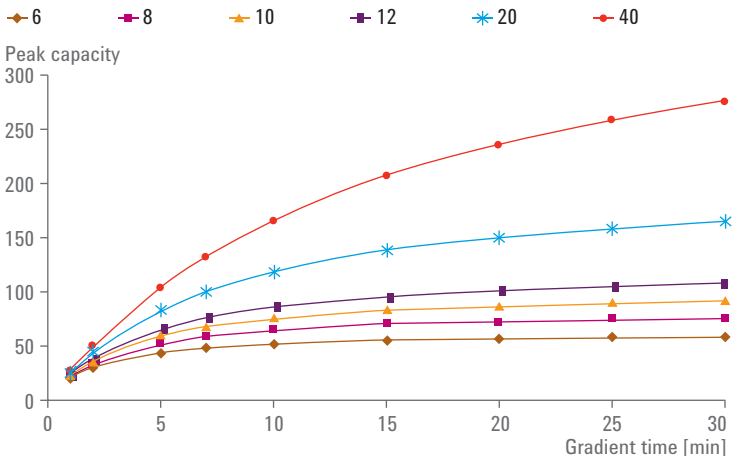


Figure 2.7 Dependence of peak capacity on gradient time and solute S calculated using Equation 2.11, with $G(p) = 1$. Values of S are given in the legend. All other variables except t_g are as in Figure 2.4 and Figure 2.5. Note the rapid initial increase and then the gradual approach to a limit beyond which there is little further improvement in peak capacity. These curves tell us that we really should increase the column length as the gradient time is increased in order to optimize the peak capacity.

Figure 2.7 shows that for a column of fixed length and flow rate the peak capacity increases with gradient time but rather rapidly reaches a limiting value. The gradient time at which 90 percent of the peak capacity is achieved is given by Equation 2.12.

$$\frac{t_g}{t_0} \geq 9S\Delta\phi$$

Equation 2.12 Gradient time required to reach 90% of limiting peak capacity.

The limiting peak capacity is given by Equation 2.13.

$$n_{C,max} \approx \frac{\sqrt{N}}{4} S\Delta\phi$$

Equation 2.13 Calculation of limiting peak capacity.

These equations (as well as Figure 2.7) clearly tell us that the peak capacity and speed of generating peak capacity depend strongly on the column's efficiency (N) and the characteristics of the solute set (S and $\ln k_w$).

Thus to get a high peak capacity we need excellent columns and a solute set that has both large S values and a wide range in solute retention to assure a big $\Delta\phi$. We should point out that theoretical plots like that in Figure 2.7 are strongly supported by many experimental measurements of peak capacity as a function of gradient time. That is, the peak capacity initially increases rapidly with increasing gradient time, and then curves over and becomes constant. This has proven to be the case for both the slow gradients (15 to 60 minutes) used in the first dimension and much faster gradients (tens of seconds) used in the second dimension of LCxLC systems. While the experimental data may not exactly fit Equation 2.11, the plots show the same limiting behavior.

Clearly the rate of production of peak capacity computed as n_c/t_g decreases with time (see Section 2.3.4 "Optimization of 1D gradient peak capacity"). Ultimately this fact combined with the undersampling problem to be discussed in Section 2.4.2 "The undersampling or remixing problem" leads to the existence of an optimum 2D gradient time that maximizes the real 2D peak capacity as described in Section 2.4.3 "Consequences of the undersampling problem".

Despite the great utility of Equation 2.11 we are compelled to point out a very serious short coming of the above approach to relating the peak capacity to the gradient time. Equation 2.11 *assumes that all of the conditions of the separation* (column length, flow rate, initial and final mobile phase composition, dead time and plate count) *are fixed as the gradient time is varied*. In fact you can definitely improve the peak capacity if you are willing to vary several conditions of the separation as the gradient time is increased (see Section 2.3.4 "Optimization of 1D gradient peak capacity"). Perhaps the most serious limitation of Equation 2.11 is that L is fixed and consequently so is N . We are quite confident that it is possible to generate a plate count of upwards of 20,000 under conditions compatible with a 30-minute gradient time. Thus we estimate that a more reasonable value of N to use instead of

3,000 at least for a gradient time of 30 minutes would be 20,000. This leads to limiting values of the peak capacity of 149 (6), 194 (8), 237 (10), 278 (12), 425 (20) and 708 (40), where the relevant S values are given in parentheses. This is a considerable increase in peak capacity over that shown in Figure 2.7.

2.3.3.1

Optimum rate of peak capacity production

Another important aspect of peak capacity that is particularly relevant for the optimization of *online* 2D-LC is the rate of production of peak capacity. This parameter is controlled by two independent factors, both of which are quite important.

- The relationship between peak capacity and gradient time.
- The time needed to re-equilibrate (t_{re-eq}) the system before the next gradient can be done.

The re-equilibration time includes the time needed to flush the gradient mixer so that its effluent reaches the initial composition used in the gradient, plus the time needed to flush the column sufficiently that repeated separations of the same solutes are reproducible. We have found that many types of RPLC columns require flushing with about two to three column volumes of the initial eluent before their retention times become fully reproducible. We do not know how long it takes HILIC or ion exchange columns to re-equilibrate. For HILIC or ion exchange chromatography (IEX) these volumes might be much longer.

The gradient elution cycle time (t_c) is defined as the sum of the gradient and re-equilibration times and thus the rate of production of peak capacity is best taken as n_c/t_c and not n_c/t_g . As discussed above the gradient time is what determines the peak capacity. Shown in Figure 2.8 are data from experimental measurements of 2n_c values as a function of 2t_g for a few low molecular weight probe solutes on a small (2.1 x 33 mm) column operated at elevated temperature and very high flow rate (3 mL/min). The experimental t_{re-eq} was actually 3 seconds but a series of curves were computed for several values of t_{re-eq} ranging from 2 to 5 seconds. It is evident that there is an optimum in the peak capacity production rate. We will see later that this will also strongly influence the optimum in a plot of 2D peak capacity versus the first-dimension sampling time for online LCxLC.

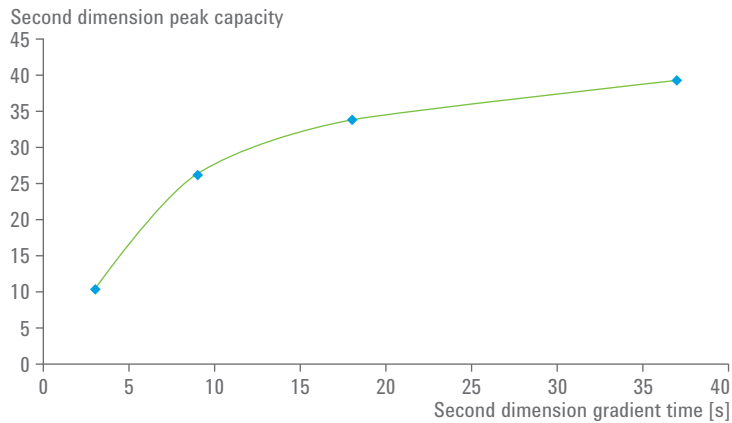


Figure 2.8 Experimental data for 2n_c versus 2t_g . Data from Huang *et al.*¹⁹ – a 2.1 x 33 mm (id) column prepared with particles of carbon-clad zirconia was operated at a flow rate of 3 mL/min, column temperature of 110 °C, using an acetonitrile/water gradient. Data were acquired on maize seed samples during LCxLC analyses. The solid points are the experimental data and the curve is the best fit given by ${}^2n_c = 50.0 \cdot {}^2t_g / (9.16 + {}^2t_g)$ with 2t_g in seconds.

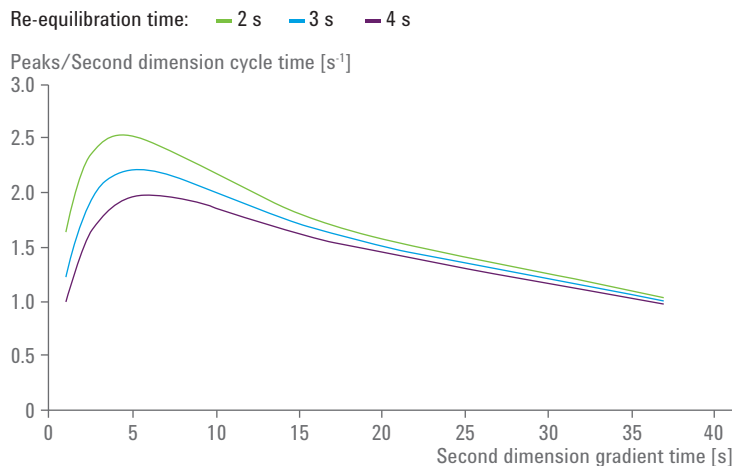


Figure 2.9 Plot of computed values of the rate of production of peak capacity versus gradient time. The curves were computed by fitting the data of Figure 2.8 to an equation of the form of Equation 2.11. The cycle times were computed by adding the re-equilibration times given in the legend to the gradient time used to compute the peak capacity. The peak capacity production rate is defined as ${}^2n_c / {}^2t_c$.

2.3.4

Optimization of 1D gradient peak capacity

For various reasons that will become clear in Chapter 3 “Practical Implementation of 2D-LC” it is very difficult to fully optimize the conditions used to develop the ^1D gradient in online LCxLC. In particular, it is quite often the case that the flow rate used in the first dimension (^1F) is well below the flow rate that maximizes the peak capacity. However, the constraint on the ^1F imposed by the ^2D separation is obviously non-existent in 1D chromatography. There have been many approaches to maximizing the peak capacity in gradient elution^{18,20} but in general the best approach is to adapt Poppe’s method²¹ originally designed for maximizing plate count in isocratic chromatography to optimize the peak capacity in gradient elution²². Poppe’s basic idea was that two conditions must be met.

- The column length and velocity are covaried so that the operating pressure is always at some desired maximum value.
- The column length and velocity are covaried so that the analysis takes place in some desired timescale. The timescale is set by the column dead time (t_0) and the retention factor of the most retained peak.

It is implicit that you are working with a *fixed particle size* at a constant temperature and eluent composition and thus at a given viscosity. If you obey the above rules one will produce a separation having the maximum possible value of N/t_0 for the particle size chosen for the system used²³.

Poppe’s approach to optimization can be adapted to gradient elution in the following way²². First, instead of optimizing plate count we optimize peak capacity using Equation 2.1. Since this equation depends on the retention times of the least and most retained solutes we must input solute dependent data, specifically the S and k_w values. Second, the timescale is based on the gradient time not the dead time of the column. Third, the gradient peak capacity depends on column length and eluent velocity, as well as initial and final eluent composition. If you want to also optimize the temperature then you must put in additional factors. Programs for doing this kind of optimization are available on the web at <http://homepages.gac.edu/~dstoll/calculators/optimize.html> (accessed November 1, 2014).

One of the most important lessons we have learned from doing gradient optimization of peak capacity is that we do not advise the use of a column of fixed length at various gradient times. It is very important to allow the column length, flow rate (eluent velocity) and eluent composition to vary with the gradient time. The results of such a study involving separations of tryptic peptides are shown in Figure 2.10. The main take-home message

from these plots is that it is necessary to gradually increase the particle size as the gradient time is increased to maximize the peak capacity. You should use the smallest possible particles to achieve the maximum peak capacity at very short times but when longer gradients are used the particle size must be increased. Furthermore it is important to understand that as you move from left to right, that is, upwards, along any of these Poppe curves the columns get longer and the velocities become slower. This should be self-evident as the pressure at any point along any of the curves in Figure 2.10 is held at 400 bar and the analysis time, that is, the gradient time, gradually increases as you move from left to right.

The plot shows that the highest peak capacities are obtained at the longest gradient times ($>> 1000$ seconds) with long columns run at low eluent velocity. Further, at longer times larger particles used in much longer columns give higher peak capacities. In contrast, the most time effective separations are obtained at very short gradient times ($<< 100$ seconds) with small particles and very short (< 5 cm) columns at high eluent velocity.

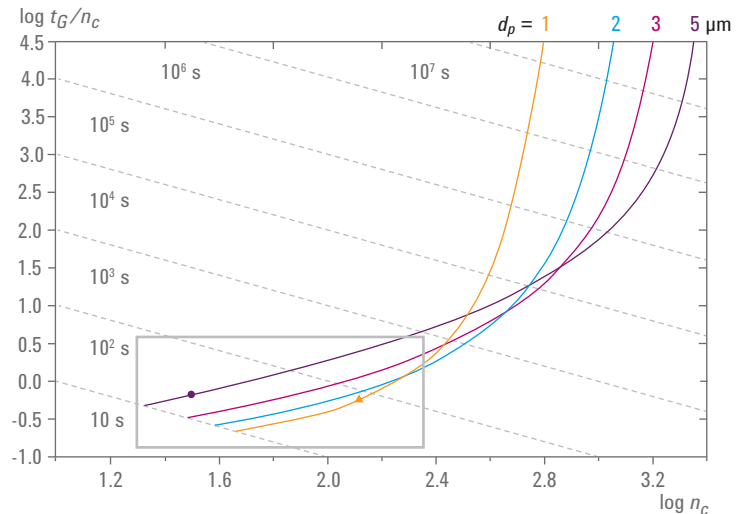


Figure 2.10 Poppe gradient plot showing relationship between gradient time and optimized peak capacity. The diagonal dotted lines are lines of constant t_g . The conditions used assume van Deemter parameters $A = 1.04$, $B = 16$, $C = 0.033$, dimensionless flow resistance factor = 500, temperature = 40°C , and $P_{\max} = 400$ bar. Adapted from Reference 22. The plot shows that the highest peak capacities are obtained at the longest gradient times ($>> 1000$ seconds) with long columns run at low eluent velocity. Furthermore at longer times, larger particles used in much longer columns give higher peak capacities. In contrast, the most time effective separations are obtained at very short gradient times ($<< 100$ seconds) with small particles and very short (< 5 cm) columns at high eluent velocity.

Both column temperature and the maximum operating pressure have big effects on the peak capacity, especially at very short gradient time. These results are shown in Figure 2.11. In the high speed region ($t_g < 100$ seconds) pressure has only a small effect on peak capacity but temperature has a beneficial effect. However, the effect of elevated temperatures at long gradient times where the highest peak capacities are obtained is small, and eventually elevating the column temperature becomes detrimental in the case of exceedingly long gradients.

There are a number of important take-home messages for 2D-LC that we can learn from these graphs.

- The ¹D separation, which is done on a long timescale (15 minutes or more) generally should be done with rather long columns (> 15 cm) at low flow rates with intermediate size particles, almost certainly not 1.8- μm particles, to get the best peak capacity at the maximum system pressure.
- As the gradient time is increased the column length should be increased and the flow rate decreased to maintain the pressure at the maximum allowable.
- Intermediate temperatures of 40 to 60 °C should be used (as long as there is no on-column sample decomposition) to lower the eluent viscosity.
- For reasons that will become clear in our discussion of instrumentation (see Chapter 3 "Practical Implementation of 2D-LC") the column diameter should be 2.1 mm or less.
- For fast ²D gradient separations (10 to 60 seconds) small (1.8 or 2.7 μm core-shell particles) should be used.
- The maximum available column temperature should be used to allow the ²D column to be run at very high flow rates. Flow rates of 3 mL/min can be used and this is exceedingly important to reduce the ²D system flush-out and column re-equilibration to a minimum.

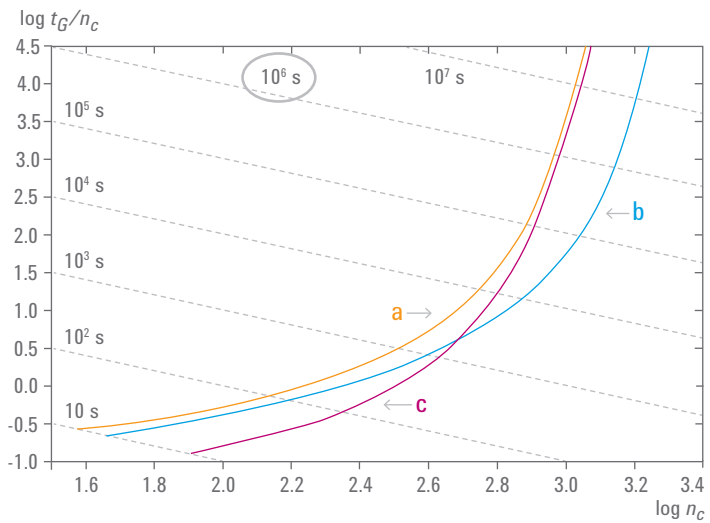


Figure 2.11 Effect of temperature and pressure on peak capacity and analysis time for tryptic peptides studied in Figure 2.10. In this case the particle size is fixed at 2 μm . a) $P_{max} = 400 \text{ bar}, T = 40^\circ\text{C}$; b) $P_{max} = 1000 \text{ bar}, T = 40^\circ\text{C}$; c) $P_{max} = 400 \text{ bar}, T = 100^\circ\text{C}$. Adapted from Reference 22. All of the comments about Figure 2.10 apply here as well. The results show that increasing column temperature is a more effective way to increase speed in the limit of high speed chromatography than is increasing the system pressure. This means that the second dimension should have small particles packed in a short column, run at high temperatures and high eluent velocity. However, in the limit of very high peak capacity, increasing temperature is counter-productive whereas increasing pressure is a significant help.

2.3.5

Other benefits of gradient elution in LCxLC

In addition to the higher peak capacity of gradient over isocratic LC, which is as such very important in 2D-LC, gradient elution affords several additional advantages, which are particularly important in the second dimension.

- By making the ²D gradient go to very strong eluent compositions (for example, high organic modifier in RPLC) you can have all of the compounds injected onto the column elute before the next ²D separation is executed. This is vital to avoid what can be called *wrap-around* in ²D separations. Suppose that the eluent composition was too weak to elute all the components before the next fraction of ¹D column effluent is injected. Those non-eluting species will eventually elute at some later time in the separation, and the peak will be associated with the wrong ¹D fraction, thus it will be given an incorrect ¹D retention time as well as the wrong ²D retention time. Use of gradient elution reduces the likelihood of such events.

- However, probably, the chief advantage of doing a ²D gradient is to focus the sample contained by the ¹D effluent on the top of the ²D column. This is vital to mitigate the drastic sample dilution that takes place in isocratic chromatography.

The sample focusing effect is not to be confused with the on-column zone compression effect discussed in Section 2.3.2 "Peak width in gradient elution", which is accounted for by the factor $G(p)$. The sample focusing effect is quite different. It has been known for a long time and is used as a preconcentration device to allow a larger volume of sample to be injected²³. One way to implement preconcentration is to place a *trapping column* in the sample loop. In essence the sample will be focused at the top of a column if it is injected in a bolus of fluid that is a very weak eluent on the stationary phase in use. Imagine that a large volume of sample contained in a noneluting eluent is flowing into a column. The leading edge of the sample experiences a great decrease in velocity once it contacts the stationary phase. This is especially effective if there is minimal mixing with the solvent that is initially in the column which is preferably a very weak eluent. The rear edge of the sample moves at the mobile phase velocity and thus the sample volume is compressed, that is, the sample is focused at the top of the column and becomes a good deal more concentrated. To a first approximation the sample concentration increases (and the effective volume decreases) by the ratio of solute retention factors in the loading solvent relative to the eluting solvent. Thus the loading solvent needs to be weak and the eluting solvent needs to be strong. In order for this to be a big effect the samples retention factor as it enters the column must be quite large – at least 10 or more. If this were so then a 20- μL volume of sample would be compressed 10 fold down to 2 μL . Thus almost all of the zone dispersion that the sample undergoes during injection onto and elution out of the ¹D column, and delivery onto the ²D column can be eliminated. Thus the degree of dilution^{25, 26} that the sample undergoes in the first dimension of a 2D-LC separation is significantly reduced.

Now let us consider what happens in the course of a 2D-LC separation. When the ¹D column is run isocratically we must make sure that the ¹D eluent is a weak eluent on the ²D column. However, if the ¹D column is run under gradient conditions we must make sure that the ¹D eluent remains a weak one on the ²D column especially at the end of the ¹D gradient. In RPxRP it is helpful to choose a ²D column that is much more retentive than the ¹D column. For example, you might use an RP cyano or RP polar embedded phase on a low surface area substrate as the ¹D column and a heavily loaded C18 phase on a high surface area substrate as the ²D column.

2.4 Fundamentals of peak capacity in LCxLC

We will say more about the use of *trapping* columns and deliberate pre-dilution of sample with very weak eluent before injection onto the ^2D column in Chapter 3 “Practical Implementation of 2D-LC”.

One of the best ways to think about the peak capacity in a two-dimensional separation is to think of breaking up a one-dimensional separation into a linear series of bins as shown in Figure 2.12, with each bin representing a unit of peak capacity, and then doing a second separation on the chemical contents of each $'\text{D}$ bin as shown in Figure 2.13. This is similar to cars parking along a road versus cars parking in a parking lot.

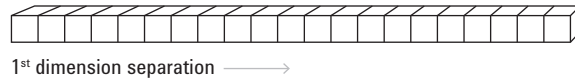


Figure 2.12 Schematic representation of the peak capacity of a one-dimensional separation.

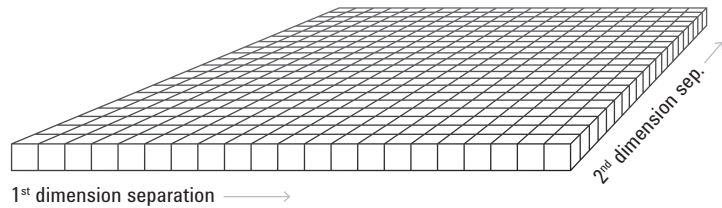


Figure 2.13 Schematic representation of the peak capacity of a two-dimensional separation.

This approach very rapidly leads the single most important concept of multidimensional separations known as the *product rule* given by Equation 2.14. Here $n_{c,2D}$ represents the peak capacity of the 2D separation, and the first-dimension (1n_c) and second-dimension (2n_c) peak capacities respectively.

$$n_{c,2D} = ^1n_c \times ^2n_c$$

Equation 2.14 Product rule given by multiplication of peak capacities.

The major importance of the product rule is that it greatly increases the peak capacity as compared to the use of tandem columns which, at best, only results in the *addition* of the peak capacities of the two columns.

Equation 2.14 tells us that if 1n_c were 50 and 2n_c were 20, then $n_{c,2D}$ would be 1000. From the outset it must be understood that *the product rule only provides an estimate of the theoretical maximum peak capacity* and applies only under certain *ideal* circumstances. As stated by Giddings²⁷ these are as follows:

- “First, it is one in which the components of a mixture are subjected to two or more separation steps (mechanisms) in which *their displacements depend on different factors.*”
- “The second criterion is that when two components are substantially separated in any single step, *they remain separated until the completion of the separation step.*”

Giddings’ rules are rather tersely stated and require amplification to be used in practice. They can be translated into practical guidelines as follows:

- A. The retention of the sample species must be controlled by two (or more) different (*orthogonal*) physicochemical properties and the two separation systems *must* separate the species by complimentary mechanisms.
- B. The location of the components after separation in time requires two time coordinates (1t_R and 2t_R) not be merely the sum of two retention times. This proviso rules out a simple tandem arrangement of columns.
- C. The sample constituents must be spread across the *entire separation space.*
- D. Once the species are separated in the first dimension there *must be no remixing* (that is, additional peak broadening) induced while doing the 2D separation.

2.4.1 Spatial coverage limitations on the product rule

Suppose that we used the same type of stationary phase and same mobile phase composition, including pH, in both dimensions. It is evident that a plot of retention time on each dimension will be a perfectly straight diagonal line (see left panel in Figure 2.14). Clearly this choice of columns and conditions does not accomplish much improvement in the separation. It fails to satisfy proviso (A) above. *This is what we will see if the separation mechanisms are strongly correlated.* This outcome will occur under two different conditions. First, suppose that the two separation dimensions fundamentally access only a single retention determining property among the sample solutes, for example, retention on the pair of columns really only responds to differences in solute based solely on their molecular size and not, for example, their charge, shape, hydrogen

bonding properties or affinity for silanol groups. Second, suppose the separation conditions do in fact respond differently to two (or more) solute properties but *in a given solute set* there is really only one difference in the solute properties that influence the separation as would be the case with a simple homologous series (for example, alkyl benzenes), a set of benzologs (for example, benzene, biphenyl, p-triphenyl, and so on) or a homopolymer (for example, glycine, diglycine, triglycine, and so on). Clearly what we require is that each dimension of the separation system interact with a different solute retention determining property and that the solute set contains at least two such properties. *This is a necessary condition for spreading the solutes out.* If the differences in solute properties are sufficiently large then the solutes will be spread over the entire space as shown by the right panel in Figure 2.14. This has become known as a highly *orthogonal* separation. More often than not we will find that the separation is only partially orthogonal (see center panel in Figure 2.14).

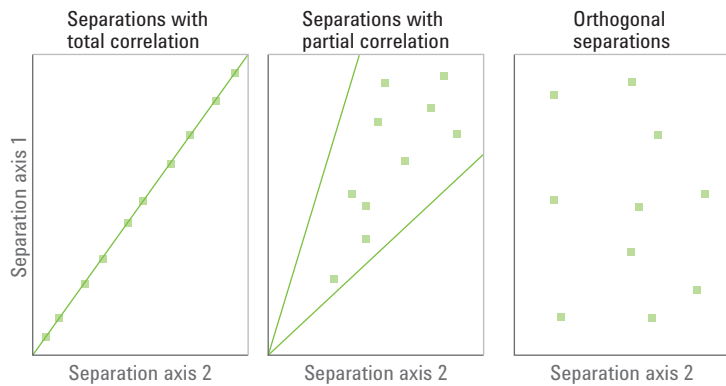
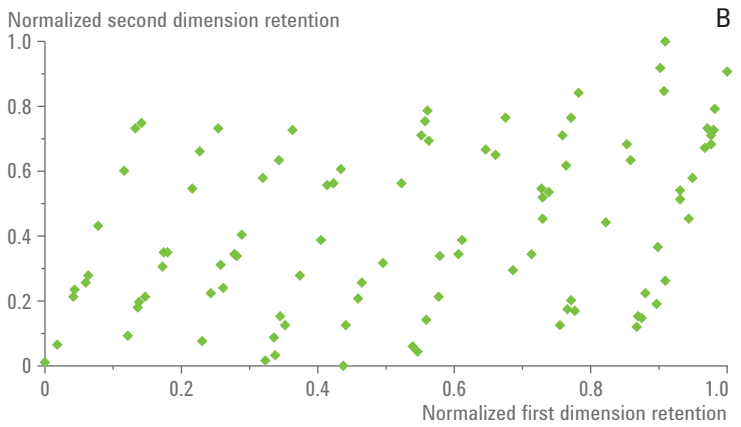
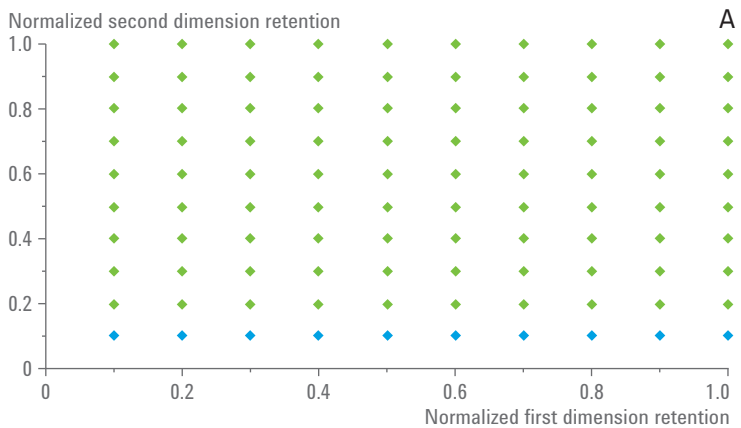


Figure 2.14 Effect of different degrees of correlation of separation mechanisms on scatter (orthogonality) in plots of first versus second-dimension retention.

Too much attention can be paid to the purely statistical or mathematical interpretation of the *orthogonality* issue as described above. It is after all only a highly desirable but not sufficient condition for attaining what we want which according to Giddings²⁸ is: a) to have minimal correlation between the two retention coordinates; b) to spread the sample components over as much of the *entire* separation space as possible; and c) to have a minimal amount of clustering of the points thereby leaving undesirable sparsely occupied regions surrounded by more densely populated regions. In an ideally ordered two-dimensional chromatogram

(see panel A in Figure 2.15), as imagined in the two-dimensional peak capacity concepts of Giddings^{27,28}, all peaks are equally spaced leaving no *gaps* or *holes* in the structure and thus no clusters. These conditions will give the maximum number of single component peaks that can be put into that separation space. A number of different depictions of what might happen are shown in Figure 2.15. Note that in all figures there are 100 components whose retentions have been assigned by different rules.



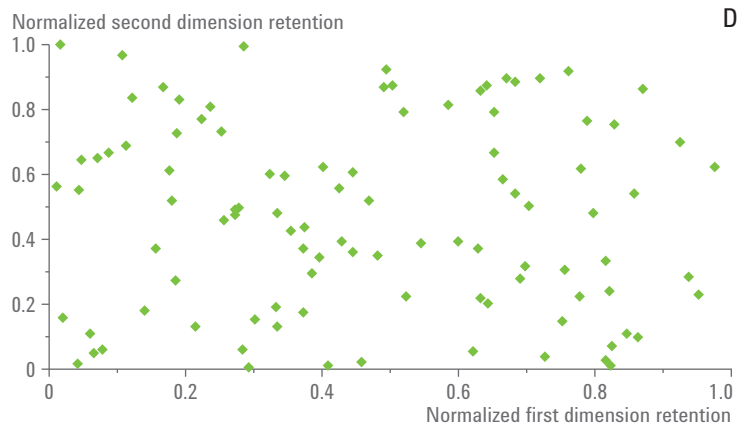
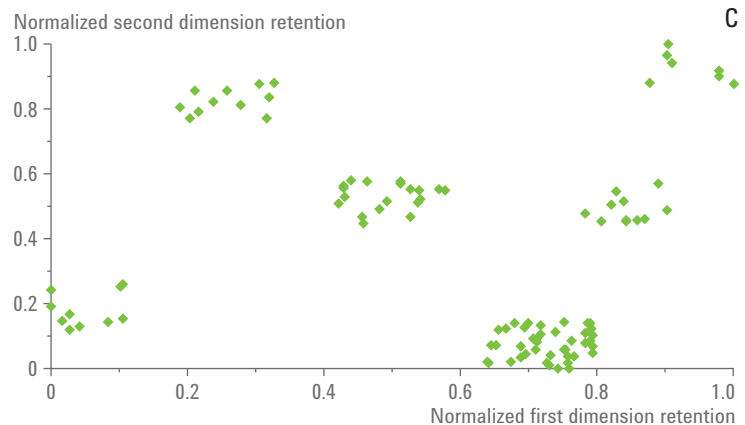


Figure 2.15

Panel A: Ideal distribution according to Giddings, showing equal resolution of all analytes with no gaps or clusters²⁸.

Panel B: A non-ideal distribution sometimes referred to as *bananagrams*²⁹.

This arrangement of peaks shows clusters and gaps in data. Comparison of panel B with panel A shows a clear deterioration of the average resolution due to clustering resulting from discontinuous change in the property controlling retention on the '1D axis. This is commonly observed in polymer separations.

Panel C: Clustergrams spread over the entire length and breadth of space but leaving huge gaps. A great reduction of peak capacity results due to very large proportion of wasted space.

Panel D: Completely orthogonal separation with all retentions assigned randomly over the entire space. Much of the peak capacity lost in panels B and C is recovered but we still see big gaps, which persist due to the randomness of the retentions. Should we count such unused space or not?

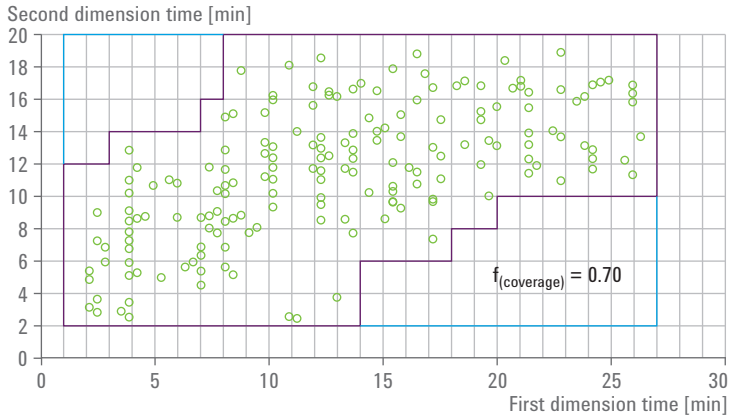


Figure 2.16 Retention coordinates in a two-dimensional separation space (green dots) obtained from a RP_xRP separation of a maize seed extract. The fractional coverage of the separation space is calculated as the ratio of the number of bins contained by the purple boundary to that contained by the blue boundary. Adapted from Reference 30.

One approach to how you might calculate and quantify the usage of the two-dimensional separation space or the so-called surface coverage is shown in Figure 2.16. This approach was used by Stoll³¹ and represents a modification of a method first presented by Gilar³². The Gilar concept is very useful and conceptually important because it gets away from a simplistic reliance on the *orthogonality* concept and *emphasizes the idea of filling the available space with peaks*. In contrast to the Gilar method the Stoll modification does not use a square grid but divides the space up in proportion to the relative peak capacity of each axis. Also the Stoll modification draws a rectilinear outline around all occupied grid locations and thus incorporates many unoccupied grid points. In this regard the Stoll method is very similar to Davis' *minimum alpha hull* approach³³ shown in Figure 2.17 and not surprisingly the two approaches give similar results. In both the Gilar method and Stoll-modified-Gilar method the separation space is segmented into a definite number of bins following some agreed upon semi-arbitrary but reasonable rule to guide the number of bins; the fractional surface coverage is then computed after determining which unoccupied bins are surrounded by occupied bins. There are a number of subjective issues involved in defining the appropriate bin size and in deciding whether or not to include an empty bin that is surrounded by occupied bins as being part of the occupied space. It is evident that the bin size selected will be a controlling factor in determining the fraction of bins which are occupied. So does the issue of whether you include unoccupied bins which are surrounded by occupied bins. Regardless of the rules followed to compute the surface coverage the objective is to

adjust the stationary and mobile phase conditions to achieve a fractional surface coverage as close to unity as possible. In any case it is evident that the more orthogonal separation in the right panel of Figure 2.14 does a better job of achieving high coverage than does the highly correlated separation in the left panel of Figure 2.14.

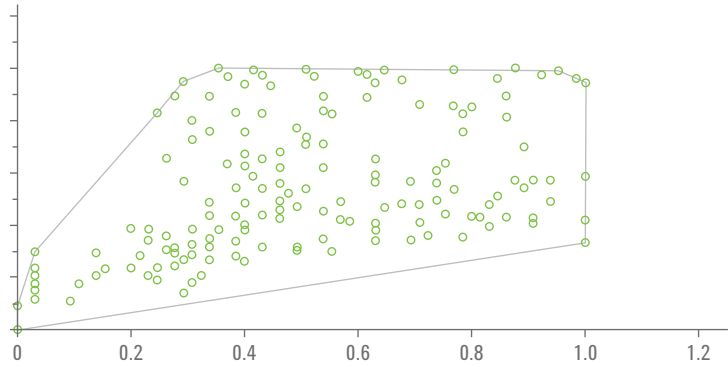


Figure 2.17 An illustration of the Davis minimum alpha hull method of determining a fractional coverage metric. Adapted from Reference 33.

A number of fundamentally different approaches have been taken to designing a metric which measures *orthogonality* or *fractional surface coverage*. It goes well beyond the scope of the present work³¹⁻³⁴ to review and explain these methods. No consensus has been reached as to the best approach or even what constitutes the characteristics of an optimum approach. It could well be that different approaches should be used depending on the characteristics of the sample set. For example, a sample set with a lot of structure (clusters) such as those shown in panels B and C of Figure 2.15 might best be characterized by one method and those lacking structure (see panel D in Figure 2.15) might be best characterized by a different method. Regardless of how the coverage metric is computed we want to choose the '1D and 2D separation conditions so that as much of the separation space as possible is occupied by the range in properties encompassed by the sample.

2.4.2

The undersampling or remixing problem

Proviso D in Section 2.4 “Fundamentals of peak capacity in LCxLC” requires that during the process of doing the ²D separation any separation achieved in the first dimension must not be undone even partially or the product rule will be violated. For a moment return to Figure 1.1 and Figure 1.2 in Chapter 1 “Introduction to Two-Dimensional Liquid Chromatography”. In order to do online or offline 2D-LC the ¹D eluent must be captured and stored temporarily until the desired volume of sample is collected. The problem is that unless the volume of sample collected is a very small fraction of the peak volume it is inevitable that some remixing must take place. Murphy, Schure and Foley were the first to address this problem in a quantitative fashion³⁵. Their basic idea is shown in Figure 2.18 where we imagine that we collect a volume equivalent to about the 4σ width of a peak. Depending on when the sample is taken relative to the center of a peak (this is called the sampling phase) it is quite possible that some degree of remixing will take place.

The Murphy-Schure-Foley guideline states that “In comprehensive 2D-LC, three to four samples in the second dimension must be taken across the 8σ width of the ¹D peak to minimize remixing effects in the sampling loop and loss in total peak capacity.”

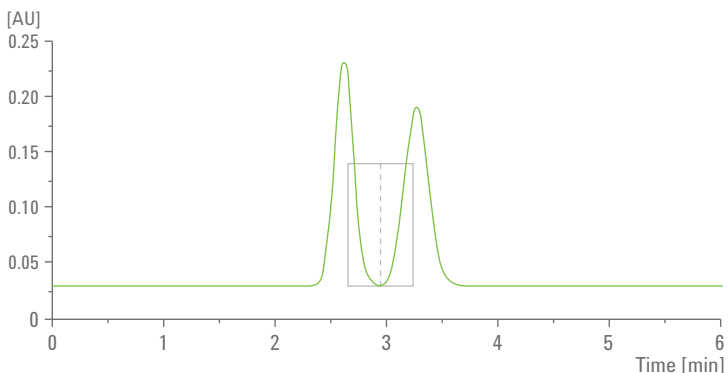


Figure 2.18 The origin of the undersampling (remixing) problem³⁵. If these ¹D peaks are sampled such that the end of the first sample is at 3 minutes and the second sample starts at 2.9 minutes, all of the separation of these two peaks by the ¹D column is preserved. However, if the sampling window is expanded such that a single sample is collected from 2.6 to 3.2 minutes, much of the resolution achieved by the ¹D separation is lost by remixing of the peaks.

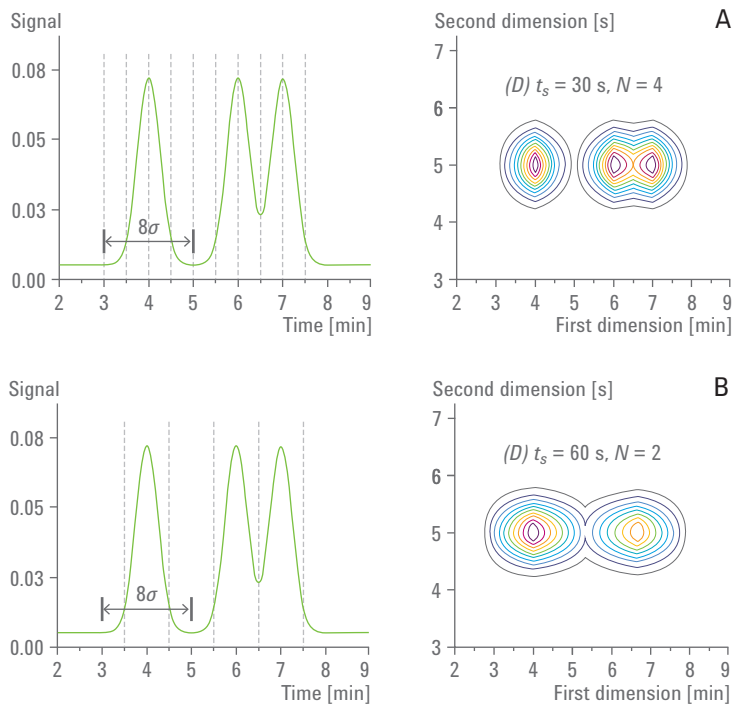
That undersampling actually results in the loss of information and peak capacity is shown convincingly in the three panels of Figure 2.19. Examination of the contour plots which result from decreasing the sampling rate from four per 8σ down to one per 8σ shows that initially

we see three distinct peak maxima (panel A), then two (panel B), and finally only one (panel C). Clearly we are losing peak capacity and the product rule no longer gives a useful estimate of the resolving power. It is important to understand that what we are losing is peak capacity from the first dimension and that the extent of this loss is related to how exactly the sampling process is done.

While the examples shown here in Figure 2.19 use the 2D contour plot to show the loss of peak capacity one can see the same effect of sampling rate in a simple 1D chromatogram (see Figure 2.20).

Remember, in the very beginning of this exposition 2D-LC was explained as adding a chemically selective detector to a normal 1D-LC system.

In panel A of Figure 2.20 a set of 100 peaks with random spacing and heights is sampled at very high speed ($N = 40/8\sigma$) and we see 51 resolved maxima, but as the sampling rate is decreased by adding up all the signal that is acquired in the sampling interval it is evident that many peak maxima that were visible at the faster sampling rate are lost. Even at the Murphy recommended minimum rate of $N = 4 \text{ samples}/8\sigma$ (panel B in Figure 2.20) we see a far from negligible loss in the number of peak maxima.



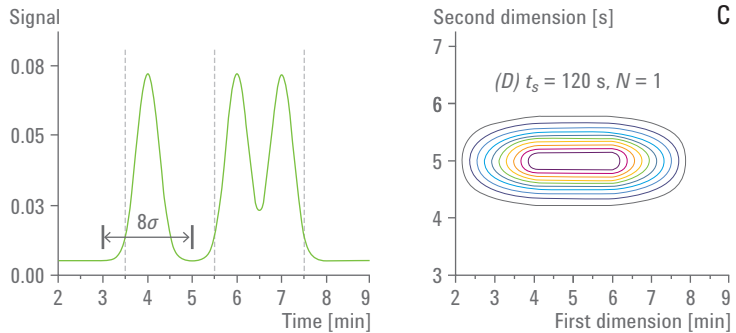


Figure 2.19 Illustration of the effect of sampling rate on the number of peaks that will be observed in LCxLC³⁰.

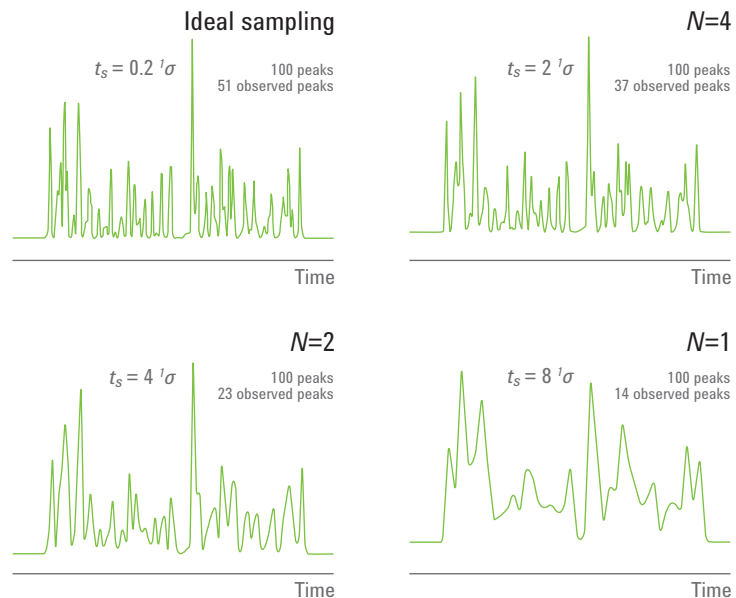


Figure 2.20 Effect of sampling rate in one-dimensional chromatography. Panel A corresponds to very fast (ideal) sampling at a rate of $N = 40$. In this case with randomly spaced peaks 51 maxima are observed although there are 100 components. Panel B corresponds to sampling at the Murphy-Schure-Foley recommended speed of $N = 4$. We already see a loss in peak maxima due to undersampling. Panels C and D correspond to quite bad undersampling at $N = 2$ and $N = 1$ respectively with a catastrophic loss in maxima and thus resolving power. Figure courtesy of Prof. Joe Davis.

While the Murphy-Schure-Foley guideline is helpful it is clearly only semiquantitative. Subsequently Davis, Stoll and Carr³⁶ developed a *quantitative undersampling factor* that allows $n_{c,2D}$ to be corrected. The Davis-Stoll-Carr work enabled random placement of component

retention times over the 2D space and thus incorporated the effect of random sampling phase. Further, the method allowed the various components to have random heights. By means of an *in silico* stochastic experiment they developed an equation for the average peak broadening factor ($\langle\beta\rangle$) as given by Equation 2.15.

$$\langle\beta\rangle = \sqrt{1 + 3.35(t_s / {}^1W)^2}$$

Equation 2.15 Calculating the average peak broadening factor.

In Equation 2.15, t_s is the sampling time and 1W is the 4σ average 1D peak width. $\langle\beta\rangle$ is to be used as a correction factor on the product rule (Equation 2.14). Thus combining Equation 2.2 and Equation 2.15 gives Equation 2.16.

$$n_{c,2D}^* = \frac{{}^1n_c \times {}^2n_c}{\langle\beta\rangle} = \frac{{}^1n_c \times {}^2n_c}{\sqrt{1 + 3.35(t_s \times {}^1n_c / {}^1t_g)^2}}$$

Equation 2.16 Combining estimation of peak capacity with peak broadening factor.

In Equation 2.16, $n_{c,2D}^*$ is the *corrected* 2D peak capacity. The form on the right is obtained by using Equation 2.2 to estimate the value of 1W . When sampling is conducted at the Murphy-Schure-Foley rate of four samples per 8σ then $t_s = 2\sigma$. Equation 2.15 tells us that at this sampling rate the corrected peak capacity will be about 36 percent less than given by the product rule. Clearly one must sample each peak quite a few times to minimize the adverse remixing effect of undersampling. Let us consider the consequences of the Murphy-Schure-Foley guideline. Suppose we do a 30-minute 1D separation having a reasonable peak capacity of 100. Based on Equation 2.2 we estimate the average 1W ($= 4 {}^1\sigma$) at about 0.3 minutes (18 seconds). This means that each sample should be taken every 18/2 or 9 seconds. No *practical* 2D-LC has as yet been done so fast although speeds of 6 seconds per 2D separation have been attained in experiments in support of theoretical studies. Thus we see that the Murphy-Schure-Foley guideline is a very stringent, nearly impossible to satisfy guideline even though it costs us about 36 percent of our peak capacity even when it is obeyed.

Although we are foreshadowing a later more detailed discussion we point out that in *online LCxLC* (with a single 2D column) *the 2D analysis time must be equal to the first-dimension sampling time*. This means that when

gradient elution is done the sum of the gradient time and the system re-equilibration time must be equal to t_s . Keeping in mind the fact that the peak capacity productivity of gradient elution rapidly diminishes as the gradient time decreases (see Equation 2.10 and Figure 2.9) the Murphy-Schure-Foley guideline greatly limits the peak capacity of online LCxLC. The Murphy-Schure-Foley guideline does not impose any time limits on the second dimension of offline LCxLC as the samples are stored before the 2D analyses are carried out. However, it does require that many samples be collected and then analyzed at a later time. In the above case of a 30-minute separation having a peak capacity of 100 we would have to collect and analyze 200 samples. This is far more than is typically done in any offline work. Further if we assume that each 2D separation was done in as little as one minute the entire 2D separation would take more than three hours.

2.4.3

Consequences of the undersampling problem

Based on the above discussion it is evident that almost all LCxLC both online and offline is done under conditions where the first dimension is seriously undersampled. This means that the second term in Equation 2.15 is the dominant term in the majority of practical work. Under these conditions Equation 2.16 can be approximated as given in Equation 2.17.

$$n_{c,2D}^* \approx \frac{^2n_c \times ^1t_g}{1.83 \times t_s}$$

Equation 2.17 Approximation of corrected 2D peak capacity.

Here we used Equation 2.2 to estimate the value of $'W$. This leads to the unexpected but very important result (see Equation 2.17) that *the first-dimension peak capacity has no influence on the corrected 2D peak capacity ($n_{c,2D}^*$)*. This result is clearly shown in Figure 2.21 where $n_{c,2D}^*$ is plotted against $'n_c$ according to Equation 2.16. At very low values of $'n_c$ where the first-dimension peaks are wide it is easy to sample them sufficiently but as $'n_c$ increases undersampling becomes more extreme until the limiting form in Equation 2.17 applies. Equation 2.16, Equation 2.17, and Figure 2.21 tell us that the corrected 2D peak capacity rapidly approaches a limit as $'n_c$ increases, and secondly the limiting corrected peak capacity increases linearly with the first-dimension gradient time. Using values of the sampling time, second-dimension cycle time (2t_c) and second-dimension peak capacity (2n_c) that are experimentally accessible we estimate that corrected peak capacities of 1400 are achievable in an analysis time of 50 minutes. This is well in excess of what can be done in fully optimized 1D-LC.

Clearly the undersampling problem imposes a very severe limit on the peak capacity that can be generated in a given time in LCxLC and especially so in online work. To a certain extent this limitation also means that there really is no point in heroic efforts to achieve the highest possible ${}^1\text{D}$ peak capacities, since above a certain ${}^1\text{D}$ peak capacity it does not increase the corrected 2D peak capacity.

It is important to note that we have not yet taken the fractional coverage into account in these calculations. We will do so in Section 2.4.4 “Maximizing the corrected 2D peak capacity” but before we do so we now need to consider another very important concept – namely the existence of an optimum sampling time which maximizes the corrected 2D peak capacity.

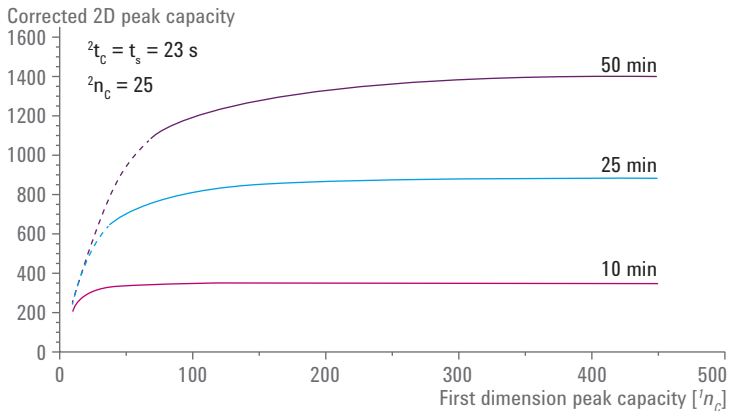


Figure 2.21 Plot of corrected peak capacity versus first-dimension peak capacity calculated using Equation 2.16 with values and conditions given in the graph. Each curve corresponds to a ${}^1\text{D}$ gradient time.

A major practical implication of this calculation is that increasing the ${}^1\text{D}$ peak capacity above about 100 just does not give a significant increase in the corrected peak capacity unless the ${}^1\text{D}$ gradient times are greater than 30 minutes.

2.4.4 Maximizing the corrected 2D peak capacity

In our discussion of gradient elution peak capacity in Section 2.3.3 “Peak capacity of gradient elution” it became evident that peak capacity as a function of gradient time first increases almost linearly but then decelerates and slowly approaches a constant (see Equation 2.12 and Equation 2.13). Both the ${}^1\text{D}$ and ${}^2\text{D}$ peak capacities exhibit the same

general time dependence. In online LCxLC we have stated that the 2D gradient cycle time (2t_c) must be equal to the 1D sampling time, which is in turn the sum of the 2D gradient time and 2D instrument and gradient re-equilibration time as given by Equation 2.18.

$$t_s = ^2t_c = ^2t_g + ^2t_{re-eq}$$

Equation 2.18 Calculating the sampling time.

When we combine these ideas with the fact that the corrected 2D peak capacity of LCxLC diminishes as t_s increases we see that in *online* LCxLC there is an optimum in $n_{c,2D}^*$ as a function of the sampling time as shown in Figure 2.22.

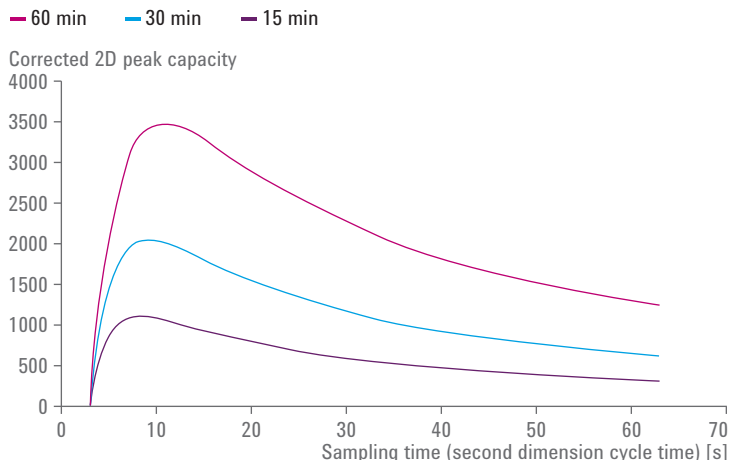


Figure 2.22 Effect of sampling time on the corrected peak capacity of online LCxLC. The 1D gradient times are shown on the legend. The corresponding 1D peak capacities are 227 (60 minutes), 190 (30 minutes) and 143 (15 minutes)¹. The 2D re-equilibration time was 3 seconds. The 2D peak capacity was taken as: $n_c = 44 \cdot ^2t_g / (6.3s + ^2t_g)$.

The optimum 2D cycle times range from about 8 to 12 seconds and increase as the 1D gradient time increases.

We see that the optimum sampling time increases from about 8 to 12 seconds as the 1D gradient time is increased. The most important point to be learned from Figure 2.22 is that there is a very strong dependence of the corrected 2D peak capacity on the sampling time due to the combined

impact of the undersampling factor and the effect of ²D gradient time on the ²D peak capacity. In several papers it was recommended that you should deliberately perform the first dimension poorly (for example, by using larger particles or suboptimal flow rates) so that the ¹D peaks are intentionally broadened and thus severe demands are not placed on the second dimension. Consensus has still not yet been reached on whether this improves peak quantification *in practice*.

However, several theoretical studies have shown that the best accuracy and precision are obtained by getting at least three samples each containing a reasonable fraction of the total peak out of each first-dimension peak.

The practical consequences of such high speed separations are addressed in Chapter 3 “Practical Implementation of 2D-LC” on the instrumentation needed to do LCxLC.

2.4.5

The effective peak capacity

Given that 2D-LC requires more complex instrumentation than 1D-LC and is more difficult to optimize 2D-LC should only be used when it offers a clear advantage in terms of analytical power. You could simplistically just compare the ideal peak capacity of 1D and 2D methods. However, in order to *fairly* compare 1D and 2D chromatography in terms of peak capacity we proposed³¹ that you should correct the ideal 2D peak capacity for both the undersampling problem and the fraction of the separation space covered by the sample. This is done by multiplying the corrected peak capacity ($n_{c,2D}^*$ in Equation 2.16) by a fractional coverage metric ($f_{cov} \leq 1$) to give Equation 2.19.

$$n'_{c,2D} = \frac{{}^1n_c \times {}^2n_c \times f_{cov}}{<\beta>}$$

Equation 2.19 Calculating the effective 2D peak capacity.

This new type of peak capacity is called the *effective 2D peak capacity* and is given the symbol $n'_{c,2D}$. Many groups have employed Equation 2.15 to estimate the undersampling factor but there does not seem to be any emerging consensus on a fractional coverage metric since each has its own merits and limitations^{33, 34}. We will return to this comparison later. For present purposes Stoll's³¹ modification of Gilar's method³² will be used both of which seem to capture the sense of a real coverage metric in contrast to an orthogonality metric.

2.5

Comparison of 1D gradient elution and online LCxLC

2.5.1

Peak capacity and number of peaks detected

Huang *et al.*¹⁹ implemented a detailed comparison of 1D and online LCxLC using Equation 2.19. They measured the ¹D and ²D peak capacities as well as the fractional coverage as a function of both the ¹D and ²D gradient times using a multicomponent extract of maize seed. The results are shown in Figure 2.23. There is clearly an optimum value of the ²D cycle time between 12 and 21 seconds. A somewhat different perspective is shown in Figure 2.24 where we plot the effective 2D peak capacity against the ¹D or 1D gradient time at four values of the ²D cycle time. The main thrust of this figure is that the effective 2D peak capacity overtakes the 1D peak capacity in a time of less than 10 minutes and if we use an optimized ¹D sampling time, effective peak capacities far in excess of those produced by 1D gradient elution chromatography can be obtained in only 10 minutes. Clearly the resolving power of online LCxLC can become much better than highly optimized 1D chromatography at rather short analysis times. A seeming discrepancy between the optimum ²D cycle time shown in Figure 2.22 and that in Figure 2.23 needs some explanation. First, the chromatographic conditions are not quite the same. Second, and more importantly, Huang *et al.* saw that the f_{cov} correction factor decreased significantly at short ²D cycle times, thereby pushing the optimum in the plot of the effective peak capacity to longer times.

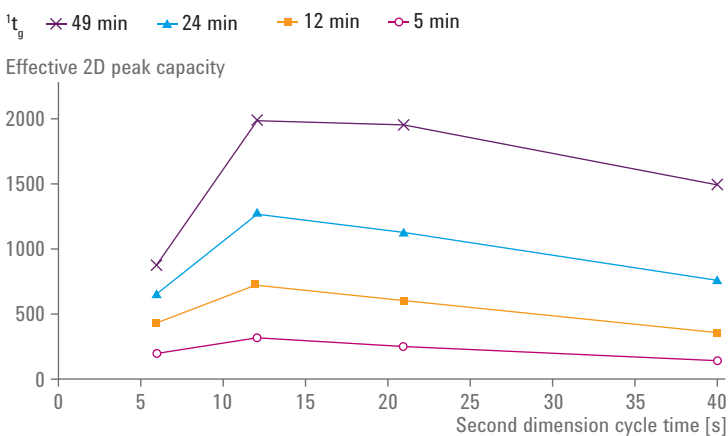


Figure 2.23 Effective peak capacity of online LCxLC obtained with maize seed extract as a function of ²D cycle time (= ¹D sampling time) and ¹D gradient time. Adapted from Reference 19.

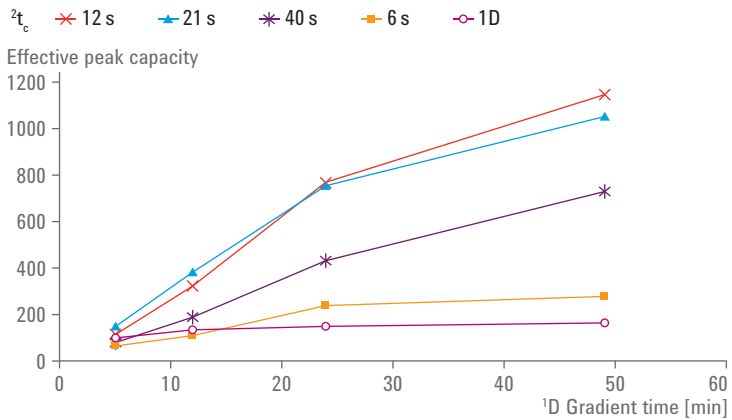


Figure 2.24 Effective 2D peak capacity vs. 1D gradient time of the first dimension of LCxLC and of 1D gradient elution. The open circles are the effective peak capacity for the 1D separations. The closed symbols are for online LCxLC. The 2D cycle times are given in the legend. The 2D re-equilibration time was 3 seconds. Note that all 2D results are better than the 1D results at times less than 5 minutes except the data collected at a 6 second 2D cycle time. Adapted from Reference 19.

2.5.2 Analyte dilution and detection sensitivity

Another factor that should be considered when comparing 1D and 2D-LC separations is the detection sensitivity at the outlet of the column in a 1D separation compared to the outlet of the 2D column in a 2D-LC separation. Under typical conditions in most types of chromatographic separation, the analyte elutes from the column at a lower concentration (that is, more dilute) compared to its concentration at the point of injection. This means that unless steps are taken to counteract this dilution process, the analyte will be even less concentrated when it elutes from the 2D column in a 2D-LC system compared to its concentration at the point of elution from the 1D column, which obviously affects detectability and quantification, especially when low abundance species are targeted. For a more quantitative treatment of this effect, we refer you to the studies of Schure²⁵, and Schoenmakers and coworkers²⁶. In practice this problem can be mitigated through careful choice of the volume of 1D effluent injected into the 2D column, and the 2D flow rate. Generally larger injection volumes help minimize differences in detection sensitivity, however you have to be careful not to inject so much that 2D peak shape suffers – we discuss this issue in more detail in Chapter 3 “Practical Implementation of 2D-LC”. Likewise, lower 2D flow rates minimize analyte dilution, but this also affects 2D separation speed, so ultimately a compromise must be made. If highest detection sensitivity is required the use of long UV-cells or high-sensitivity mass-selective detection might be considered as well.

2.6 Summary

By far the two most important messages that should be taken from this chapter are:

- As a 2D-LC user you must make the corrections recommended here (that is, the undersampling correction based on $\langle\beta\rangle$ and some form of correction for f_{cov}) by use of Equation 2.16. If not, you will vastly overestimate the peak capacity of 2D-LC and fall into the trap of using 2D-LC when a 1D-LC gradient separation, which is easier to implement and optimize, should be used. The devil is indeed in the details.
- Even after making both of these corrections the effective peak capacity of 2D-LC does exceed that of fully optimized 1D-LC in only a few minutes of analysis time provided that you use the optimized 2 D cycle time.

Successful development of LCxLC methods involves consideration of several tradeoffs and compromises that are not encountered in conventional 1D-LC method development. In this chapter we discuss the practical aspects of setting up a LCxLC method. These include:

- Required components of a LCxLC and their typical characteristics
- Effects of pump gradient delay volume on LCxLC performance
- Considerations related to the choice of first and second dimension conditions (column size, type, particle size, and so on)
- Considerations related to detection

3.1

Setting up a LCxLC system

Along with the potential for increased resolving power in 2D-LC comes increased complexity, both in terms of instrument design and in method development, as the numbers of decisions required to set up a 2D-LC method is more than two times the number of decisions needed for a conventional 1D-LC method. In this chapter we discuss important practical considerations related to each component of the 2D-LC system, and attempt to articulate best practices for setting up 2D-LC methods.

3.1.1

The general issue of the effect of gradient delay volume on re-equilibration time

Since many applications of LCxLC require gradient elution conditions in one or both dimensions of the separation, we first review the important practical issues related to this elution mode. As long as the available equipment on the market or existing older equipment already available in your laboratory remains quite variable in terms of performance characteristics it will be very important for you to understand the influence that the characteristics of *the pumping systems* have on LCxLC methods.

The ability of a given pumping system to accurately and precisely deliver a specified solvent gradient to the HPLC column inlet affects the performance of a LCxLC method, mostly in terms of the repeatability of retention times in both separation dimensions. This is an important factor in situations where large numbers of samples are analyzed as part of a large dataset, as peaks must be in the *same* locations in each chromatogram throughout the experiment. An even more significant factor, however, is the gradient delay volume(s) associated with the pumping systems used in the two dimensions of the 2D-LC system.

Figure 3.1 shows the basic components of a liquid chromatograph that is capable of gradient elution. It is critical to understand that the volume of the components between the solvent mixing point and the column inlet is finite, and results in a time (and volume) delay between the start of the programmed solvent change, and the actual arrival of that composition change as observed at the column inlet. Historically this volume has been much larger than would be expected based on a simple calculation of the volume of the pieces connecting the mixer to the injector and column, which means that most of the volume is attributed to the mixing element itself.

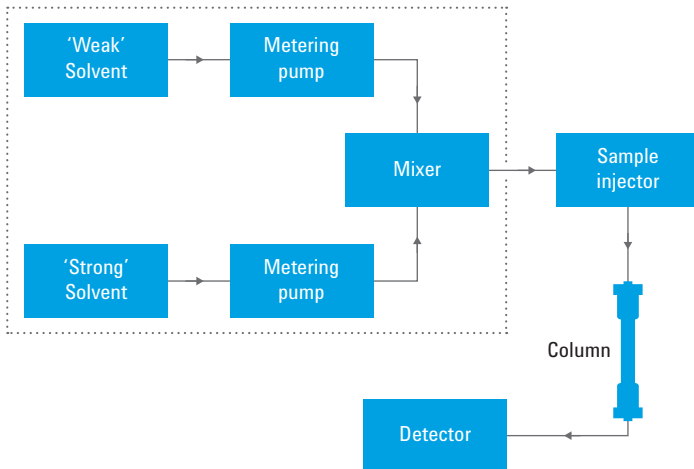


Figure 3.1 Diagram showing the essential elements of a HPLC system, with an emphasis on the flow path of the eluent and its components before and after the mixing point.

When two solvents with relatively similar viscosities are used (for example, acetonitrile and water) as is the case in RPLC, little volume is required to actually mix the fluid. Instead, the large mixing volume has historically been required to effectively smooth out temporary variations in the composition of the mixed mobile phase that resulted from imperfections in the delivery of the individual solvent components over time. Particularly in the case of legacy HPLC pumps, turbulences in the flows of the individual solvents are observed at the end of the piston stroke in reciprocating style pump designs. Figure 3.2 shows a

comparison of the performance of two pumping systems with significantly different gradient delay volumes and times in terms of the number of gradients that can be executed in a given time. The red trace shows the change in solvent composition as it would be programmed into the instrument control software, and the dashed blue line shows the actual solvent composition observed at the column inlet as a function of time. The offset of the blue dashed line from the red line at the start of a gradient is what we refer to as the *gradient delay time* (t_d). This delay time is a function of the gradient delay volume (V_d), which is a characteristic of a particular pumping system, and the flow rate (F), see Equation 3.1.

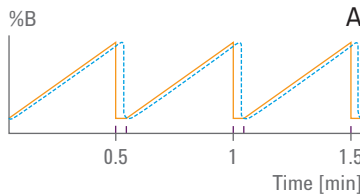
$$t_d = \frac{V_d}{F}$$

Equation 3.1 Relationship of delay time to gradient delay volume and flow rate.

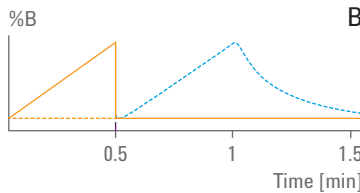
The fact that the onset of the solvent change at the column inlet is delayed is not so detrimental by itself, because this delay can be anticipated. The bigger impediment to producing a large number of solvent gradients in a short time is the fact that the time required to flush the strong solvent (the organic component in RPLC) from the pumping system at the end of a gradient is much greater than t_d . We refer to this time as the flush-out time (t_{flush}), and typically assume it is simply $2 \times t_d$. The precise multiplier depends on the construction of the eluent mixer which is the chief cause of the delay. Figure 3.2 shows the impact of this flush-out time on gradient throughput using conditions typically encountered in the second dimension of a LCxLC system, and V_d values representing both a rather low (50 µL) and a high (1000 µL) volume gradient mixing system. In a high delay volume system we see that when rapid solvent gradients are used, most of the analysis time is spent waiting for the strong solvent to flush out of the system in preparation for execution of the next solvent gradient.

We will discuss this issue in more detail in Section 3.1.4 “Considerations for the configuration of the second dimension”, but it is convenient to note here that this factor essentially prohibits the use of pumps with high gradient delay volumes much larger than 100 µL in the second dimension of fast online LCxLC systems.

On the other hand, a system with a much smaller V_D on the order of tens of microliters yields t_D values around a few seconds at flow rates in the range of 1 to 3 mL/min. Equation 3.1 clearly tells us that high flow rates in the second dimension separation are quite beneficial and perhaps even mandatory. This means that even when rapid solvent gradients are used, a large fraction of the analysis (cycle) time is spent on the gradient elution profile itself, and the time flushing the strong solvent from the system is minimized, as shown in Figure 3.2. This factor can also be quite important in the first dimension of a LCxLC system as well, albeit for different reasons. We will discuss this too in more detail in Section 3.1.6 “Considerations for the configuration of the first dimension”.



$$\begin{array}{ll} t_g = 30 \text{ s} & t_D = 1.5 \text{ s} \\ V_D = 50 \mu\text{L} & t_{flush} = 3.0 \text{ s} \\ F = 2 \text{ mL/min} & \end{array}$$



$$\begin{array}{ll} V_D = 1000 \mu\text{L} & t_D = 30 \text{ s} \\ F = 2 \text{ mL/min} & t_{flush} = 60 \text{ s} \end{array}$$

Figure 3.2 Comparison of the performance of two different pumping systems in terms of the number of gradients that can be carried out in 2 min. System A has a gradient delay volume of 50 μL , whereas system B has a much larger volume of 1000 μL ; the flow rate is assumed to be 2 mL/min.

3.1.2 Generic LC_xLC system diagram

It is convenient here to introduce a generic LC_xLC system diagram, indicating all of the major components that will be discussed in turn in the following sections. Figure 3.3 shows the components involved in a conventional LC_xLC system.

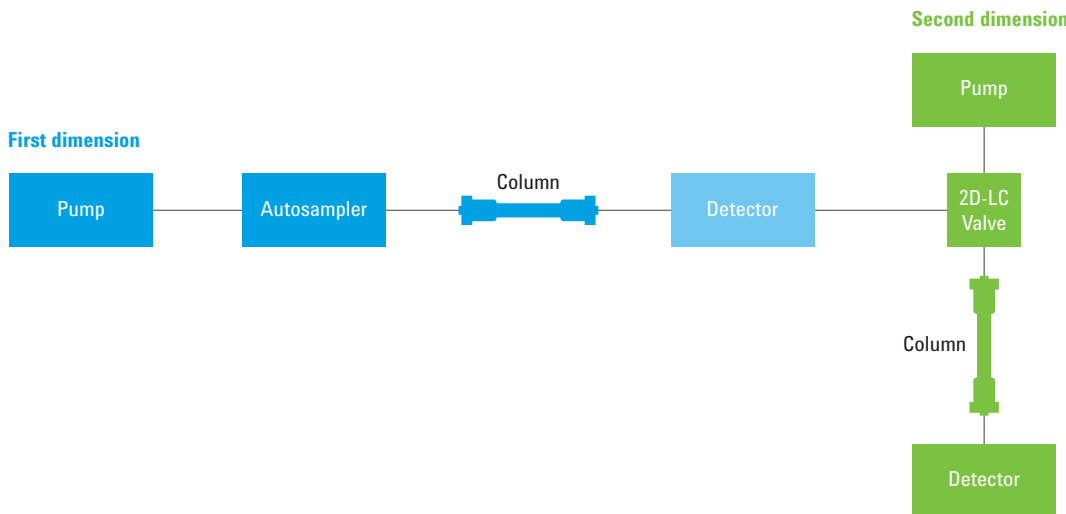


Figure 3.3 Block diagram showing the main components of a system for online LC_xLC.

3.1.3 Example of method development process for LC_xLC

As with all chromatographic methods, the process of developing LC_xLC methods is primarily a matter of managing the compromises that must be made when the two chromatographic dimensions are coupled together. Although guidelines for method development in LC_xLC are not nearly as advanced they are in 1D-LC, at least preliminary guidance can be found in the literature^{37,38}. Table 3.1 illustrates the sequence of decisions that must be made to set up a LC_xLC method – here the separation of 14 taxanes (see core structure in Figure 3.4) is used for this case study, because the separation problem is well defined and the chemistry of the solutes is well understood.

Step	Compromise made	Conditions
Choose ² D separation conditions	² D speed versus efficiency	² D column: 4.6 x 50 mm (1.8 μ m) Agilent ZORBAX Plus Phenyl-Hexyl ² F: 4.0 mL/min 20 to 33 % ACN gradients from 0 to 20 s
Choose interface loop volume and sampling time	Detection sensitivity versus undersampling effects	Loop volume: 40 μ L 2t cycle: 30 s
Choose ¹ D separation conditions	Separation speed versus ¹ D peak volume	¹ D column: 2.1 x 150 mm (3.5 μ m) Agilent ZORBAX Eclipse Plus C18 ² F: 0.060 mL/min 30 to 100 % MeOH gradients from 0 to 37 min

Table 3.1 Decision table for LCxLC method development.

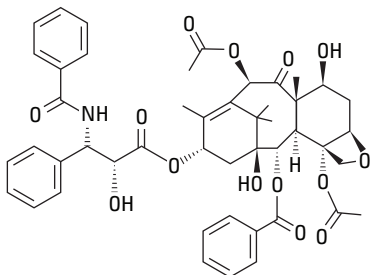


Figure 3.4 Structure of taxol – the compounds shown separated in Figure 3.5 are all structurally similar compounds.

In Table 3.1 we state the conditions used for each component of the system, and briefly comment on the compromise that is made at each step. In subsequent sections we will explain in more detail the basis for these tradeoffs, and the compromises that are made in each case. There is by no means one set of *right* conditions for a given method, nor is there an algorithmic approach for developing these conditions, and there certainly will be applications where it makes sense to have major departures from the kind of setup discussed here. However, what is discussed here amounts to a set of *best practices* to follow generally in method development. The resulting LCxLC separation of this mixture is shown in Figure 3.5.

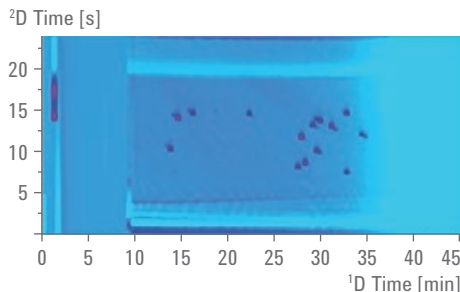


Figure 3.5 LCxLC separation of 14 taxane standards (10 µg/mL each) using UV detection at 228 nm and the conditions described in Table 3.1.

3.1.4 Considerations for the configuration of the second dimension

3.1.4.1 Column considerations

As we discussed in Section 2.4 “Fundamentals of peak capacity in LCxLC”, both the raw speed and the productivity of the ²D separation in LCxLC have a large impact on the overall performance of the LCxLC system. Because of the importance of this component of the system, we recommend starting the method development process by choosing the dimensions of the ²D column and the corresponding operating conditions. Since the ²D separations generally must be fast (and especially so for online LCxLC), the ²D column will typically be short (< 5 cm) and narrow (2.1 mm id – for various technical reasons we do not recommend 1-mm or narrower columns; see below).

Table 3.2 and Table 3.3 show the maximum achievable flow rates through such columns as a function of column length and diameter, for 2.7 mm core-shell particles at 40 °C and maximum pressure drops of 500 or 1000 bar. In this discussion we have chosen 500 and 1000 bar pressure limits to represent conditions that allow some head room for small pressure increases when working with pumps with either 600 or 1200 bar pressure limits. Along with the maximum flow rate, the corresponding column dead times (t_o) are indicated in parentheses. These two pieces of information are the most important for making a decision about the physical dimensions of the column – the column dead time ultimately controls the raw speed of the ²D separation given a particular t_g/t_o value in gradient work or the desired k range in isocratic work. The practicality of the possible combinations of column length and diameter under these conditions is indicated by color code. The major considerations here are:

- The flow rate must not be so high that an inordinate amount of solvent is consumed – here we have chosen 3 mL/min as a desirable upper limit
- The flow rate must not be so low that the gradient flush-out time (t_{flush}) is long in comparison to the gradient time itself (see section 3.1.1) – here we chosen 1 mL/min. as a desirable lower limit, as this corresponds to a t_{flush} of 6 seconds for a system with a V_D of only 50 μL .

In Table 3.2 and Table 3.3 impractical options are highlighted in red, optimal conditions are highlighted in green, and marginal conditions are highlighted in yellow. Whereas Table 3.2 and Table 3.3 assume a fixed particle size of 2.7 μm , it is also instructive to consider the same kind of analysis, but with the column diameter fixed at 2.1 mm and look at different combinations of column length and particle size. This is shown in Table 3.4 and Table 3.5 for column lengths of 3, 5, and 7.5 cm and particle sizes of 1.8, 2.7, and 3.5 μm . From these tables we draw the following practically important conclusions.

- Even with very low V_D values, 1.0 mm id columns are not useful for fast ²D separations because the achievable flow rates are too low to obtain acceptable t_{flush} values. This limitation can be ameliorated somewhat by working at higher temperature and pressures, but even then the use of small particles in 1.0 mm id columns is prohibitive.
- It is clear that 2.1 mm id columns will be optimal for most situations; reasonable flow rates are accessible both for longer columns with larger particles, and shorter columns with smaller particles.
- The use of small particles (that is, less than 2.7 μm) is highly recommended but requires the use of UHPLC pumps or temperatures above 40 °C, columns shorter than 3 cm, or some combination of these approaches.

Flow rate [mL/min]		Column id [mm]			
		1.0	2.1	3.0	4.6
L [cm]	3.0	0.63 (1.1)	2.8 (1.1)	5.7 (1.1)	13 (1.1)
	5.0	0.38 (3.2)	1.7 (3.2)	3.4 (3.2)	8.0 (3.2)
	7.5	0.25 (7.1)	1.1 (7.1)	2.3 (7.1)	5.3 (7.1)

Table 3.2 Maximum achievable flow rates* provided a maximum pressure of 500 bar, column temperature of 40 °C, and 2.7 µm core-shell particles (column dead times are indicated in seconds).

* Other conditions: Mobile phase, 20/80 ACN/water; $\epsilon_o = 0.38$, $\epsilon_i = 0.20$, see list of symbols.
Dimensionless column permeability based on the use of interstitial velocity, 500.

Flow rate [mL/min]		Column id [mm]			
		1.0	2.1	3.0	4.6
L [cm]	3.0	1.3 (0.57)	5.5 (0.57)	11 (0.57)	27 (0.57)
	5.0	0.75 (1.6)	3.3 (1.6)	6.8 (1.6)	16 (1.6)
	7.5	0.50 (3.6)	2.2 (3.6)	4.5 (3.6)	11 (3.6)

Table 3.3 Maximum achievable flow rates* provided a maximum pressure of 1000 bar, column temperature of 40 °C, and 2.7 µm core-shell particles (column dead times are indicated in seconds).

* Other conditions: Mobile phase, 20/80 ACN/water; $\epsilon_o = 0.38$, $\epsilon_i = 0.20$, see list of symbols.
Dimensionless column permeability based on the use of interstitial velocity, 500.

Flow rate [mL/min]		Particle size [µm]		
		1.8	2.7	3.5
L [cm]	3.0	1.2 (2.6)	2.8 (1.1)	4.7 (0.68)
	5.0	0.74 (7.1)	1.7 (3.2)	2.8 (1.9)
	7.5	0.49 (16)	1.1 (7.1)	1.9 (4.2)

Table 3.4 Maximum achievable flow rates* provided a maximum pressure of 500 bar, column temperature of 40 °C, and 2.1 mm column diameter (column dead times are indicated in seconds).

* Other conditions: Mobile phase, 20/80 ACN/water; $\epsilon_o = 0.38$, $\epsilon_i = 0.20$, see list of symbols.
Dimensionless column permeability based on the use of interstitial velocity, 500.

Flow rate [mL/min]		Particle size [μm]		
		1.8	2.7	3.5
L [cm]	3.0	2.5 (1.3)	5.5 (0.57)	9.3 (0.34)
	5.0	1.5 (3.6)	3.3 (1.6)	5.6 (0.94)
	7.5	1.0 (8.0)	2.2 (3.6)	3.7 (2.1)

Table 3.5 Maximum achievable flow rates* provided a maximum pressure of 1000 bar, column temperature of 40 °C, and 2.1 mm column diameter (column dead times are indicated in seconds).

* Other conditions: Mobile phase, 20/80 ACN/water; $\epsilon_e = 0.38$, $\epsilon_i = 0.20$, see list of symbols. Dimensionless column permeability based on the use of interstitial velocity, 500.

The information in Table 3.2, Table 3.3, Table 3.4 and Table 3.5 is very helpful in narrowing the choices of particle size, column diameter, and column length. However this perspective only addresses the issue of the raw speed of the separation, and totally neglects the performance of these columns in terms of efficiency (that is, plate count, N) or peak capacity (n_c), or both. As we discussed in Section 2.3.3 “Peak capacity of gradient elution”, estimation of peak capacities under gradient elution conditions requires some assumptions about the properties of the sample constituents, thus this is difficult to do in a general way. We can move in this direction by first examining the dependence of the plate count (N) on the column parameters discussed above, in addition to the operating conditions including temperature (T) and pressure (P). The relationships between column efficiency (N) and the major operating variables including: particle size (d_p), eluent velocity (u_e , and thus flow rate, F), column length (L), column temperature (T), and pressure drop across the column (P) are well established. If you are interested in the derivations of the following equations and their significance, please refer to Reference 23. Here we present the relevant final expressions for reference, and discuss the implications of these relationships in the context of ²D separations in LCxLC systems.

To effectively use these expressions we begin by asking the following question; what values of particle size, column length, and eluent velocity will provide the optimum performance for my ²D separation in terms of efficiency (N) or peak capacity (n_c)? To make the discussion manageable we first make the reasonable assumption that the column that provides the most plates (N) will also provide the most peak capacity (n_c), and then further assume that we will maintain a value of 10 for the ratio of the gradient time to the column dead time (t_g/t_m). For example, suppose we

want the optimum values of d_p , L , and u_e (F) for a 2D gradient time (t_g) of 30 seconds; this immediately sets the column dead time (t_m) at 3 seconds. Once t_m has been decided, then the optimum values of d_p , L , and u_e (F) for a given operating temperature (T) and pressure (P_{max}) are given by Equation 3.2, Equation 3.3 and Equation 3.4, where Φ is the dimensionless column permeability (typically approximated as 500), η is the eluent viscosity, D_m is the diffusion coefficient of the analyte in the eluent, B and C are van Deemter fitting coefficients, and λ is the ratio of interstitial (ϵ_e) and total column porosities (ϵ_{tot}).

$$d_p = \left[\frac{\Phi \eta^B / C}{P_{max}} \right]^{1/4} (\lambda t_0)^{1/4} D_m^{1/2}$$

Equation 3.2 Calculation of optimum particle size.

$$L = \left[\frac{P_{max}^B / C}{\Phi \eta} \right]^{1/4} (\lambda t_0)^{3/4} D_m^{1/2}$$

Equation 3.3 Calculation of optimum column length.

$$u_e = \left[\frac{P_{max}^B / C}{\Phi \eta \lambda t_0} \right]^{1/4} D_m^{1/2}$$

Equation 3.4 Calculation of optimum eluent interstitial velocity (flow rate).

These relationships are very powerful in this context in that we can calculate the values of d_p , L , and u_e (F), which will give the highest possible plate counts (N) for column dead times that correspond to gradient times of interest in the second dimension, and we can do this for different combinations of operating temperature and pressure. It is important to understand that it is impossible to make this treatment completely general given all of the variability in particle technology currently available for liquid chromatography. Thus, we have chosen parameters that describe a generic particle (see figure captions for details), and point out that variation in the particle type (for example, fully porous versus superficially porous particles) will lead to changes in the absolute values of the values presented in these figures. Nevertheless, we believe that the trends we see in these results are reliable (realistic) and can serve as a guide for method development choices. Figure 3.6, Figure 3.7, and Figure 3.8 show the results of these calculations for gradient times ranging from 5 to 60 seconds,

and temperature/pressure combinations of 25/500, 25/1000, 100/500, and 100/1000 ($^{\circ}\text{C}/\text{bar}$). Figure 3.6 shows that the optimum particle size increases with increasing gradient time, and with increasing temperature. The transparent blue box over the bottom portion of the figure indicates particle sizes that are currently not commercially available, thus these optimum conditions are not accessible experimentally. Similarly Figure 3.7 shows the optimum column lengths and Figure 3.8 shows the optimum flow rates for different column diameters ($T = 60\ ^{\circ}\text{C}$, $\Delta P = 500$ bar, dashed lines, or 1000 bar, solid lines), again with blue boxes indicating experimentally inaccessible (in the case of L) or undesirable (in the case of F) conditions. These figures are helpful to understand the trends in the optimal parameters as a function of gradient time.

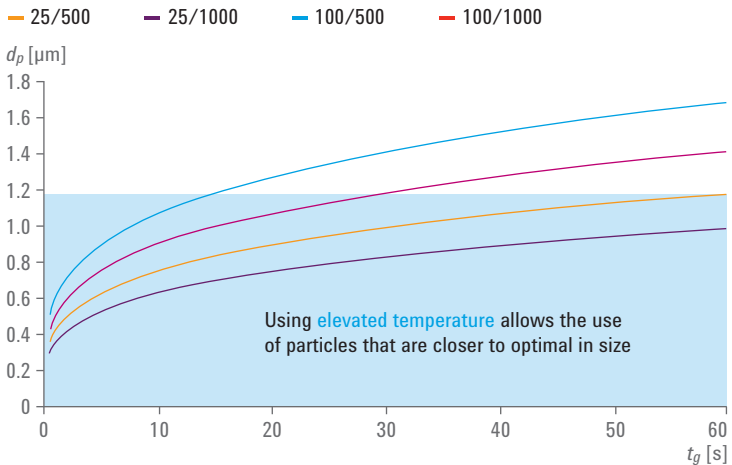


Figure 3.6 Dependence of the optimum particle size on gradient time under different combinations of operating conditions. The blue box indicates conditions that are experimentally inaccessible using current commercially available materials. Assumptions: The ratio t_g/t_0 is fixed at 10; Dimensionless van Deemter parameters are 1.0, 5.0, and 0.05; D_m ($40\ ^{\circ}\text{C}$), $1.0 \times 10^{-5} \text{ cm}^2/\text{s}$; ϵ_e , 0.38; ϵ_r , 0.30.

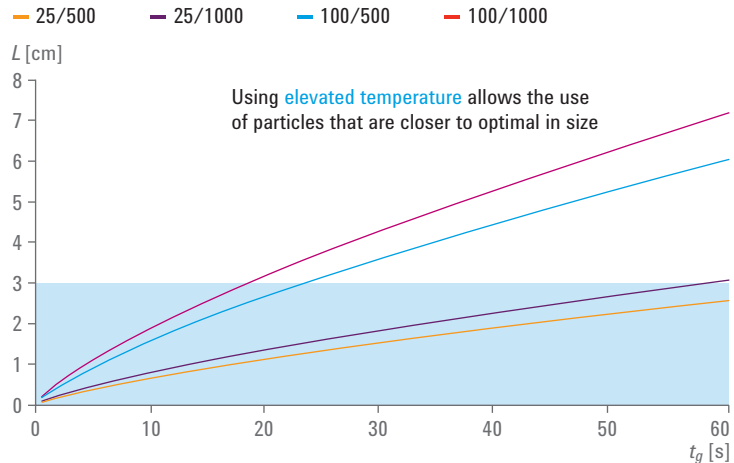


Figure 3.7 Dependence of the optimum column length on gradient time under different combinations of operating conditions. The blue box indicates conditions that are experimentally inaccessible using current commercially available columns. Assumptions: The ratio t_g/t_0 is fixed at 10; Dimensionless van Deemter parameters are 1.0, 5.0, and 0.05; D_m (40 °C), 1.0×10^{-5} cm²/s; ϵ_o , 0.38; ϵ_r , 0.30.

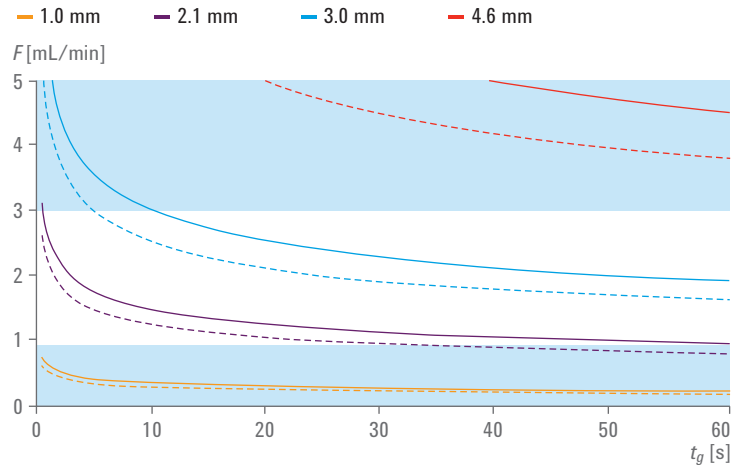


Figure 3.8 Dependence of the optimum flow rate on gradient time for different column inner diameters, assuming a column temperature of 60 °C and a maximum pressures of 500 bar (dashed lines) or 1000 bar (solid lines). The blue box indicates conditions that are undesirable in practice.

Assumptions: The ratio t_g/t_0 is fixed at 10; Dimensionless van Deemter parameters are 1.0, 5.0, and 0.05; D_m (40 °C), 1.0×10^{-5} cm²/s; ϵ_o , 0.38; ϵ_r , 0.30.

A different perspective is required, however, to efficiently appreciate the effects of temperature and pressure on the *optimal combinations of column characteristics*. These combinations of optimal d_p , L , and F are presented in Table 3.6 and Table 3.7 for a gradient times of 15 or 30 seconds and assuming a gradient delay volume of 50 μL and pressure limits of 500 or 1000 bar. A few important observations follow from these results.

- The most striking observation is that the optimal conditions are at the current limits of commercially available systems and columns. This means that no matter how the second dimension is configured, some level of performance sacrifice will be made, and the degree of sacrifice depends heavily on exactly how the column is configured.
- Increasing the column temperature from 25 to 100 °C or increasing the available pressure from 500 to 1000 bar provides a similar performance gain, adding approximately 50 percent to the number of achievable plates under these conditions.
- If both the temperature and pressure can be increased, another 50 percent gain in plates can be realized compared to changing only one of these two variables.
- Working at intermediate pressures and temperatures (for example, the 60/500 option) provides performance gains that are similar to those resulting from an extreme change in either temperature or pressure alone.

	Conditions: temperature [°C] / pressure [bar]				
	25/500	25/1000	100/500	100/1000	60/500
d_p [μm]	0.8	0.7	1.2	1.0	1.0
L [cm]	0.9	1.1	2.1	2.5	1.4
Column id [mm]	3.0	3.0	2.1	2.1	3.0
F [mL/min]	1.5	1.7	1.7	2.0	2.3
t_{flush} [s]	4.0	3.5	3.5	3.0	2.6
N	5500	7800	9000	12700	7100

Table 3.6 Optimal parameters* for a gradient time of 15 seconds, given a pumping system with a gradient delay volume of 50 μL .

* Other conditions: Mobile phase, 40/60 ACN/water; $\epsilon_e = 0.38$; $\epsilon_i = 0.20$; Dimensionless column permeability (based on the use of interstitial velocity), 500.

	Conditions: temperature [°C] / pressure [bar]				
	25/500	25/1000	100/500	100/1000	60/500
d_p [μm]	0.8	0.7	1.2	1.0	1.0
L [cm]	0.9	1.1	2.1	2.5	1.4
Column id [mm]	3.0	3.0	2.1	2.1	3.0
F [mL/min]	1.5	1.7	1.7	2.0	2.3
t_{flush} [s]	4.0	3.5	3.5	3.0	2.6
N	5500	7800	9000	12700	7100

Table 3.7 Optimal parameters* for a gradient time of 30 s, given a pumping system with a gradient delay volume of 50 μL .

* Other conditions: Mobile phase, 40/60 ACN/water; $\epsilon_o = 0.38$; $\epsilon_i = 0.20$; Dimensionless column permeability (based on the use of interstitial velocity), 500.

Since none of the combinations of d_p , L , and F presented in Table 3.6 and Table 3.7 are realizable in practice, in Table 3.8 and Table 3.9 we present a set of optimal compromise combinations of characteristics for each combination of temperature and pressure, and 2D gradient times of 15 or 30 seconds. These characteristics provide the best performance that is achievable with current particle sizes and column lengths, keeping in mind that we are trying to maintain reasonable flow rates and gradient flush-out times in making these choices. The performance differences between different conditions (T/P combinations) are far more dramatic in this case than in the fully optimized case presented in Table 3.6 and Table 3.7. First, the low plate count associated with the 25 °C/500 bar condition is primarily a consequence of the minimum column length of 3 cm. The only way to achieve a short column dead time of 1.5 seconds with a 3-cm long column is to use large particles. However, at the high eluent velocities required to achieve this high speed, peaks are severely broadened due to slow mass transfer in and out of the large particles, and the resulting plate count is very low. A ninefold improvement in plates can be realized by raising the column temperature to 100 °C, whereas a four-fold improvement can be realized by raising the operating pressure to 1000 bar. This improvement resulting from the pressure increase is not as significant as in the fully optimal case, again because of the column length limitation which requires 2.7 μm particles to be used to achieve a column dead time of 1.5 seconds. The results suggest that the most dramatic performance gain can be realized by combining the benefits of increased temperature and pressure, which enables the use of sub-two-micron particles in a 3 cm column. In the event that such high temperature and pressure capabilities are not available, the 60 °C/500 bar option actually

provides highly competitive performance compared to the 25/1000 option. Comparison of Table 3.8 and Table 3.9 shows that slightly more optimal performance can be achieved with gradient times of 30 seconds.

	Conditions: temperature [°C] / pressure [bar]				
	25/500	25/1000	100/500	100/1000	60/500
d_p [μm]	5.0	2.7	2.7	1.8	3.5
L [cm]	3.0	3.0	3.0	3.0	3.0
Column id [mm]	2.1	2.1	2.1	2.1	2.1
F [mL/min]	2.4	2.4	2.4	2.4	2.4
Pressure [bar]	260	900	340	760	320
t_{flush} [s]	2.5	2.5	2.5	2.5	2.5
N	320	1100	2800	5530	1100
Percent loss from Optimal	94	86	69	56	85

Table 3.8 Optimal compromise parameters* for a gradient time of 15 seconds, given a pumping system with a gradient delay volume of 50 μL and a minimum column length of 3 cm.

* Other conditions: Mobile phase, 40/60 ACN/water; $\epsilon_e = 0.38$ $\epsilon_i = 0.20$; Dimensionless column permeability (based on the use of interstitial velocity), 500.

	Conditions: temperature [°C] / pressure [bar]				
	25/500	25/1000	100/500	100/1000	60/500
d_p [μm]	2.7	1.8	1.8	1.8	3.5
L [cm]	3.0	3.0	3.0	5.0	5.0
Column id [mm]	2.1	2.1	2.1	2.1	2.1
F [mL/min]	1.2	1.2	1.2	2.0	2.0
Pressure [bar]	450	1000	380	1050	450
t_{flush} [s]	5.0	5.0	5.0	3.0	3.0
N	1900	3900	7600	10200	2200
Percent loss from Optimal	76	65	40	43	78

Table 3.9 Optimal compromise parameters* for a gradient time of 30 seconds, given a pumping system with a gradient delay volume of 50 μL and a minimum column length of 3 cm.

* Other conditions: Mobile phase, 40/60 ACN/water; $\epsilon_e = 0.38$ $\epsilon_i = 0.20$; Dimensionless column permeability (based on the use of interstitial velocity), 500.

3.1.4.2

Instrument considerations

At several points we have emphasized the importance of achieving a small gradient delay volume in the ^2D solvent delivery system, as V_d has a large impact on the productivity of the ^2D separation, as well as the overall performance of the LCxLC system. Table 3.10 shows the impact of the gradient delay volumes associated with different types of pumps on the fraction of different analysis times available for actual separation. For each type of pump (that is, legacy, and modern) we show the results associated with typical conditions in both the first and second dimensions. These values emphasize the point that gradient delay volumes in excess of 500 μL make very fast gradient work utterly impractical, and delay volumes less than 100 μL are highly desirable, particularly in the second dimension of the LCxLC system.

Pump type	Gradient delay volume (V_d , [μL])	Flow rate [mL]	Gradient delay time (t_d)	Analysis time	Fraction of analysis available for separation
Legacy	1000	0.25	4 min	30 min	74 %
	1000	3.0	20 s	60 s	33 %
Modern	100	0.25	24 s	30 min	97 %
	100	3.0	2 s	30 s	88 %

Table 3.10 Effect of gradient delay volume on the fraction of analysis time available* for separation under typical first and second-dimension conditions.

* Assumes the main detriment is a flush-out time that is $2t_d$.

Aside from the characteristics of the pumping-mixer system, the other major consideration in configuring the second dimension is the impact of sources of extracolumn (that is, system) dispersion on the widths and shapes of ^2D peaks. Assuming that most ^2D separations are carried out in the gradient elution mode such that the effects of *precolumn* broadening sources are minimized, the major potential sources of post-column broadening are the tubing connecting the column to the detector, the detection element volume (for example, the flow cell in a UV or DAD detector, or the spray chamber in a LC-MS system), and the detector response time.

A representative chromatogram obtained in the second dimension of a LCxLC system under fast gradient elution conditions (30 mm by 2.1 mm id column packed with 1.8 μm SB C18 particles operated at 60 $^\circ\text{C}$ and 2 mL/min) is shown in panel A of Figure 3.9. Under these conditions the volumes of the narrow peaks (calculated at the 4σ peak width) are about 10 μL , and the corresponding peak variances in volume units are also

very small. This means that the variances associated with broadening of these peaks in postcolumn connecting tubing and the detector flow cell must also be very small to avoid a significant increase in the observed peak width. Table 3.11 shows the volumes of connection tubing for different combinations of length and diameter that would reasonably be used to connect the ²D column to a detector. The use of 0.003-inch (75-mm) id tubing is attractive because of the low volume and corresponding low contribution to total peak variance. However, its use in the second dimension is quite restricted because the pressure to push the effluent through the tubing scales with the fourth power (not the square) of the flow rate. As for the effect of flow cell volume, Figure 3.9 shows a comparison of ²D peak width and shape in chromatograms obtained with the *standard* Agilent 1290 Infinity DAD flow cell, and the ultralow delay volume version with $V_\sigma = 600 \text{ nL}$. Here we see that there is a significant effect of the reduced flow cell volume on both the width (narrower) and the shape (more symmetrical) of these narrow peaks, whereas larger tubing volumes have a large effect on the peak width than the peak shape.

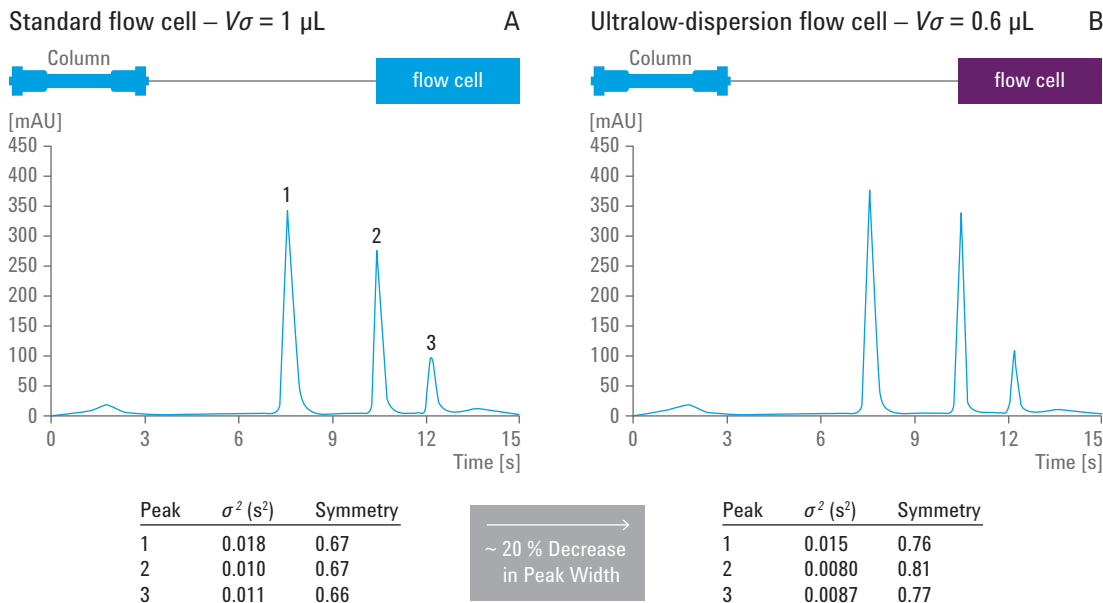


Figure 3.9 Comparison of ²D chromatograms obtained under fast gradient elution conditions, with two different DAD flow cells installed. Chromatographic conditions: Column, 2.1 x 30 mm, SB C18, 1.8 micron; Temperature, 60 °C; Gradient elution from 2 to 100 % over 12 s; Flow rate, 2 mL/min.; Postcolumn connection tubing, 25 cm x 0.005 inch id; 40 μL injection of nitropropane (1), nitropentane (2), and dipropylphthalate (3) in water.

Diameters [in] / [mm]			
Length [cm]	0.003/0.075	0.005/0.12	0.007/0.17
5	0.2	0.6	1.2
10	0.5	1.3	2.5
20	0.9	2.5	5.0
30	1.4	3.8	7.4

Table 3.11 Volumes of connection tubing of different lengths and diameters [μL]

3.1.5

Considerations for the configuration of the interface between separation dimensions

In many respects we consider the interface between the two separation dimensions in an LCxLC system to be the heart of the system, because choices made about this piece of the hardware directly affect most aspects of the first and second dimensions, and the overall performance of the system. Included in the notion of the *interface* here are:

- the specific valve design (there are many options presented in the literature) and mode of operation;
- the sampling loops used to collect ^1D effluent and transfer it to the second dimension. In the following subsections we will discuss each of these aspects in turn, reviewing what is known about how these decisions affect the performance of the LCxLC system.

3.1.5.1

Interface valve designs

In principle, the function of the interface valve is simple – its purpose is to collect ^1D effluent and transfer it to the ^2D column for separating the sample constituents that were not already separated by the ^1D column. However, doing this precisely and quickly, at high pressure, tens or hundreds of times during a single LCxLC analysis is difficult. These challenges have led to much variability and evolution in the designs that have been used since the initial demonstration of an online LCxLC separation in 1978 by Erni and Frei³⁶. Panel A in Figure 3.10 shows a flow diagram for the 8-port/2-position valve used in this early work. We see that one sample loop is loaded with ^1D effluent in the same direction that it is unloaded into the ^2D column, while the other loop is loaded in the direction opposite to which it is unloaded. In this way, one loop is operated in the so-called first-in-last-out (FILO) configuration, while the other loop is operated in the first-in-first-out (FIFO) configuration. Van der Horst and Schoenmakers³⁹ have shown that this asymmetry in operation can lead to differences in peak shape, width, and retention time that depend on which of the two loops is used to hold a specific ^1D fraction. In their paper, they argued that a 10-port/2-position valve configured as

shown in Figure 3.11 could be used to eliminate these differences. This design is symmetric in the sense that both sample loops can be unloaded in the same direction that they are loaded. However, unfortunately it is also asymmetric in the sense that the small *bridge* connector that is used to complete the flow path adds a small amount of volume to the flow path of each loop, but is *in front* of the loop in one path, and *behind* the loop in the other path. This also leads to small, but detectable and important determinate shifts in ²D retention time that depend on which path is traversed. These shifts in retention time for typical ²D flow rates and the dimensions of the bridge connection are presented in Table 3.12. We see that at a realistic ²D flow rate of 2 mL/min the expected retention shift is on the order of 40 ms, which is about 10 percent of the peak widths encountered in a typical fast ²D chromatogram in LCxLC. Panels A and C in Figure 3.12 show that this fluctuation in retention time is easily observed when the ²D separation is highly reproducible. In the most recent evolution of valve technology for LCxLC, Agilent Technologies has developed a symmetric so-called 2-position/4-port duo valve design (see Figure 3.13) that both allows loading/unloading of the two sample loops in the same direction, and eliminates the need for the bridge connection that causes problems in the 10-port/2-position design. The consistency of ²D separations from the two sample loops of the valve is markedly improved as shown in panels B and D of Figure 3.13. This consistency in ²D retention time and peak shape is especially helpful during peak identification and assignment in complicated LCxLC chromatograms.

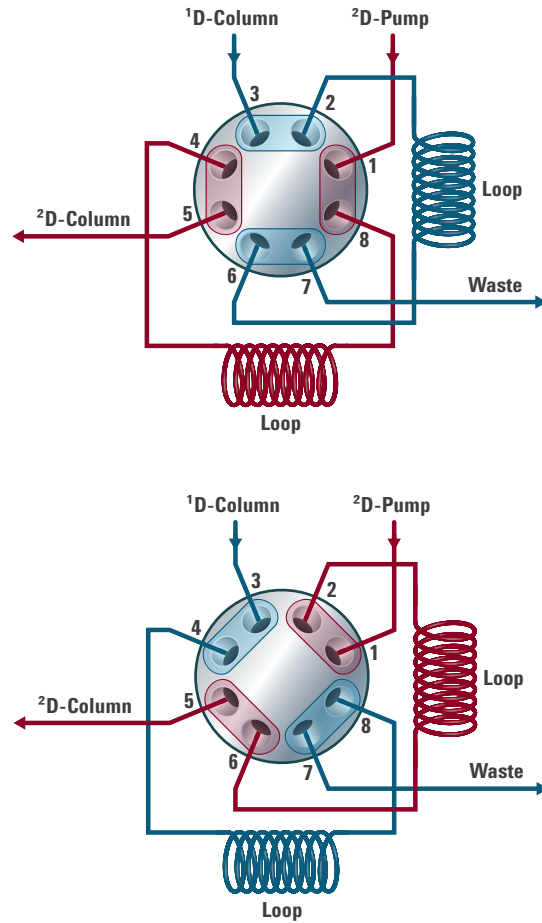


Figure 3.10 Flow paths for the two positions of an 8-port/2-position valve used for LC_xLC.

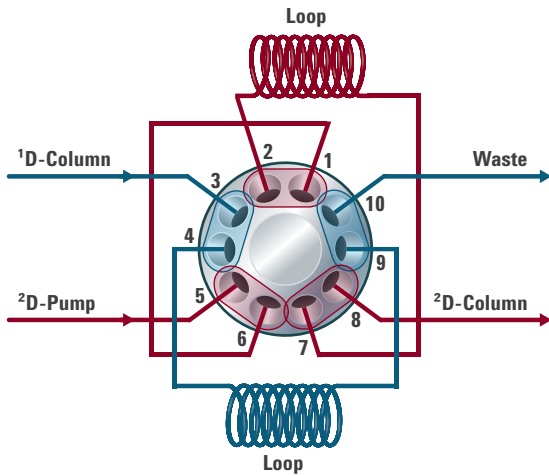


Figure 3.11 Flow path through a 10-port/2-position valve used for LCxLC.

Flow rate [mL/min]	Bridge volume [μL]	Retention shift [ms]
1	1.3	78
2	1.3	39
3	1.3	26

Table 3.12 Retention shifts expected as a result of different flow path volumes associated with the valve design shown in Figure 3.11.

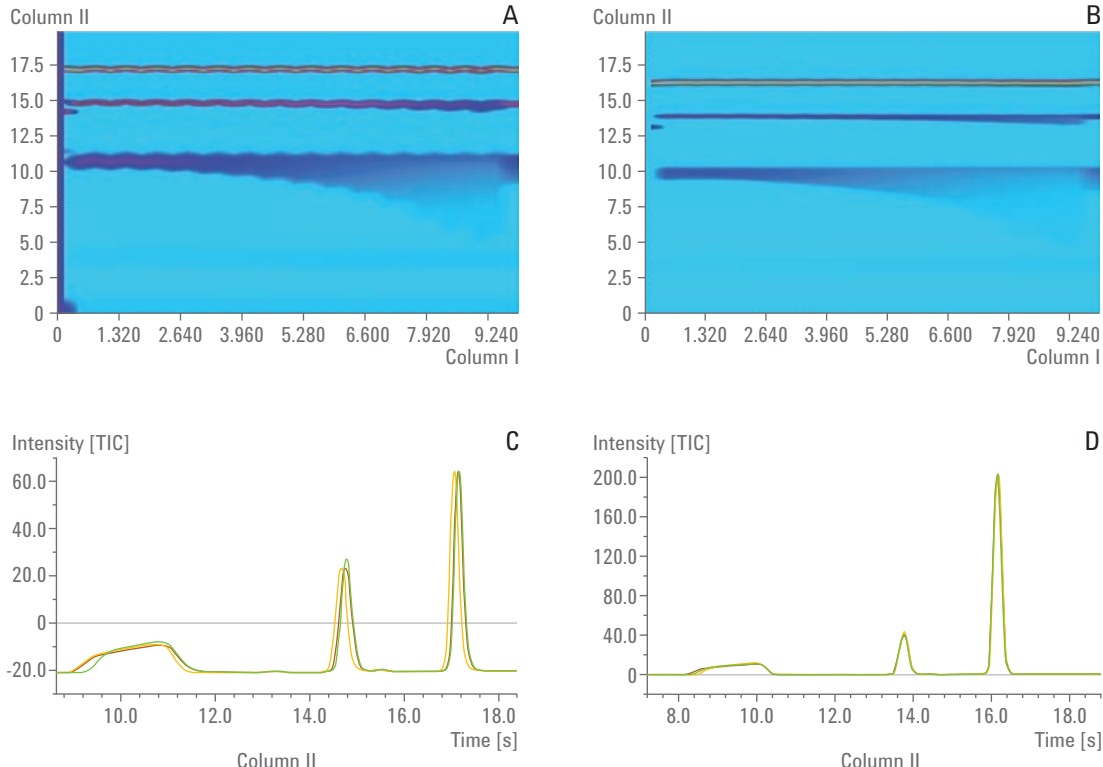


Figure 3.12 Comparison of the loop-to-loop 2D retention consistency for two different valve designs. Panels A and C were obtained using a valve with the design shown in Figure 3.11, and Panels B and D were obtained using a valve with the design shown in Figure 3.13.

Panels A and C: Asymmetric 10-port/2-position valve (see Figure 3.11)

Panels B and D: Symmetric 8-port/2-position valve (see Figure 3.13)

Panels A and B show contour plots from LCxLC separations with test compounds infused directly into the valve such that compounds show up as stripes in the plot.

Panels C and D are chromatogram overlays from three consecutive 2D separations.

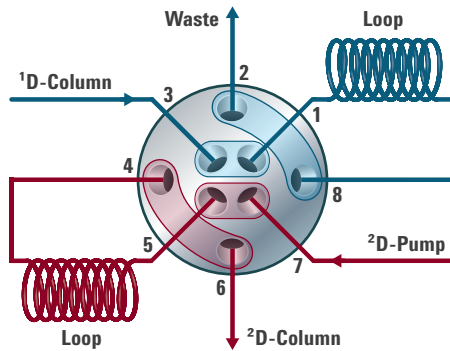


Figure 3.13 Symmetric flow paths through a 8-port/2-position valve designed for LCxLC.

3.1.5.2 Sample loop volume

The simplest approach to determining the loop volume for the two samples appended to the interface in Figure 3.3 is to recognize that the required storage volume is simply the product of the $'F$ flow rate ($'F$) and the sampling time, t_s .

$${}^2V_{inj.} = t_s \times {}^1F$$

Equation 3.5 Calculating the required storage volume.

However, as is the case in conventional 1D chromatography, it is important to understand that when the $'D$ effluent fills a sample loop the two-fold higher linear velocity at the center of the tube will cause some loss of sample when the loop volume is chosen to be exactly that calculated using Equation 3.5. To compensate for this, it is generally a good practice to choose a loop volume that is on the order of 30 percent larger than the volume calculated using Equation 3.5, to obtain the most precise results. Of course, this is not an absolute rule, and in fact the loops can be overfilled when purely qualitative results are desired. Finally, it should be noted that the volume of both loops does not need to be highly accurate but it should be precisely the same for both loops to keep the two flow paths as similar as possible.

3.1.5.3 Connection between $'D$ flow rate and 2D injection volume

Perhaps the most difficult aspect of developing methods for LCxLC is that there are so many interactions between the various parameters of the method that several compromises, some of which can be severe, must be made. One particularly important interaction is that between the $'D$ flow rate ($'F$) and the 2D injection volume (${}^2V_{inj.}$) that we discussed in Section 3.1.5.1 “Interface valve designs”. The importance of these parameters

can be better appreciated by inspection of Table 3.13, which shows the required interface sample loop volume as a function of $'F$ and sampling time (t_s). The volumes are color-coded to indicate those that are favorable (green) in light of the fact that columns with very small volumes must be used in the second dimension for optimum performance (see Section 3.1.4 "Considerations for the configuration of the second dimension"). For example, the dead volume of a 30 mm by 2.1 mm id column dimension packed with fully porous particles is only about 60 μL . The volumes highlighted in green (< 15 μL) can be injected into a small column without severe effects on peak broadening if proper attention is paid to the solvent strengths of the ^2D eluent and the ^1D effluent that is injected. Injecting the volumes highlighted in yellow requires very careful attention (for example, choosing IEX in one dimension and RP in the other so that solvent strength effects are minimized, or pre-injection dilution of ^1D effluent with weak solvent) otherwise the performance of the ^2D column will be severely compromised. The volumes highlighted in red are nearly entirely impractical due to both the solvent strength problem, and the fact that the required sample loop volume introduces a large, additional source of delay volume, which slows down the ^2D separation.

	Sampling time [s]			
$'F$ [mL/min]	10	20	30	60
0.025	4.2	8.3	13	25
0.05	8.3	17	25	50
0.1	17	33	50	100
0.2	33	67	100	200
0.5	83	167	250	500
1.0	167	333	500	1000

Table 3.13 Injection volumes [μL] associated with different combinations of ^1D flow rate and sampling time.

On the surface it seems that the volumes presented in Table 3.13 are not a problem because we can simply choose to use a small loop volume for the interface. However, if the ^1D separation is going to be sampled comprehensively, these small volumes must be accompanied by very low ^1D flow rates or very short sampling times, or both. The seriousness of this challenge is emphasized by Table 3.14 that contains ^1D gradient delay times ($'t_g$) calculated as a function of the gradient delay volume of the

1D pumping system (1V_D) and the 1D flow rate (1F). Here, acceptable t_d values (< 1 min) are highlighted in green. Clearly this is a subjective designation, driven primarily by the fraction of the total 2D analysis time that one is willing to sacrifice to the delay time at the beginning of the 1D separation, and perhaps more importantly, at the end when the strong solvent is flushed from the pumping system (t_{flush} , see Figure 3.2). The values highlighted in yellow represent marginal values, which may or may not be acceptable, depending largely on the overall LCxLC analysis time. The values in red are impractical except in the unusual case that the LCxLC analysis time is on the order of several hours.

	First-dimension gradient delay volume [μL]			
1F [mL/min]	20	100	200	1000
0.025	0.8	4	8	40
0.05	0.4	2	4	20
0.1	0.2	1	2	10
0.2	0.1	0.5	1	5
0.5	0.04	0.2	0.4	2
1.0	0.02	0.1	0.2	1

Table 3.14 First-dimension gradient delay times [s] for different combinations of 1D flow rate and 1D gradient delay volume.

Again, superficially it seems that we should simply choose a pumping system with a 1V_D of 20 to 100 μL and a 1F of 0.5 to 1.0 mL/min., but it is normally not this easy. First, most of the HPLC pumping systems in use today (as of 2013) are characterized by 1V_d volumes of > 500 μL . It is only in the latest generation of pumping systems that we have seen 1V_D volumes decreased into the 50 to 200 μL range. Second, the main problem with using large 1F values is that this leads to very large sampling volumes, as was discussed above in this section. Thus, in most situations, a serious compromise is necessitated in choosing 1F and t_s .

3.1.5.4

Effect of the solvent strength of the sample injected into the second dimension

One of the most limiting difficulties in LCxLC method development is the problem of incompatibility between the 1D effluent that constitutes the sample solvent, which gets injected into the 2D column, with the initial strength or nature of the eluent chosen for the 2D column. As a simple example, suppose that two different types of RP columns (such as a conventional C18 phase and a polar embedded phase) are used in the two dimensions of a LCxLC system, and both columns are operated in

the gradient elution mode. Late in the LCxLC separation the ¹D eluent will be rich in organic solvent in order to elute strongly retained compounds from the ¹D column. This usually results in a situation where a relatively large volume (several tens of microliters) of this organic-rich (for example, 50 percent by volume) solvent is injected into a small ²D column where the solvent gradient starts at composition that is much weaker (for example, 10 percent organic by volume) than the injected sample. This results in severe distortion of ²D peaks, at least of the early eluting ones, whose retention times are shortened because analytes are eluting in the sample solvent (from the ¹D effluent) rather than in the intended ²D eluent. This difficult situation has prompted study of a variety of solutions, each with its own advantages and disadvantages as discussed below.

- *Use of a ²D column that is generally (much) more retentive than the ¹D column* – this approach minimizes the problem because on average the eluent used in the ¹D column will be weaker and the eluent used in the ²D column will be stronger. This is generally a very good idea, and a good guiding principle⁴⁰.
- *Minimizing ${}^2V_{inj}$ to minimize the impact of the sample solvent on the ²D separation* – this approach minimizes the problem by reducing the volume of injected ¹D effluent while leaving the ²D column volume fixed. At some point (for example, 1 μ L injected into a 30 mm by 2.1 mm id column) the composition of the sample will not matter. This approach works well when detector sensitivity is not a concern. Achieving such low injection volumes in a LCxLC system requires the use of very small diameter ¹D columns (for example, 0.5-mm id relative to a 2.1 or 4.6-mm id ²D column), substantial splitting (such as 9:1) of the ¹D flow such that a small fraction is injected into the ¹D column, or both. In either case detection sensitivity is compromised because when very small columns are used in the first dimension the mass of sample that can be injected is quite small, and if flow splitting is used some fraction of the sample is discarded before it reaches the ²D detector.

- *Use of trapping columns in the interface*^{41,42} – this approach effectively extracts analytes eluting from the ¹D column from the ¹D effluent prior to their injection into the ²D column as narrow bands. In principle this approach totally eliminates the solvent strength problem; however, this benefit comes at a cost, and results in other performance compromises. The trapping efficiency is a function of the trap volume, which can be significant in comparison to the volume of the ²D column itself⁴³, adding another element to the ²D gradient delay volume that is a problem for very fast ²D separations. Small variations in trap volume and packing may lead to differences in retention time and peak shape observed in the ²D separation depending on which trap a particular fraction originated from. While the trapping concept has been demonstrated by a number of groups, at this time we are unaware of any long-term, systematic study of their performance demonstrating that this approach is robust enough to be used in practice for studies involving hundreds of LCxLC analyses. This is an area of research that deserves more attention in the future.

An example of the importance of the solvent strength of the sample injected into the second dimension is shown in Figure 3.14. Here the analyte is phenytoin (neutral under the conditions of the experiment) and the column is a 2.1 x 30 mm C18 column. Panel A shows a typical peak shape and width when a small volume (1 µL) of sample (containing 35 % ACN by volume) is injected into a small column (2.1 x 30 mm) under simulated LCxLC conditions with an eluent composition of 35 % ACN and 65 % dilute phosphoric acid in water at 1.0 mL/min. The performance is excellent because the injection volume is small relative to the column volume, even though the sample and eluent solvent strengths are the same. Panel B shows how badly the performance suffers when a larger volume of a sample of slightly higher solvent strength (45 % ACN) is injected, which is more representative of the actual injection volume (20 µL) used in a real LCxLC experiment. At this point the ²D separation is no longer useful. Panel C shows that excellent performance of the ²D column can be maintained even when large injection volumes are used, as long as the volume fraction of ACN in the sample is at least 10 percent lower than the composition of the ²D eluent. Clearly more work is needed to develop similar guidelines for other separation modes (for example, HILIC) and gradient elution conditions.

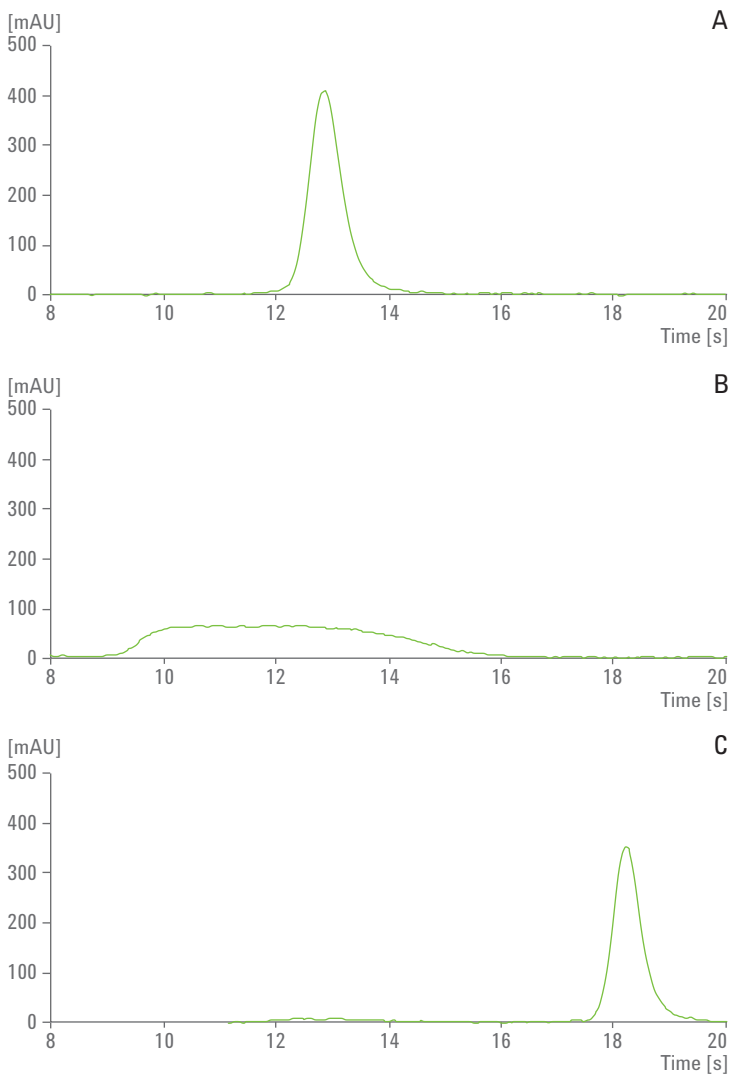


Figure 3.14 Demonstration of the effect of the solvent strength of samples injected into the ^2D column on the quality of ^2D separation. All chromatograms were obtained using conventional 1D instrumentation and a single 2.1×30 mm core-shell C18 column with a mobile phase of 35/65 ACN/dilute phosphoric acid at 1.0 mL/min .

Panel A shows the excellent peak shape obtained when a $1 \mu\text{L}$ sample of phenytoin in 35/65 ACN/dilute phosphoric acid is injected.

Panel B shows the devastating effect of injecting a $20 \mu\text{L}$ sample containing 45 % ACN, as might be encountered in a LCxLC experiment.

Panel C shows how excellent peak shape can be obtained even when injecting samples as large as $75 \mu\text{L}$, as long as the sample contains at least 10 % less organic solvent than the ^2D eluent.

3.1.6

Considerations for the configuration of the first dimension

Some of the requirements for the first-dimension instrument components (that is, pump, detector) are similar to those in the second dimension, while others are quite different. The major differences originate from the fact that ^1D separations are always given much more time than ^2D separations in online LCxLC work. Table 3.15 provides a comparison of the requirements in general terms, as well as typical sets of parameters, recognizing that there is quite a bit of variability across different LCxLC methods.

	First		Second	
	General	Typical	General	Typical
Column dimensions	Longer; similar or smaller diameter	2.1 x 150 mm	Shorter; similar or larger diameter	2.1 x 30 mm
Pump gradient delay volume	Should be less than 200 μL	100 μL	Must be less than 200 μL	100 μL
Pump flow capability	Low flow capability is important to minimize sampling volume	20 to 200 $\mu\text{L}/\text{min}$	Increased flow rate limits provide more operational flexibility	1 to 3 mL/min
Pump pressure capability	High pressure is not important because columns are best operated at their optimal velocities	< 600 bar	Increased pressure limits provide more operational flexibility	< 1200 bar
System dispersion	Should be low in terms of volume		Must be low in terms of both time and volume	
Column temperature	Higher temperatures favor lower organic content in the eluent, however temperature must not be too high to avoid analyte degradation during long analyses	30 to 50 °C	Higher temperatures enable the use of higher eluent velocities and flow rates, thereby improving the throughput of each ^2D separation	40 to 100 °C

Table 3.15 Comparison of typical instrument parameters associated with the first and second dimensions of a LCxLC system.

3.1.7

Detection considerations

3.1.7.1

First-dimension detectors

We strongly recommend using some kind of detector following the ^1D column, as shown in Figure 3.3, at least during the setup of the system or development of the method. Even if the signals from this detector are not ultimately used for qualitative or quantitative purposes, we find that in practice the insight that this ^1D detector yields about the performance of the ^1D pumping system and column in real time is invaluable. However, care must be taken to make sure the flow path through this first detector (for example, a UV detection flow cell and connecting tubing)

does not add too much to the ^1D peak width. As discussed in Section 3.1.6 “Considerations for the configuration of the first dimension” we recommend the use of narrow columns (for example, 1.0 or 2.1-mm id) in the first dimension to minimize the volume of samples of ^1D effluent injected into the second dimension. These small columns, especially if they are efficient, can have very small peak volumes that are on the order of the volumes of some large UV detector flow cells. This situation should be avoided and a smaller volume flow cell should be used.

3.1.7.2

Second-dimension detectors

Whereas there is potential for significant broadening of ^1D peaks because of their low volumes relative to the detection element, there is also significant potential for broadening of ^2D peaks both because they are typically very narrow in time units (as low as 200 ms at half-height), and because they have very small volumes (on the order of tens of microliters). This means that the ^2D detector must be capable of sampling at a minimum of 40 Hz (forty data points per second), and preferably higher than 80 Hz. This is not a problem with modern UV absorbance detectors, but it can be a significant problem with some types of MS detection. The small volumes associated with ^2D peaks means that the volume of the detection element (for example, the flow cell in a UV detector) must also be carefully considered to be sure that its volume is small compared the volumes of the chromatographic peaks.

3.1.7.3

Special considerations for MS detection

In addition to the considerations described above concerning detection frequency and the volume of the detection element, in the case of MS detection the ^2D mobile phase flow rate is also a major concern. In Section 3.1.4 “Considerations for the configuration of the second dimension” we discussed the complex interplay between the productivity of the ^2D separation in a LCxLC system and the ^2D column diameter, flow rate, and gradient delay volume associated with the pumping system. For the sake of discussion we assume that the upper limit of the flow rate that can be wholly directed to a mass spectrometer equipped with an electrospray ionization source (ESI-MS) is 0.25 mL/min. From Section 3.1.4 “Considerations for the configuration of the second dimension” we see that most of the ^2D flow rates that optimize LCxLC peak capacity are well in excess of 1 mL/min. If a 2.1-mm id column is used in the second dimension, which requires either a high-flow compatible MS-interface, a portion of this flow must be split off and diverted to waste prior to the MS inlet, or some of the LCxLC separation performance must be compromised by choosing narrower ^2D column, lower ^2D flow rate, or both.

3.2

Heart-cutting 2D-LC Methods

Although the focus of this Primer is on LCxLC, heart-cutting 2D-LC (denoted LC-LC) is also a very powerful technique that warrants mention here. In contrast to LCxLC, in LC-LC only a single fraction of ¹D effluent captured from a particular ¹D peak is transferred to the second dimension for further separation. Thus, LC-LC is a much more targeted 2D-LC approach that is especially useful when very high resolution information is needed on a relatively small number of peaks in the ¹D chromatogram. Figure 3.15 shows the configuration of an 8-port/2-position valve that can be used to carry out a LC-LC separation.

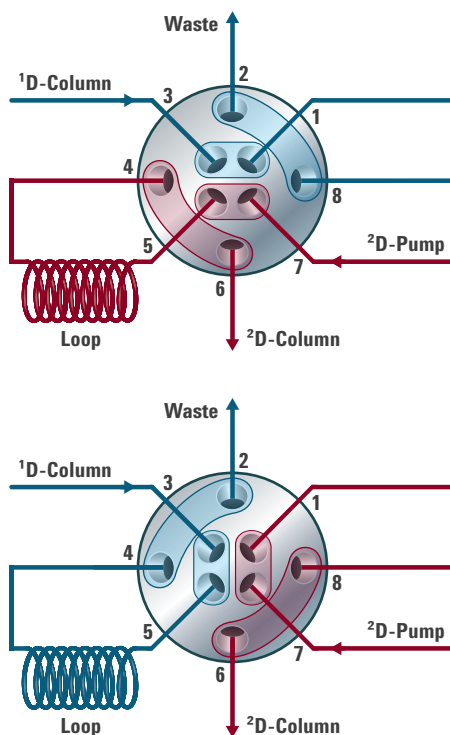


Figure 3.15 Configuration of an 8-port/2-position valve needed to execute a LC-LC separation.

In the following example LC-LC separation an active pharmaceutical ingredient (API) is first separated from several impurities by a ¹D separation, see Figure 3.15. Then, 1D effluent is captured in an 80 μ L loop fixed to the valve shown in Figure 3.15 over a 15 second period from 20.75 to 21.00 minutes and immediately injected into the second column for further separation.

Figure 3.16 shows that an additional impurity (G), which had co-eluted with the API in the first dimension, is easily resolved by the ²D separation. The chromatographic conditions used in this case are summarized in Table 3.16.

Parameter	First dimension	Second dimension
Column	Agilent ZORBAX Eclipse Plus C18, 2.1 x 150 mm, 1.8 µm	Agilent ZORBAX Eclipse Plus Phenyl-Hexyl, 3.0 x 50 mm, 1.8 µm
Mobile phase	Acetonitrile, 0.1 % formic acid in water	Methanol, 0.1 % formic acid in water
Flow rate	0.2 mL/min	3.0 mL/min
Temperature	25 °C	60 °C
Transfer volume	80 µL	80 µL

Table 3.16 Chromatographic conditions used in the resolution of an impurity from a pharmaceutical API by LC-LC. Adapted from Agilent Application Note 5991-0834EN.

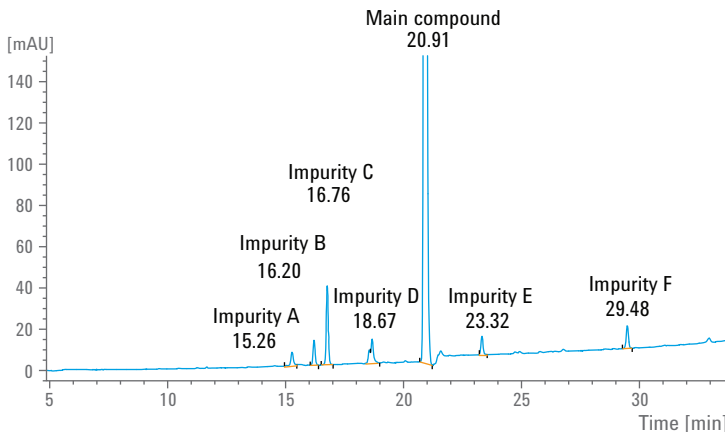


Figure 3.16 Separation of an API and several impurities in a conventional ¹D separation. Adapted from Agilent Application Note 5991-0834EN.

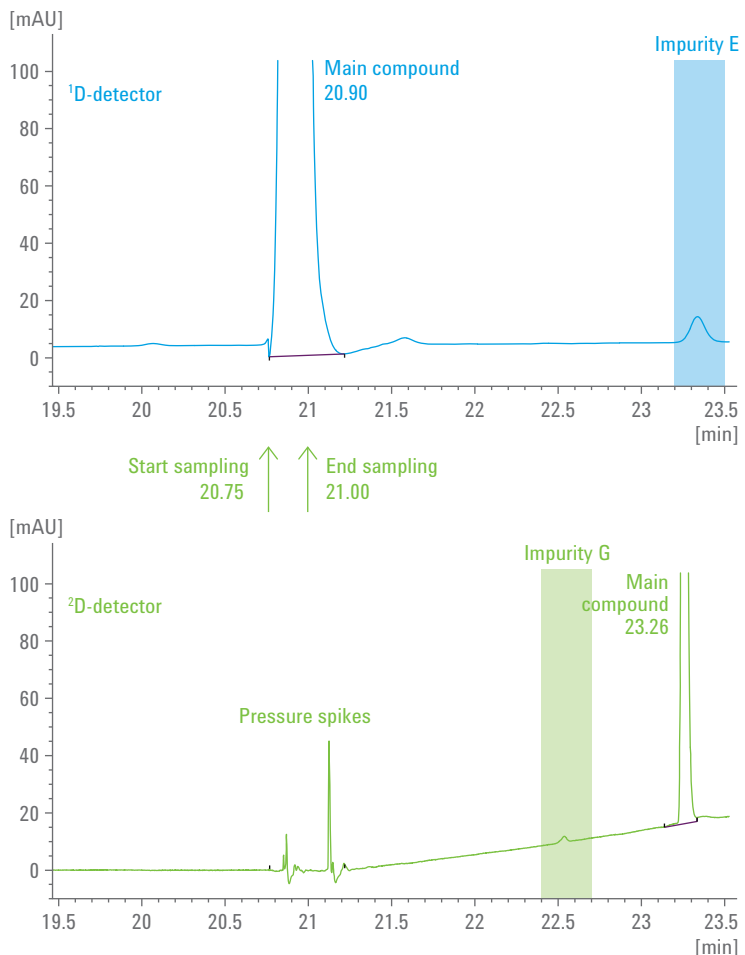


Figure 3.17 Panel A shows a close-up view of the main API peak in the ¹D chromatogram and the sampling window from 20.75 to 21.00 minutes. Panel B shows the ²D separation of the API from an additional impurity (G) that co-eluted with the API in the ¹D separation. Adapted from Agilent Application Note 5991-0834EN.

Aside from the major decisions about the instrument parameters discussed above, the method development process for LC_xLC must begin with choosing the mode of separation (that is, separation mechanism) and specific stationary phase chemistry for each of the separation dimensions. To some extent the choice of column dimensions and other instrumentation parameters depends on the separation modes and columns that are chosen, so those decisions may have to be revised slightly as a result of the considerations discussed below.

4.1 Possible combinations of separation modes

Giddings pointed out early in the development of LC_xLC⁴⁴ that there are a large number of possible combinations of separation modes, which leads to an even larger number of possible combinations of stationary phase chemistries. In our view, however, a significant majority of the possible combinations of modes are far less than ideal in most situations for a number of reasons, which fortunately simplifies method development a bit. In Table 4.1 we attempt to *score* a number of interesting mode combinations, by assigning scores based on a variety of important operational characteristics. A detailed discussion of this comparison can be found in a review article⁴⁰. In spite of the difficulty associated with finding pairs of RPLC columns that are sufficiently different to be useful in a LC_xLC separation, the particular combination of RPxRP is clearly very attractive by all but one metric, albeit a very important one. For this reason we have focused most of our own experimental work, as well as the subsequent discussion in this section, on this combination. There is no question that some of the other modes combinations in Table 4.1 will be very useful in addressing specific separation problems, which may well change the scoring scheme such that the RPxRP combination is no longer the clear winner. However, we believe that the RPxRP combination will be as good as or better than any other combination for a large number of applications of LC_xLC methods. In our view there is tremendous potential for applications involving the RPxRP combination by using eluents buffered at different pH in the two dimensions such that the ionization states of ionogenic analytes change dramatically. This concept has been explored briefly³², but it is likely that much more will be done along these lines. In the next decade we anticipate that the outlook for other mode combinations will change as more fundamental studies establish the limitations of the RPxRP relative to other mode combinations.

Mode	IECxRP [45]	SECxRP [46]	NPxRP [47]	RPxRP [2]	HILICxRP [48]	HILICxHILIC [43]	ACxRP [49]	SECxNP [50]	SECxIEC [7]	LCCCxRP [51]
Orthogonality	++	++	++	+	+	-	++	+	+	++
Peak capacity	+	+	+	++	+	+	-	-	--	+
Peak capacity/ time	-	--	+	++	+	+	-	--	--	+
Solvent compatibility	+	+	--	++	+	++	+	+	+	-
Applicability	+	+	-	++	+	-	+	-	-	-
Score	4	3	1	9	5	2	2	-2	-3	2

Table 4.1 Comparison of different mode combinations for LCxLC⁴⁰.

References to examples of each type of implementation are indicated in the column headings. Abbreviations: IEC – ion-exchange; RP – reversed-phase; SEC – size-exclusion; NP – normal phase; HILIC – hydrophilic interaction; AC – argentation; LCCC – liquid chromatography under critical conditions.

As an illustration of where the RPxRP combination is especially attractive and perhaps the only viable mode combination, we will discuss the features of the solute set shown in Figure 4.1. This is a group of acetic acid derivatives of indole, some of which are uncharged, some are cationic in a certain pH range, some are anionic, and some can even be zwitterions. These compounds are known as plant auxins and are involved in many aspects of plant growth and development. This great diversity of chemistries in one sample rules out the combination of ion-exchange with RPLC. Similarly, all of them are nominally in the same molecular weight range, which rules out the use of size-exclusion in combination with RPLC. Most of these solutes would have low or negligible solubility in low polarity solvents that are typically used in NPLC. These kinds of considerations lead us to think seriously about using RPLC in both dimensions of an LCxLC separation.

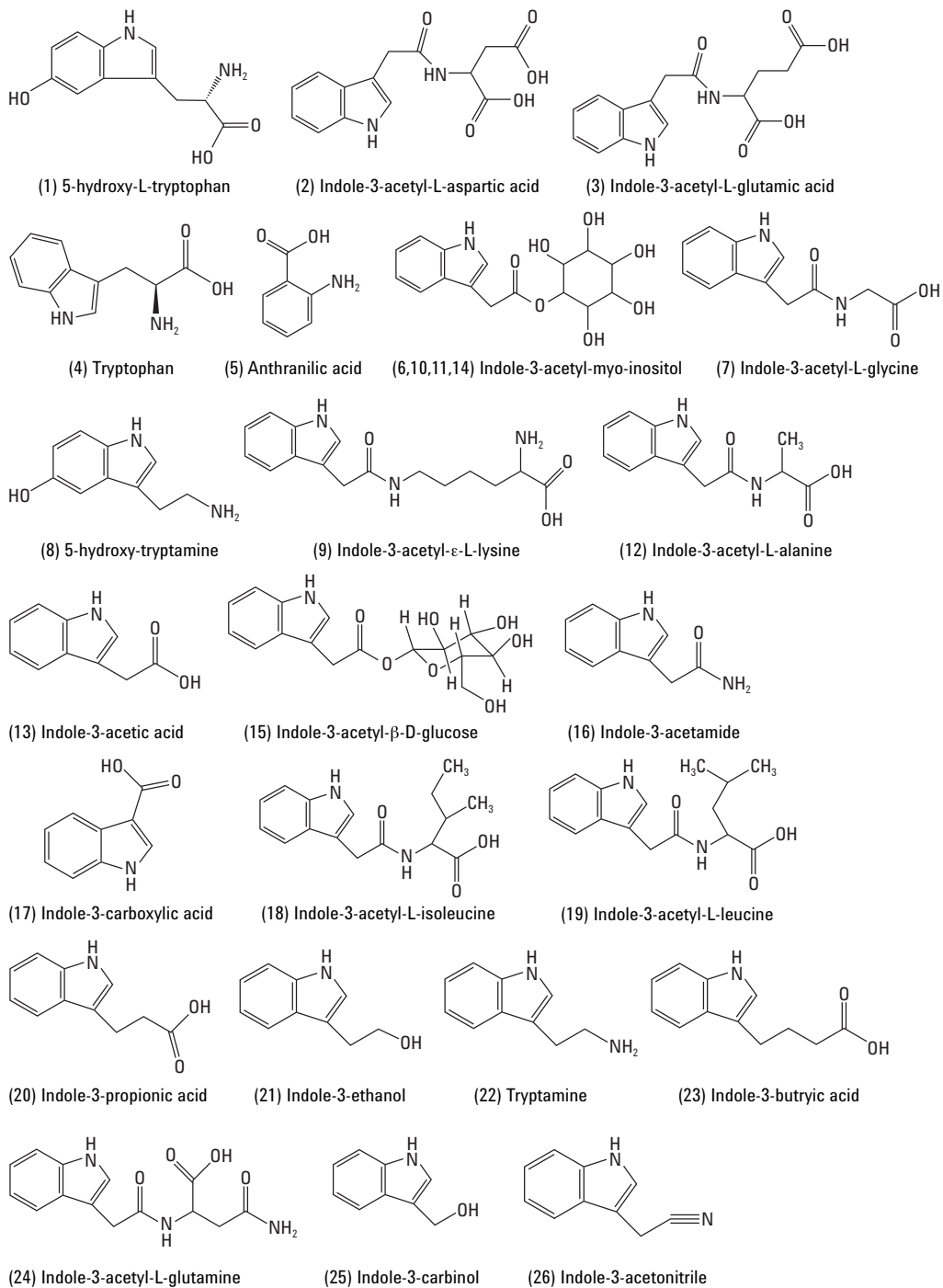


Figure 4.1 Structures of 26 metabolites related to indole-3-acetic acid found in plants.

4.2

Choosing stationary phases in RP_xRP

Over the past two decades a number of groups have worked to develop models of RPLC retention^{52,53}. The most comprehensive of these efforts has been led by Snyder and Dolan, and their collaborators⁵⁴, in which they have developed an exceptionally useful system of classifying reversed phase columns in terms of properties that differentiate the columns according to their *chromatographic selectivity*. This system is based upon the so-called Hydrophobic Subtraction Model of selectivity, and will be referred to hereafter as the HSM. This system is useful here in that it can help us understand which reversed phase columns can be paired as the ¹D and ²D columns to increase the likelihood of using a large fraction of the 2D separation space as measured by the f_{cov} value. The details of how the column classification system was developed are relatively unimportant here (see Reference 55 for details). What matters is that the interactions between various types of RPLC phases and different solutes can be described in terms of five fundamental properties including the solute's hydrophobicity (η'), steric resistance (σ'), hydrogen bond basicity (β'), hydrogen bond acidity (α'), and ion-exchange character (κ'). The phase *hydrophobicity* (H) is the dominant factor that controls retention and selectivity. A schematic explaining the other factors is given in Figure 4.2. These five factors are sufficient to accurately account for the selectivity of the more common phases such as alkyl-bonded silicas, but need to be augmented with two additional factors, namely their ability to interact with π electrons and the extent to which they are affected by dipolar interactions, for the system to accurately describe the selectivity of phenyl-, fluoro- and certain polar-embedded phases.

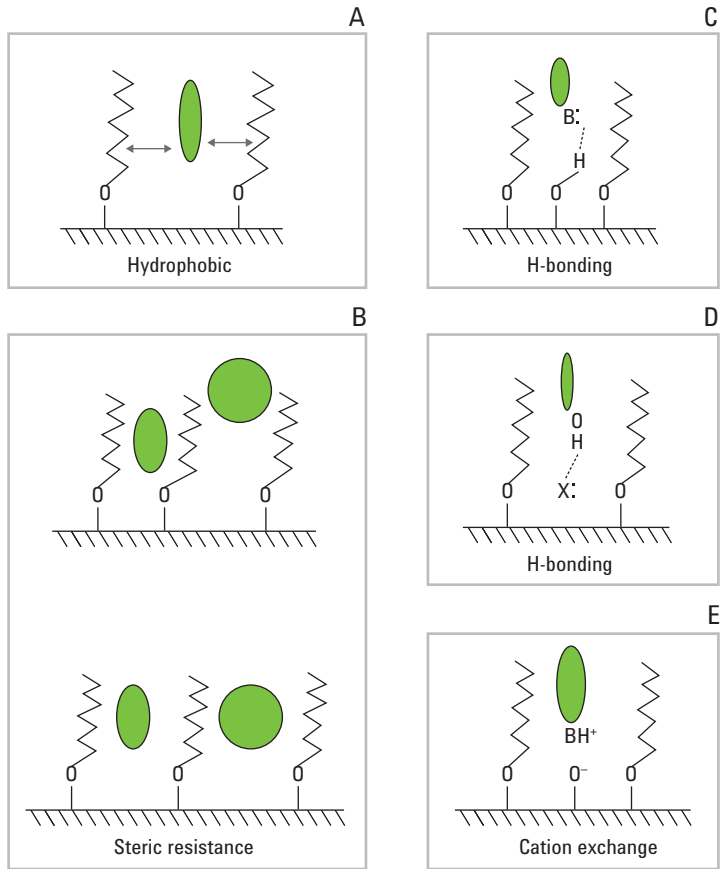


Figure 4.2 Schematics showing the different physicochemical interactions between analytes and RP stationary phases that are quantified by the HSM. Adapted from Reference 55.

Snyder *et al.* showed that the ratio of retention factors (α) of a probe solute relative to ethyl benzene is given simply by Equation 4.1.

$$\ln(\alpha) = \ln\left(\frac{k_{\text{solute}}}{k_{\text{ethylbenzene}}}\right) = H\eta' - S^*\sigma' + Aa' + B\beta' + Ck'$$

Equation 4.1 Ratio of retention factors.

Where H , S^* , A , B and C are the phase characteristics *complementary* to the corresponding set of solute characteristics as depicted in Figure 4.2. Since the capital Latin letters represent stationary phase characteristics, their values for a very common type of C18, Type B silica are all very close to zero except for the H term which is very close to unity for such

a column. A stationary phase differing from a typical C18 material could have an H factor either greater than unity or less than unity depending upon whether it is more or less hydrophobic compared to an *average* C18 phase. The other factors can be positive or negative depending upon whether they augment or reduce solute retention relative to that on the prototypical C18 phase (see Table 4.2). As an example, consider a stationary phase that at a particular pH has acquired a negative charge larger than the *standard* C18 phase. The stationary phase would have a positive C factor and thus would show enhanced retention of cations relative to the *standard* C18 phase. Perhaps the greatest strength of the Snyder-Dolan classification system is that the characteristics of over 640 different RPLC columns have been measured and are freely available as a web-based resource, see www.hplccolumns.org, accessed November 1, 2014^{56,57}.

Average column parameter					
Column property or type	H	S*	A	B	C (pH 2.8)
Type-B C ₁₈ (end-capped)	1.00	0.01	-0.07	-0.01	0.05
Change in type-B C18 column parameters for a change in column properties					
1 C3 to C18	0.40	0.09	0.27	0.02	0.18
2 Non-end-capped to end-capped	0.02	0.03	-0.38	0.02	-0.22
3 6 to 30-nm pore	-0.20	-0.05	-0.16	0.09	0.14
4 0.9 to 2.9 $\mu\text{mol}/\text{m}^2$	0.37	0.10	0.19	-0.07	0.16
Average values of column parameters for each column type					
5 Type-B C18	1.00	0.01	-0.07	-0.01	0.05
6 Type-B C8	0.83	0.00	-0.11	0.02	-0.02
7 Type-A C18	0.84	-0.06	0.12	0.05	0.78
8 EPG	0.68	0.00	-0.54	-0.17	-0.65
9 Polar-group end-capped	0.94	-0.02	-0.01	0.01	-0.14
10 Polymeric alkylsilica (type-A)	0.94	0.04	0.42	-0.02	0.69
11 Cyanopropyl	0.41	-0.11	-0.58	-0.01	0.07
12 Phenylpropyl	0.60	-0.16	-0.23	0.02	0.07
13 Bonded zirconia	1.03	-0.01	-0.43	0.05	2.08
14 Fluoroalkyl	0.70	-0.03	0.10	0.04	1.03

Table 4.2 Average variation in column selectivity parameters as a function of column properties and column type (Adapted from Reference 54).

Another important factor in using the HSM is that to a first approximation the phase characteristics are independent of the volume fraction of organic modifier of the eluent. Their dependence on the nature of the modifier is not quite so simple because we know the stationary phase absorbs a significant amount of organic modifier. It is very important to note that the *C* term is strongly dependent upon the mobile phase pH. Measurements of the *C* term are available at pH 2.8 and 7.0. You should also note that the values reported on the website noted above are all determined in a 50:50 acetonitrile/water mixture containing 60 mM phosphate buffer at both pHs.

4.2.1

Use of HSM to judge phase suitability in LCxLC

Two reversed phases can be compared in terms of an overall selectivity metric, the column selectivity factor (F_s), defined as in Equation 4.2.

$$F_s = [(H_1 - H_2)^2 + (S^*_1 - S_2)^2 + (A_1 - A_2)^2 + (B_1 - B_2)^2 + (C_1 - C_2)^2]^{1/2}$$

Equation 4.2 Column selectivity factor.

In order to use F_s to make accurate predictions of similarity in selectivity for a given set of *typical* solutes, we must apply a representative *weighting factor* to each term as given by Equation 4.3.

$$F_s = [(12.5 \cdot (H_1 - H_2))^2 + (100 \cdot (S^*_1 - S_2))^2 + (30 \cdot (A_1 - A_2))^2 + (143 \cdot (B_1 - B_2))^2 + (83 \cdot (C_1 - C_2))^2]^{1/2}$$

Equation 4.3 Column selectivity factor including weighting factors.

However, these weighting factors must be used judiciously. For example, if a given sample contains no charged analytes then the weighting factor of the *C* term should be set to zero and the F_s metric would change appropriately. When the F_s value for two phases is less than three the average selectivity difference between the two phases will be less than about 0.03. Conversely when F_s is greater than 50 the two phases would be considered as being quite different and possibly useful for a 2D-LC pairing. It must be kept in mind that both the chemical nature of the solute set and the characteristics of the phases determine whether or not the fractional coverage will be high. Thus although a given pair of stationary phases might be quite appropriate for one mixture it could well fail to give a high coverage with a second mixture. Both of the websites referred to above^{56,57} provide the ability to sort the entire column database on the basis of similarity to, or difference from, a particular target column.

4.2.2

Stationary phase selectivity triangles for visualizing differences between phases

An approach to visualizing the entire set of HSM data for a large number of phases has been developed⁵⁸. The selectivity governing properties can be reduced to four numbers with no loss in information by normalization of the S^* , A , B and C parameters relative to the H term. Thus in principle we can display all of the information in a set of four 3-parameter (*triangle*) plots ($S\text{-}C\text{-}A$, $S\text{-}C\text{-}B$, $S\text{-}A\text{-}B$ and $C\text{-}A\text{-}B$). These plots are shown in Figure 4.3. It turns out that the stationary phase A -term is generally not very important because only a relatively few solutes (for example, amides) are strong hydrogen bond bases. Consequently in Figure 4.4 we show an expanded $S\text{-}C\text{-}B$ triangle in which the data are centered a bit more, and the coordinates of three specific stationary phases are highlighted. These particular phases were selected to make a connection between their coordinates in the triangle, the calculated F_s values compared to Agilent ZORBAX SB C18, and the experimental chromatograms obtained for the separation of the Snyder-Dolan probe compounds that very clearly show the similarities and differences between these phases (see Figure 4.5).

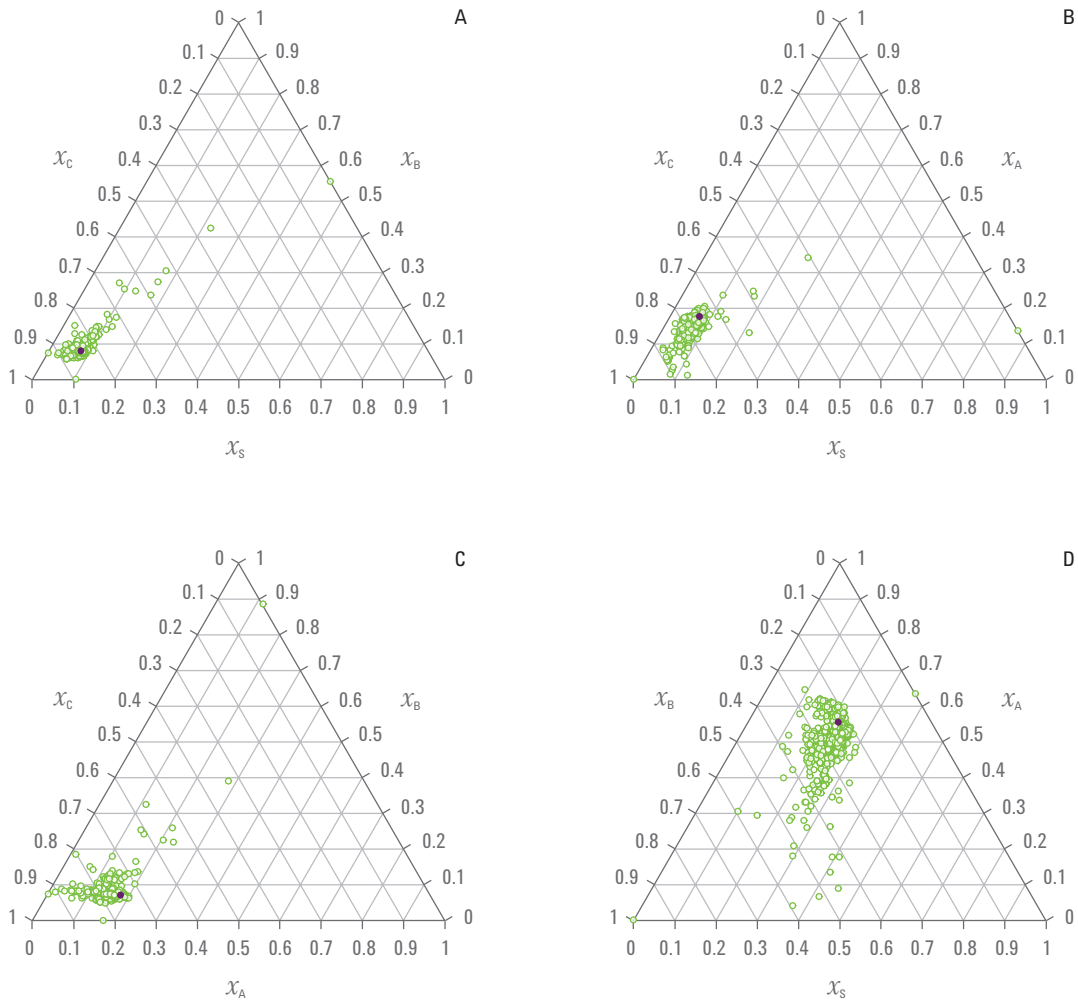


Figure 4.3 Selectivity classification of 366 reversed phased columns – a) $S\text{-}B\text{-}C$; b) $S\text{-}A\text{-}C$; c) $A\text{-}B\text{-}C$; d) $S\text{-}A\text{-}B$ triangle. Adapted from Reference 58. In these plots each point represents a single stationary phase, where the location of a particular point in the triangular selectivity space is dictated by the relative contributions of the three factors (for example, S , B , C – see text for explanation of these factors) to the selectivity of that particular phase. The location of the *average C18-type phase* is indicated by the purple dot.

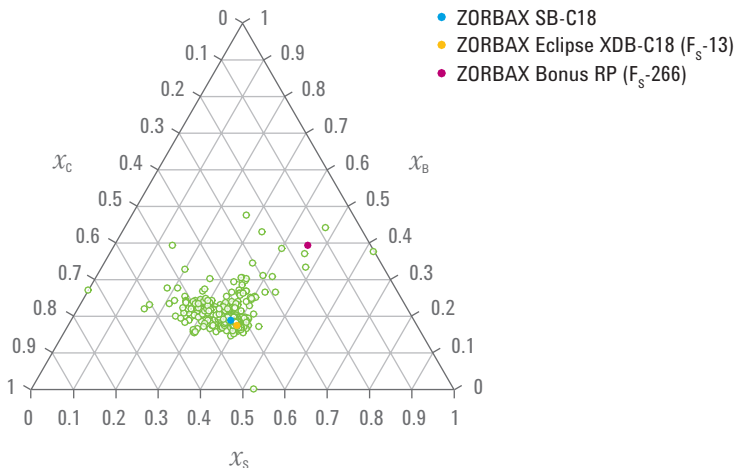


Figure 4.4 Selectivity classification of 648 reversed phase columns using the *S-B-C* triangle with weighting factors calculated using the second method described in Reference 58, which achieves more spreading of the phases over the available selectivity space for better visualization. The coordinates of three specific phases are highlighted, along with the calculated F_s values for two of the phases in comparison to Agilent ZORBAX SB-C18.

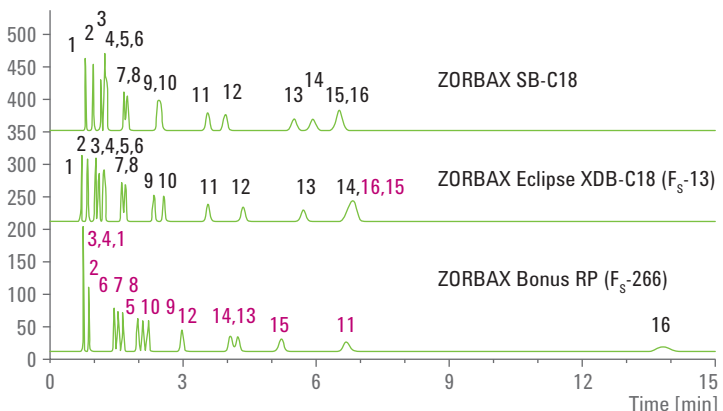


Figure 4.5 Comparison of the separations of 16 probe solutes used in the Snyder-Dolan HSM on three different columns, two of which are very similar.
 Solutes: 1) N,N-dimethylacetamide, 2) N,N-diethylacetamide, 3) Nortriptyline,
 4) Amitriptyline, 5) p-nitrophenol, 6) 5,5-diphenylhydantoin, 7) Acetophenone,
 8) Benzonitrile, 9) 5-phenylpentanol, 10) Anisole, 11) n-butylbenzoic acid, 12) Toluene,
 13) cis-chalcone, 14) Ethylbenzene, 15) trans-chalcone, 16) Mefenamic acid.
 Chromatographic conditions: 50/50 ACN/60 mM phosphate buffer, pH 2.8; 35 °C.

4.2.3

Representative applications using different separation modes

Table 4.3 gives a list of a variety of applications of 2D-LC to different sample types, along with the separation modes and phases used. This is not an exhaustive list, but it does give a sense for the different ways various separation modes and stationary phases have been used successfully for LCxLC.

Application	Mode/Stationary phase		
	First	Second	Reference
Small molecule pharmaceuticals	RP/C18 (low pH)	RP/C18 (pH 8.6)	59
Surfactants	HILIC/Zic-HILIC	RP/C8-Aqua	48
Traditional Chinese medicine	RP/CN	RP/C18 (low pH)	60
Lipids	Argentation (Silver ion)	RP/C18	49
Carotenoids	NP/Bare silica	RP/C18	61
Peptides	RP/C18 (pH 1.8)	RP/C18 (pH 10)	62
Peptides	IEX/Phosphate modified zirconia	RP/C18 (low pH)	45
Polymethacrylates	RP/C18	SEC/C18 (critical conditions)	63

Table 4.3 Representative recent applications of LCxLC and the separation modes used.

4.3

Optimizing performance through use of separation space or shifted gradients

In Section 2.4 “Fundamentals of peak capacity in LCxLC” we emphasized the importance of utilizing as much of the 2D separation space as possible to capitalize on the potential benefit of the product rule that describes the multiplicative peak capacity of LCxLC separations. Nevertheless, in spite of best attempts to find highly complementary stationary phases for use in the two dimensions of a LCxLC system, chromatograms of the kind shown in Figure 4.7⁶⁰ are typical in the sense that significant portions of the 2D separation space are unoccupied by peaks (indicated here by the two triangles labeled A and B). In this work the authors acquired this chromatogram for the separation of a Traditional Chinese Medicine sample using a so-called *full gradient* in the second dimension of the LCxLC system. A comparison of different LCxLC elution modes is shown in Figure 4.6. The value of the so-called *shifted gradient* (Panel D in Figure 4.6) for spreading peaks off of the diagonal to utilize more of the 2D separation space was first demonstrated by Bedani *et al.*⁶⁴, and elaborated further by Li and Schmitz. Figure 4.8 clearly shows that a properly designed shifted gradient can be used very effectively to spread peaks in to the previously unoccupied A region. Presumably further manipulation of the gradient would also allow spreading of peaks further into the B region as well.

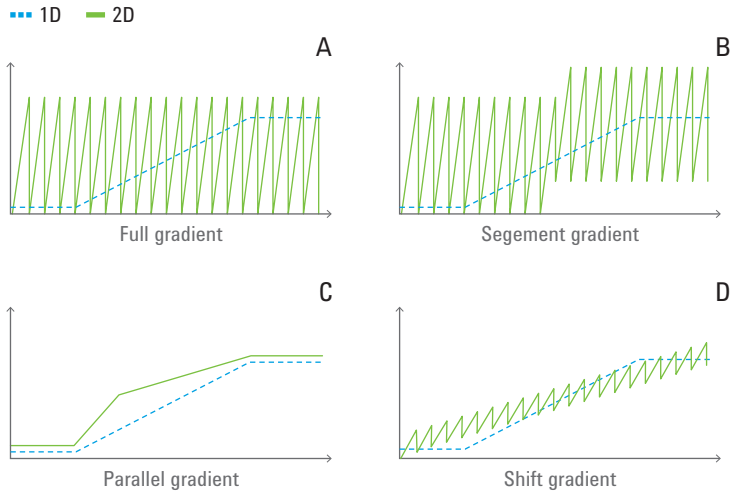


Figure 4.6 Different types of gradient profiles used in the first and second dimensions of LCxLC separations. Adapted from Reference 60.

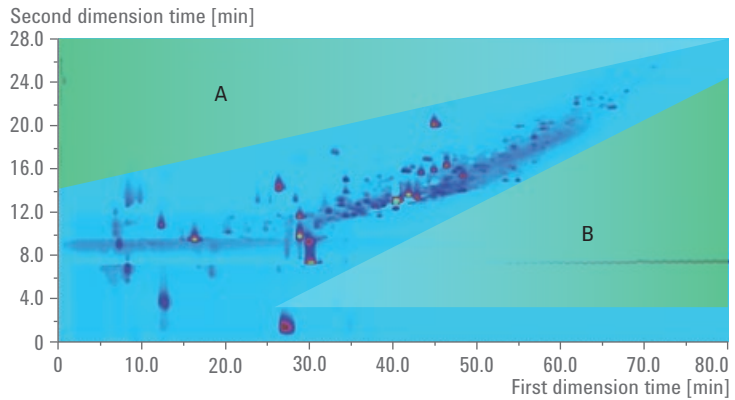


Figure 4.7 LCxLC separation of an extract of a traditional Chinese medicine (TCM), with full gradients used in the second dimension. The regions labeled A and B are largely unoccupied by chromatographic peaks.

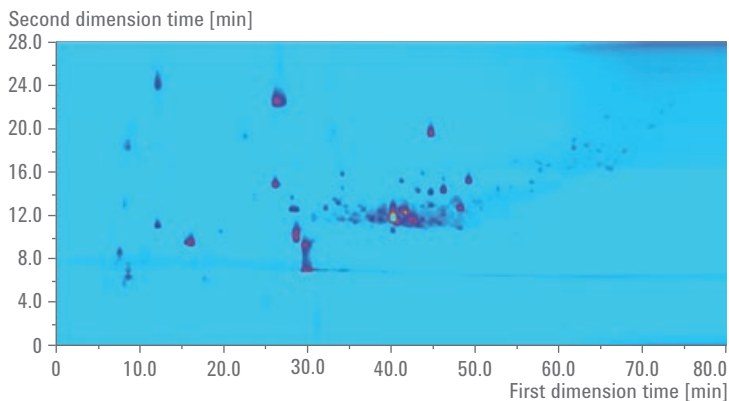


Figure 4.8 LCxLC separation of the same TCM extract as in Figure 4.7, but with the use of a shifting gradient in the second dimension. The A region from Figure 4.7 is now highly occupied by peaks. The B region is still not fully occupied, but presumably this could be achieved with further adjustment of the shifting gradient profile.

Here a point of caution is warranted to avoid misidentification of peaks when the shifted-gradient scheme is used. Because the gradient program varies slightly in adjacent 2D separations, the same compound eluting in adjacent 2D chromatograms will appear at slightly different retention times along the 2D axis. When viewing these chromatograms you need to be aware of this potential shift to avoid assignment of the two peaks to different chemical entities.

4.4

Managing the trade-off between performance, robustness, and operating cost

When considering the implementation of a 2D-LC method, concerns naturally arise about the cost and robustness of 2D separations because of the increased complexity compared to conventional 1D separations. Two aspects of this consideration warrant discussion here. First, method robustness and cost of operation should be considered when making decisions about operating parameters. The discussion of optimization of 2D methods in Section 2.4 “Fundamentals of peak capacity in LCxLC” was highly theoretical in nature, and should serve as a source of guiding principles, rather than absolute rules. For example, Figure 2.22 shows that a 2D peak capacity of 3500 can be achieved in a particular situation by using a sampling time of 10 seconds, whereas the 2D peak capacity is reduced to 2500 if the sampling time is increased to 30 seconds. From the point of view of peak capacity, the 30 seconds is not optimal, but from the point of view of method robustness the sampling time 30 seconds may be better because injections will be made into the 2D column much less frequently (only 30 percent of the injections and valve switches compared to the 10-seconds sampling time). Similarly, much of the discussion of

operating parameters for the second dimension in LCxLC in Section 3.1.4 “Considerations for the configuration of the second dimension” was focused on method performance as measured by peak capacity. In some situation it will be important to consider other metrics of performance, such as mobile phase consumption, and in these situations a method that has lower peak capacity but consumes less solvent may be preferred.

The second point to consider here is that while 2D instruments are generally more expensive upfront because of the additionally required components, development of effective 2D methods will recover this upfront cost through savings when compared to alternative analyses by conventional means. For example, if a single 2D method can replace multiple 1D methods that are required to resolve different critical pairs (for example, achiral/chiral separations in a single analysis compared to one achiral separation plus one chiral separation), or if the need for costly mass spectrometric detection can be avoided by doing a better, 2D separation, then the 2D method will be more cost effective in the long run.

4.5

Method development case studies

4.5.1

Case study 1 – Separation of degradation products of a photosensitive active pharmaceutical ingredient

There are so many possible configurations of an LCxLC system and these configurations are highly sample dependent, so it is difficult to generalize any more than we already have in Chapter 3 “Practical Implementation of 2D-LC” and Chapter 4 “Method Development in LCxLC” about method development. Thus, we feel it is most effective to use examples of real methods to develop a sense for the kinds of decisions that must be made in developing an LCxLC method.

Pharmaceutical active ingredients (APIs) are routinely subjected to forced degradation using heat, pH, light, or other variables to study the stability of the molecules under these stressing conditions. Sometimes these studies produce samples that are sufficiently complex to warrant separation by LCxLC. The conditions described below were developed to separate the degradation products of a low molecular weight API exposed to UV light.

4.5.1.1

Step 1 – Choose separation modes and stationary phases

As we discussed in Section 4.1 “Possible combinations of separation modes”, combining two RP stationary phases is particularly attractive because of the inherent compatibility of the eluents used in the first and second dimensions, and the versatility of these phases. In Section 4.2.2 “Stationary phase selectivity triangles for visualizing differences between phases” we discussed the use of selectivity triangles to guide selection of complementary RP phases, and showed that the combination of the

Agilent ZORBAX SB C18 and Agilent ZORBAX Bonus-RP phases has the potential to be very powerful for RPxRP separations, and we have used this pairing for this application.

4.5.1.2

Step 2 – Choose column dimensions and elution conditions

In Sections 3.1.6 “Considerations for the configuration of the first dimension” and 3.1.4 “Considerations for the configuration of the second dimension” we discussed considerations for choosing the dimensions of the columns used in the first and second dimensions. Using these guidelines, and keeping in mind a target analysis time of about 15 minutes, we chose the following column dimensions and initial elution conditions to ensure elution of all sample components from the columns.

First dimension

- Agilent ZORBAX Bonus-RP, 2.1 x 100 mm, 3.5 µm
- 35-70-95-95-35 % B from 0-22-24-26-26.01-30 minutes, with 10 mM perchloric acid in water as the A solvent, and acetonitrile as the B solvent
- Flow rate: 0.080 mL/min
- Column temperature: 40 °C

Second dimension

- Agilent Poroshell 120 SB-C18, 2.1 x 30 mm, 2.7 µm
- Change in %B from 0-0.20-0.21-0.25 minutes, with 10 mM perchloric acid as the A solvent, and acetonitrile as the B solvent
- Flow rate: 3.0 mL/min
- Column temperature: 60 °C

4.5.1.3

Step 3 – Configure the interface

In Section 3.1.5 “Considerations for the configuration of the interface between separation dimensions” we discussed a number of factors to consider when choosing the sampling time and ²D injection volume. In this case we have configured the sampling valve between the two dimensions with 20-µL loops and set the sampling time to 15 seconds. This combination of parameters is compatible with the 0.080-mL/min flow rate entering the loops, resulting in about complete filling of the sample loops with 20 µL of ¹D effluent every 15 seconds.

4.5.1.4

Step 4 – Adjust elution conditions to maximize use of the separation space

The ²D elution conditions were adjusted to maximize the use of the separation space using the shifted gradient approach as shown in Figure 4.9. This yielded the RPxRP chromatogram shown in Figure 4.10. We see that several peaks that are either partially or fully overlapped in the first dimension of this separation are easily resolved by the ²D separation. This additional information about the sample is obtained quickly, with minimal method development.

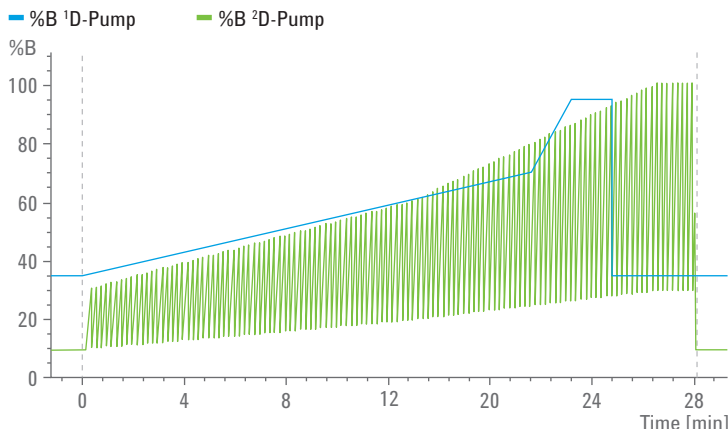


Figure 4.9 Shifted gradient profile used in the second dimension to maximize usage of the 2D separation space.

Column II [s]

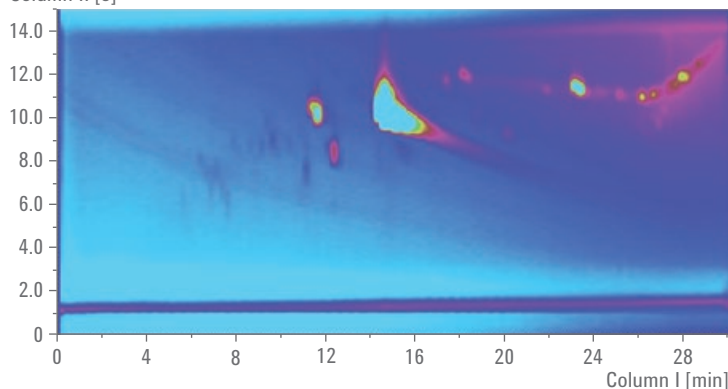


Figure 4.10 RPxRP separation of a sample of photodegraded naproxen (nominal concentration is 1 mg/mL) using a shifted gradient in the second dimension as shown in Figure 4.9. Color intensity indicates absorbance at 210 nm. The main API peak appears at about 14.5 minutes/10 seconds. A major degraded peak that co-elutes with the API in the first dimension is observed as a well separated peak following the API in the second dimension.

4.5.2

Case study 2 – Separation of a mixture of ionic and non-ionic surfactants

Although we have advocated for the widespread use of RPxRP separations, there certainly are situations where the combination of Hydrophilic Interaction Liquid Chromatography (HILIC) and RP is an excellent pairing for use in LCxLC because of the complementary nature of the retention mechanisms of these separation modes. In the following case study we summarize the work of Elsner and Schmitz *et al.*⁴⁸ on the development of a HILICxRP method for the separation of a complex surfactant mixture. The general structures of the surfactant classes separated in this work are shown in Figure 4.11.

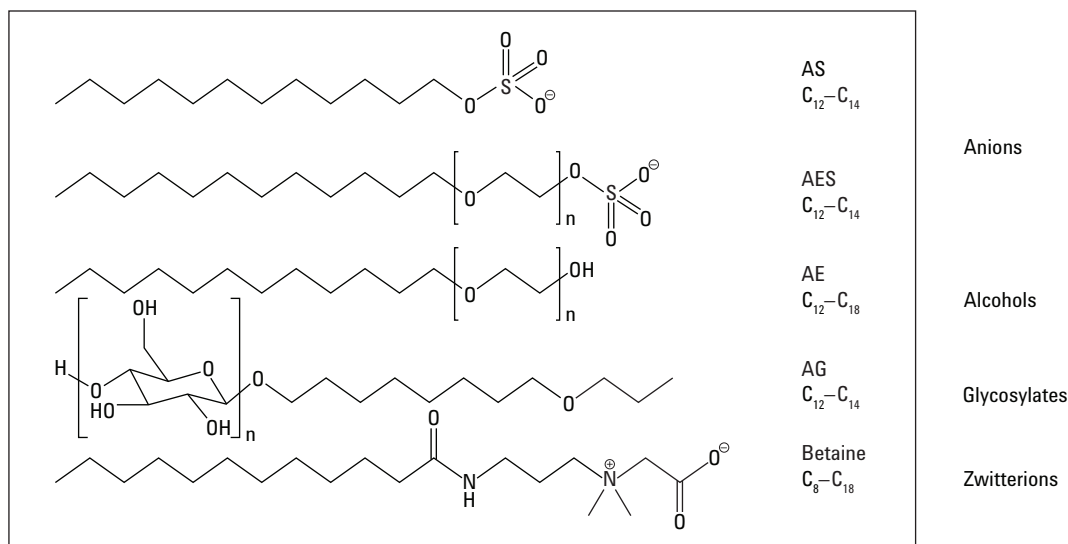


Figure 4.11 General structures of five different surfactant classes separated by a HILICxRP method.

4.5.2.1

Step 1 – Choose separation modes and stationary phases

Given the diversity and types of analyte chemistry shown in Figure 4.11, the pairing of the HILIC and RP separation modes is a natural choice in this case. In this type of scenario the HILIC separation will generally separate the mixture according to analyte polarity and extent of ethoxylation, whereas the RP separation will separate analytes according to alkyl chain length within a given analyte class.

4.5.2.2

Step 2 – Choose column dimensions and elution conditions

In this case the goal of the separation was to achieve baseline resolution of all of the main components of the mixture, according to both functional group and chain length. Thus, the focus of this work was not necessarily on separation speed *per se*.

First dimension

- SeQuant, Sweden, ZIC-HILIC, 2.1 x 250 mm, 5 µm
- 5-5-20-40-40 %B from 0-40-50-90-110 minutes, with acetonitrile as the A solvent, and 50 mM ammonium acetate (pH 5.3) in water as the B solvent
- Flow rate 0.025 mL/min
- Column temperature ambient

Second dimension

- Reprospher C8-Aqua, 4.6 x 30 mm, 3 µm, (Dr. Maisch GmbH)
- 50-50-70-95-95-50-50 %B from 0-3-6-36-42-48-60 seconds, with 50 mM ammonium acetate (pH 5.3) in water as the A solvent, and methanol as the B solvent.
- Flow rate: 3.0 mL/min, with splitting for compatibility with MS inlet
- Column temperature: ambient

4.5.2.3

Step 3 – Configure the interface

In this case the sampling valve between the two dimensions was configured with 25 µL loops and set the sampling time to 60 seconds. This combination of parameters results in 100 percent filling of the sample loops. It is important to note here that the ratio of ²D injection volume to ²D column volume (25 µL/600 µL, or 0.042) is much smaller than that used in “Case study 1 – Separation of degradation products of a photosensitive active pharmaceutical ingredient” (that is, 80 µL/60 µL, or 1.3), but this is necessary to avoid the serious broadening of ²D peaks that would occur if much larger volumes of the organic rich (~80% ACN) ¹D effluent were injected into the ²D column where relatively weaker eluents (~75% MeOH) are used. Indeed, this is one of the limitations of pairing HILIC and RP separations, in that relatively small ²D injection volumes must be used, which limits the detection sensitivity of the ²D separation relative to the first dimension. The conditions described here yield the separation shown in Figure 4.12, which is a beautiful example of the complementarity of the HILIC and RP separation modes, and effective use of the 2D separation space.

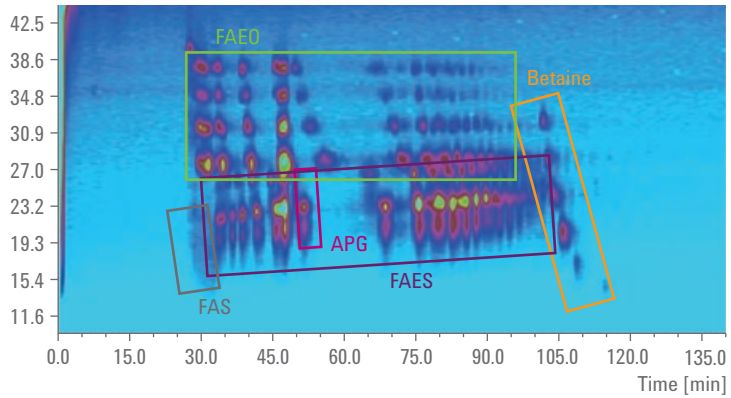


Figure 4.12 HILICxRP separation of a complex mixture of several different surfactant classes, with MS detection. Labeled peaks indicate that 110 different surfactants were separated and detected. Adapted from Reference 88.

5.1

Introduction

Data analysis is one of the most challenging aspects of using multidimensional separations in practice, especially for untargeted LCxLC analysis. At this time, approaches for working with 2D-LC data lag behind their 1D counterparts in terms of both effectiveness and ease of use. The LCxLC mode of separation in particular presents several unique challenges that simply are not present in 1D-LC, thus the following discussion is focused on this mode of operation.

Several fundamentally different approaches have been used to analyze data produced by LCxLC separations:

- A. The data can be treated as a series of 1D chromatograms each of which is analyzed in a more or less conventional fashion^{65,66}. Subsequently the 1D chromatograms must be merged into one or more types of 2D representations (see Figure 1.8).
- B. The data stream of sequential 2D chromatograms is turned into a 2D image at the outset and then treated by various techniques of image and feature analysis⁶⁷⁻⁶⁹.
- C. The higher order structures of the data (two chromatographic dimensions plus multiple wavelengths or multiple m/z coordinates) are treated as trilinear (or higher order) data structures and analyzed by chemometric methods such as parallel factor analysis (PARAFAC), the generalized rank annihilation method (GRAM), or multivariate curve resolution-alternating least squares (MCR-ALS). This is an area of intensive research. The two groups most involved in this approach are those of Synovec⁷⁰⁻⁷² who has focused on GCxGC with MS detection, and Rutan^{73,74} whose focus has been LCxLC with DAD detection. Although in principle the chemometric methods can be used for both GCxGC and LCxLC, there are several different sets of challenges posed by the two different kinds of chromatography. Although this may in fact be the most powerful approach to analysis of 2D chromatographic data, there is currently no commercial or open source software available that applies these methods to LCxLC data. Further, many problems associated with implementation of these methods are related to characteristics of the instrumentation used for LCxLC, and remain to be solved.

We will not describe this approach any further here as it requires detailed knowledge of chemometric factor analytic methodology and its routine application is still in the future, see Chapter 7 "The Future of 2D-LC".

Both approaches A and B involve some common steps including:

- Baseline correction
- Noise evaluation
- Data smoothing (filtering)
- Peak detection (including finding the times at which the peak starts, stops, reaches its maximum and measurement of the peak height above baseline)
- The merging/aligning of 2D peaks for the same species to form a single 1D peak
- Peak area/volume determination, or some form of quantitation
- Determination of the chemical identity of one or more peaks in the chromatogram
- Comparing samples (optionally)

In the first approach some form of peak merging must be done on a series of contiguous 1D chromatograms to combine the ^2D daughter peaks belonging to the same parent ^1D peak. This, in fact, is a challenging problem especially when a detector is used that does not deliver extensive qualitative information able to differentiate between different chemical constituents. To keep our discussion brief in the following sections, we will assume application of a univariate detector (for example, single-channel UV detector, or SIM in MS).

5.2 Baseline detection

Consider the structure of the data shown Figure 5.1, which is a series of ^2D chromatograms run under conditions precisely representative of an online LC \times LC separation. These were obtained during a dummy analysis in which there no sample was injected into the ^1D column, so they represent the ^2D detector baseline that must be removed so that we can better see and quantify our peaks. When an absorbance detector is used we see that the baseline changes during a single ^2D chromatogram are complex, large in magnitude, and vary as the ^1D eluent changes in composition during the ^1D gradient separation. Thus the first step in data analysis is some form of *baseline subtraction*. Unfortunately the baseline under the entire

LCxLC analysis is not as reproducible as we would like so methods more sophisticated than simple *blank* baseline subtraction correction have been developed. They generally involve fitting a polynomial⁷⁵ to individual 1D chromatograms and subtracting the polynomial from the chromatogram, or using a median filter to strip narrow peaks away from a more slowly varying baseline⁷⁶.

One of the most powerful of these baseline correction techniques is the orthogonal background correction (OBGC) method of Filgueira⁷⁷. Much of the LCxLC background observed with a DAD detector is due to its sensitivity to changes in the refractive index of the eluent; however, we have found that the total ion current response of an MS detector produces a background that is just as complex as that observed with a DAD. Fortunately a selected ion signal will be much cleaner but you must know what you are looking for so this approach is effectively limited to targeted analysis.

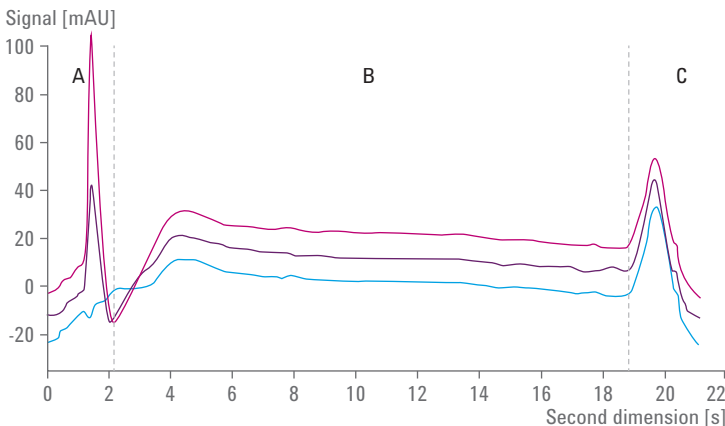


Figure 5.1 Structure of the LCxLC background represented by three single 2D chromatograms obtained from a dummy analysis sampled at different times of the gradient in the first dimension. The amount of acetonitrile in the sample solvent transferred from the 1D to the 2D (region A) corresponds to 10 percent (blue curve), 30 percent (purple curve), and 50 percent (red curve). Region B is where most peaks elute, and region C shows the system flush-out peak.

5.3

Determination of noise level

To determine if a *blip* above the baseline is large enough to be considered a peak we need an estimate of the short-term noise. Inspection of Figure 5.1 will show that there are many such blips present in the baseline (some exceeding several milliabsorbance units (mAU) in height) even though nothing was injected into the 1D column. Various methods have been described to determine the noise that is then used to set a threshold setting beyond which a signal is recognized as a real peak⁶⁵. This threshold is most commonly set at a level equal to three times the noise level.

5.4

Data smoothing and filtering

A great many techniques have been used in 1D chromatography including various polynomial, Fourier domain, and tuned filters as well as wavelet filters. We strongly prefer the use of tuned Gauss filters over Savitsky-Golay polynomial filters. However, we also recommend that very narrow (3 to 5 point) median filters do an excellent job of suppressing impulse noise.

5.5

Peak detection

One of the most common ways that chromatographic data systems determine peak start, stop and maximum times in any 1D chromatogram is by examining the first and second time derivative of the chromatogram⁷⁷. This method has also been used in 2D-LC by several groups. The peak height is generally measured by fitting a quadratic polynomial to a few points around the maximum or by fitting a number of points above the half-width to the Gauss equation.

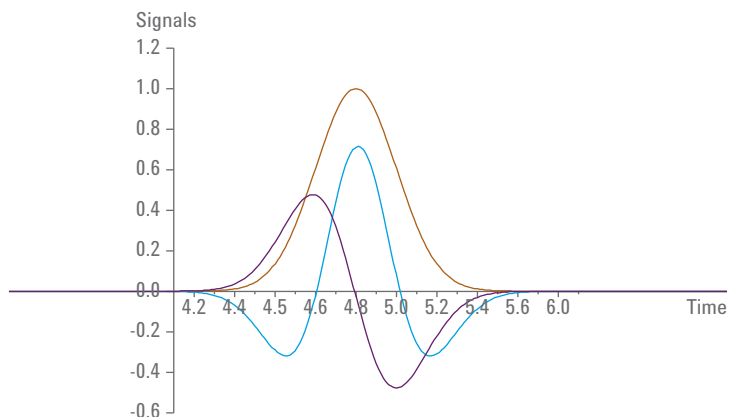


Figure 5.2 Plot of a Gaussian peak (brown), and its first (purple) and second (blue, multiplied by -1) derivative versus time. Note the first derivative is zero at the peak maximum and the second derivative is zero at $t_R + \sigma$ and $t_R - \sigma$. The peak start and stop is usually taken as $t_R \pm 2\sigma$. Only peaks with a ratio of peak maximum height to noise level greater than 3 are measured. Further, a threshold is sometimes needed for the second derivative especially when working against a highly curved baseline or when trying to find the start of a peak on the shoulder of another peak.

Reichenbach and his group have developed a quite different method for peak detection^{69,78}. In contrast to the above method, which examines the sequential 2D chromatograms and locates peaks by the same methods as simple 1D chromatography, their method is based on using the 3D image. Imagine the 3D image as a landscape that has been completely flooded so that no points of land are visible above the water level. Now one gradually drains the water away. Peaks will become evident in order of their heights, that is, the tallest peak appears first, then the second tallest and so on.

This approach is known as the *drain* algorithm. Algorithmically you first sort all of the intensities in order from largest to smallest into a queue and examine them sequentially. The algorithm initiates detection at the top of the tallest peak, that is, the most intense signal in the queue, and iteratively adds all smaller neighbors until no smaller points border the peak (see Figure 5.3). Each point drawn from the queue is compared with its neighbors. If the neighbors are of equal or larger value, the extracted point is given the same label as its largest neighbor. However, if the data point drawn is larger than its neighbors, it is given a new label to indicate that it is part of another peak. This procedure is repeated until the queue is empty. One of the major virtues of this approach is that you do not need to take any derivatives to locate the start and stop of a peak and thus it should be less sensitive than the classical methods of peak detection; clearly it is not entirely immune to noise, which can create false maxima. The drain algorithm is used in a commercial software package (LC Image) for 2D-LC data processing.

330	207	8
521	827	81
329	1306	328
83	824	519
7	208	331

Figure 5.3 Diagram of a peak apex and its surrounding smaller nearest neighbors.

5.6

Peak area measurement

The area under each peak is usually determined by use of the trapezoidal rule. Difficulties arise when we have to deal with two (or more) incompletely resolved peaks. In the simplest case of two equal height ($R_s < 1.5$) peaks two options must be considered (see Figure 5.4). The area of peak 1 can be defined by dropping a vertical from the valley to the baseline, which is extended horizontally from before to after the fused peaks (see baseline type 1 in Figure 5.4). Alternatively you can assume that the baseline is formed by drawing a line from before the peak to the valley point as in baseline type 2 in Figure 5.4.

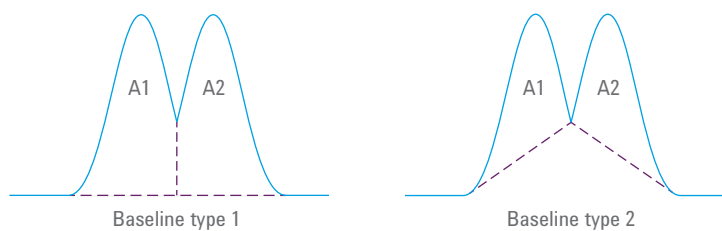


Figure 5.4 Two methods of establishing the baseline for peak area measurement.

5.7

Merging ^2D daughter peaks from the same ^1D parent peak

When a ^1D peak is properly sampled and, further, if fractions of this peak do not suffer excessive dilution so that the S/N is degraded to below the peak detection threshold, the same compound will show up as a peak at the same ^2D retention time in more than one sequential ^2D chromatogram. Since these individual ^2D peaks are derived from a single ^1D peak, it makes sense to merge them into a single 2D peak. This task would be trivial if the ^2D peak retention time were always *exactly* the same; however, this is seldom the case. Further, poorly resolved ($R_s < 1$) large neighboring peaks can significantly affect the position of the peak maximum of the target peak, the solvent composition delivered to the ^2D column varies slightly from one ^2D separation to the next, and the ^2D column inevitably exhibits different retention properties as it ages under the demanding conditions in the second dimension of a LCxLC system. Given these challenges, various algorithms have been developed to determine when it is appropriate to merge ^2D peaks and assign them the same parent (that is ^1D) retention time. An example of the peak merging process is shown in Figure 5.5. We refer you to the work of Peters *et al.* and Stevenson *et al.*^{65,66} for detailed descriptions of the merging algorithms. The basic problem is that for a given ^1D main peak all of the ^2D retention times of a series of subpeaks are not identical. This is shown in the upper panel of Figure 5.5 where we see two clusters of points labeled a-b-c and d-e-f

inside elliptical region 1 and a third cluster g-h-i-j-k inside region 2. The question arises do a-b-c belong to the same main peak and should they be joined to d-e-f or not? Two independent criteria govern these decisions. First, even though the retention times are not the same for peak a, b and c it is deemed that there is enough overlap in their start and stop times to say that they really belong to the same main peak. Indeed, the overlap in terms of time is enough to warrant combining both a-b-c and d-e-f. However, the second criteria, that is the monomodality of the main peak tells us not to combine the two clusters. Inspection of the lower panel of Figure 5.5 shows that there is an intensity maximum in the a-b-c cluster and a second maximum in the d-e-f cluster thus if the two would be combined it would result in a main peak that had two maxima, which for a chromatographic peak is physically absurd.

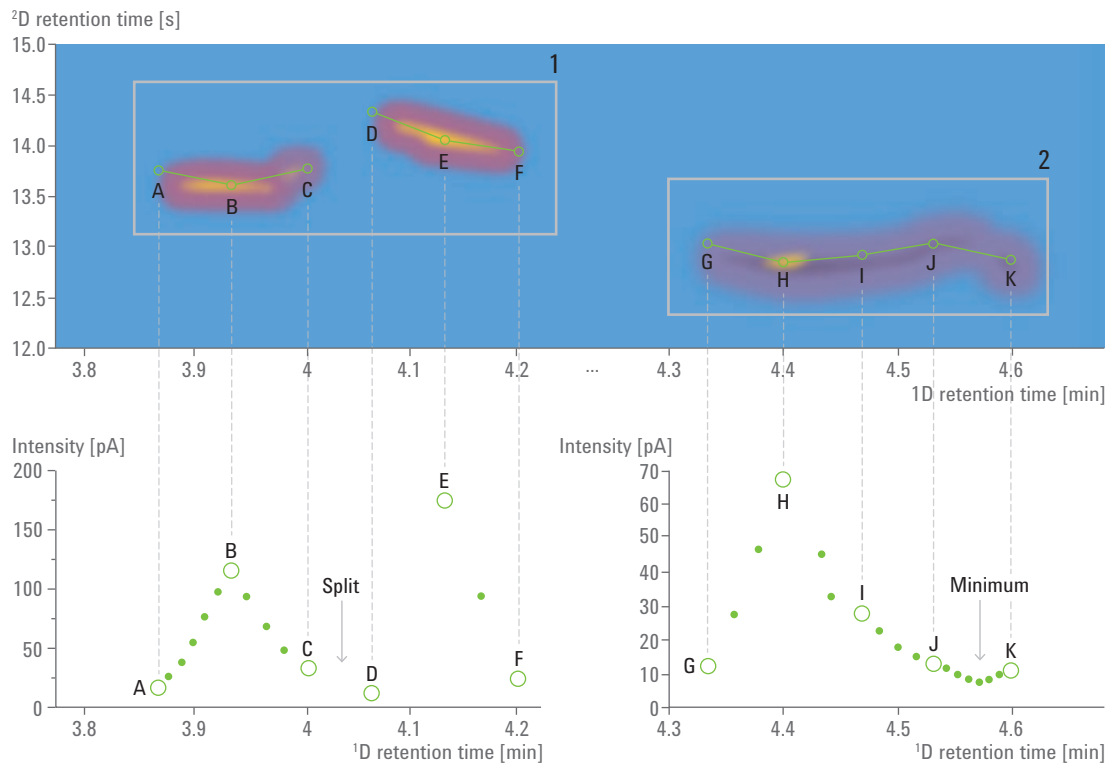


Figure 5.5 Theoretical chromatogram for illustration. In the lower panel, green circles show peak maxima profile, whereas green dots show interpolated points.

5.8

Total peak size

In 3D coordinates the integral of a peak would actually have units of volume but most commonly we simply add up the area or the peak heights of the individual ^2D peaks that are merged as described above. Some commercially available 2D-LC data analysis software packages indeed calculate the peak volume.

5.9

Comparison of quantitative performance of 1D-LC and LCxLC

There has been very little experimental work in which the precision of peak size measurements in 1D-LC and LCxLC were compared. Stoll *et al.*³¹ did report such a comparison for peaks from six compounds in 1D-LC and LCxLC. It is clear that the average precision of the 2D method is worse than that of the 1D method; some cases are much worse. However, if the values would be compared to typical 1D-LC/MS-quantifications the results would be comparable and one must not forget, that the 2D-LC approach will frequently be used because such complex samples will be handled that either a simple 1D-LC/UV approach would not work or a 1D-LC/MS approach would be required.

Solute	%RSD of 1D peak area	%RSD of 2D peak volume
Tyrosine	0.2	1.6
5-hydroxytryptophan	0.4	1.5
Tryptophan	0.3	4.5
Indole-3-acetic acid	2.2	3.0
Indole-3-propionic acid	1.2	8.0
Indole-3-acetonitrile	0.6	4.7

Table 5.1 Comparison of precision of peak size in 1D-LC versus 2D-LC (data from Reference 31).

In contrast there have been quite a few theoretical studies of the precision of 2D-LC^{73,79,80}. These studies point out that there are a number of issues that inherently complicate quantification in multidimensional chromatography relative to 1D-LC. First, any ^1D peak is generally modulated into a number of ^2D *subpeaks* (also called daughter peaks) thus each subpeak is necessarily smaller than the parent full peak. This inherently lowers their signal-to-noise ratio. Second, run-to-run variations in the ^1D system parameters (gradient, temperature, and so on) and column lead to variations in the retention times of the ^1D peaks, and this in turn leads to fluctuations in the sampling phase, which has some impact on the ^2D peak size and can lead to variations in the sum of the sub-peak areas. Third, baselines in fast ^2D chromatograms show substantially greater variation throughout the gradient as well as increased

short term noise. Fourth, in Stoll's work³¹ the ²D peaks were substantially tailed compared to his ¹D peaks, and thus more difficult to integrate accurately.

Note that the total peak size in 2D chromatography corresponds to a volume. It can be obtained in two distinct ways. The simplest and most direct way is merely to add up all the individual areas of the sub-peaks that comprise the main peak. This is known as the moments method. However, two groups^{79,81} have studied an alternative approach; namely, one fits the subpeak areas to a Gauss function of unknown total area, retention time and peak standard deviation (σ). To do this one needs to have at least three subpeaks from each parent peak. Provided that there are at least three subpeaks the Gaussian fit method gives impressively precise results which are substantially free of dependence on the modulation ratio and sampling phase. The work of Stoll was based on the simpler moments method. One can also quantify peaks by using the height of the sub-peaks; however, one report⁸¹ states that this approach is not as precise as using sub-peak areas. It is clear that a great deal more work needs to be done in the area of quantification. In Chapter 7 "The Future of 2D-LC" we delve into this issue in some detail especially in terms of the use of multivariate chemometric methods.

Jens Trafkowski

Product Manager for
2D-LC Solutions at
Agilent Technologies,
Walldbronn, Germany

As we already described in Section 1.4 “Fields of application of 2D-LC”, 2D-LC offers a wide variety of possible applications. In this chapter different applications are presented, illustrating that separation problems can be solved in many application fields when applying 2D-LC. The wide variety of 2D-LC work in general is illustrated by applications for several different analytical tasks, as well as various combinations of stationary phases and detection possibilities. It is clear that not all possibilities can be covered, however, the applications shown here give you a good overview of what can be achieved now and in future.

While this chapter presents a selection of 2D-LC applications from fields such as biopharmaceuticals, foods and natural products, further applications can be accessed through the Agilent Application Finder at: www.agilent.com/chem/application-finder

6.1**Natural products and
herbal extracts –
Analysis of taxanes**

Taxol (paclitaxel, see Figure 6.1) is one of the best chemotherapeutic ingredients that originate from a natural source. It is obtained from the bark and from cell cultures of *Taxus brevifolia*. There is much interest to farm the plant with the highest possible taxol concentration as the natural amounts are actually very low. Therefore an accurate analysis of the amount is necessary but at the same time very demanding due to the low concentration and the complex sample matrix.

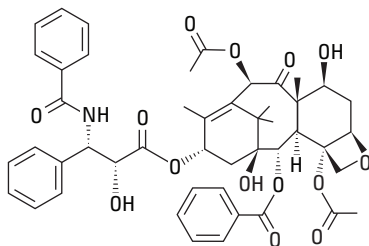


Figure 6.1 Structure of taxol (paclitaxel).

Figure 6.2 shows clearly the large impact of the matrix on the one-dimensional LC separation and the need to dramatically enlarge the peak capacity. It is questionable whether an optimized 1D method would lead to a satisfactory separation at all. Hence comprehensive 2D-LC is the method of choice. In this example RP columns were used in both dimensions for separation of analytes and the matrix, and for separation of the analytes themselves (RP_xRP). Identification, qualitative confirmation and quantitative analysis are performed using a DAD or single quadrupole MS in positive and negative APCI mode.

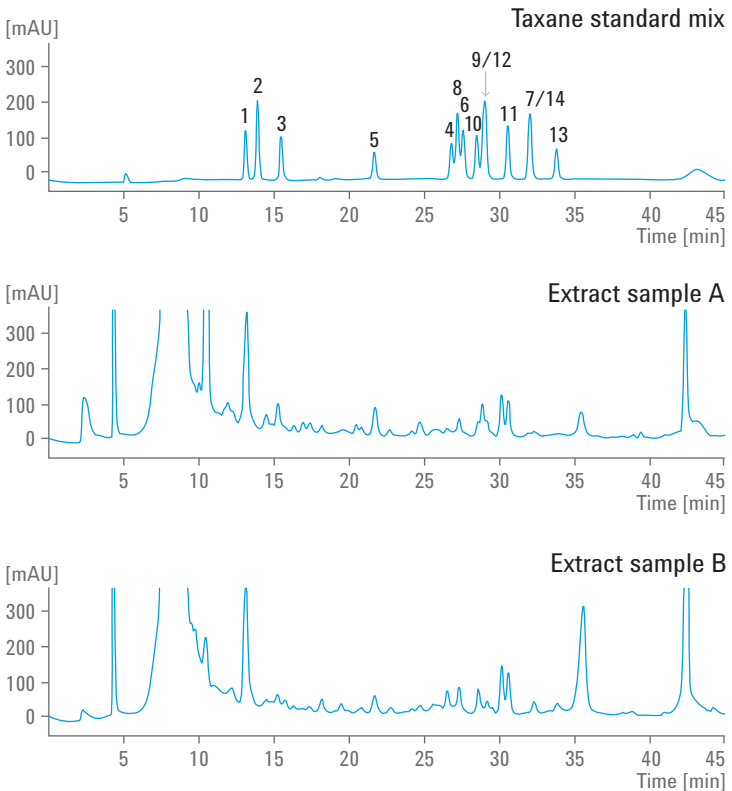


Figure 6.2 Comparison of a one-dimensional analysis of the taxane standard mixture (10 µg/mL each) and *Taxus* sp. extracts.

Figure 6.3 shows the 2D separation of two different extracts compared to a standard. The two most interesting taxanes, cephalomannine (10) and paclitaxel (12), were found in both extracts and could be quantified. With this information it is possible to determine which plant candidate should be farmed as having the highest amount of these important taxanes.

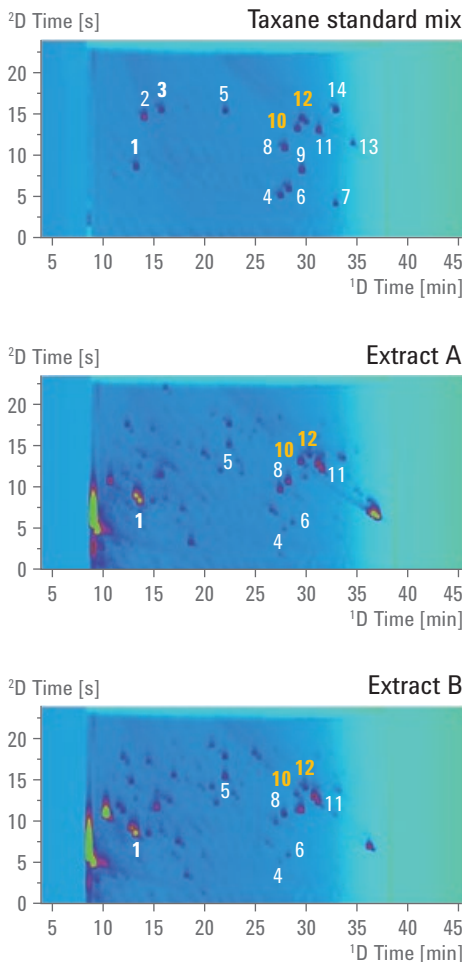
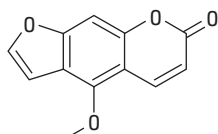


Figure 6.3 Comparison of comprehensive two-dimensional (LC_xLC) analysis of the taxane standard mixture (4 µg/mL each) and extracts.

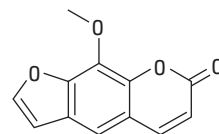
6.2

Natural product profiling – Analysis of citrus oil extracts

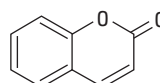
Citrus oils are widely used in cosmetics. However, due to the carcinogenic potential of furocoumarins it is important to determine their concentrations in the essential oils, which are widely used in personal health care products. Essential oils are by nature characterized by high matrix loads and their analysis suffers from the lack of sufficient separation, a fact directly leading to the idea of using 2D-LC to enable the best possible separation. For this matrix the highly orthogonal combination of normal phase and reversed phase chromatography (NPxRP) is challenging but leads to very good separation results. Single quadrupole MS in positive APCI mode and DAD were used for detection.



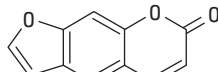
5-MOP (5-methoxysoralen, bergapten)



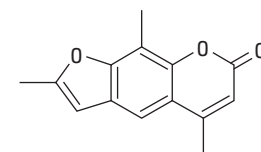
8-MOP (8-methoxysoralen, xanthotoxin)



Coumarin



Psoralen



Trioxsalen (trimethylpsoralen)

Figure 6.4 Structure of commercially available furocoumarins.

5-MOP was chosen as target compound and could be determined in three out of four samples, whereby UV spectra were used for confirmation. The presence of this carcinogenic compound shows the need to take a closer look at this group of ingredients for several cosmetic products to evaluate potential risks to the consumer. Not only the qualitative, but also the quantitative analysis can be done by applying comprehensive 2D-LC – a very important criteria for risk evaluation.

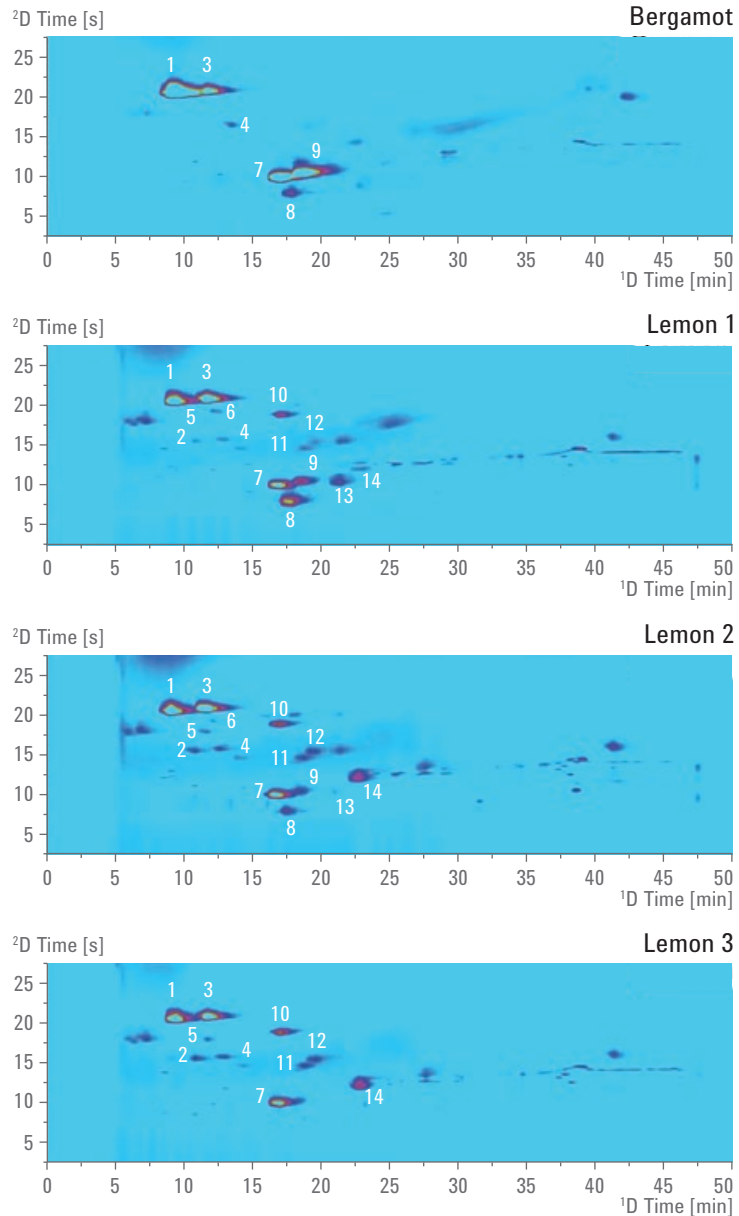


Figure 6.5 Comprehensive 2D-LC analysis of citrus oils.

- | | |
|--------------------------------------|---|
| 1 5-Geranyloxypsoralen | 9 5-MOP |
| 2 Unknown | 10 5-Geranyloxypsoralen |
| 3 5-Geranyloxy-7-methoxycoumarin | 11 Unknown |
| 4 5-Isopentenyloxy-7-methoxycoumarin | 12 5-Isopentenyloxy-8-(2,3-epoxyisopentenyloxy)psoralen |
| 5 5-Geranyloxy-8-methoxysoralen | 13 5,8-Dimethoxysoralen |
| 6 Unknown | 14 5-(2,3-Epoxyisopentenyloxy)psoralen |
| 7 5,7-Dimethoxycoumarin | |
| 8 Unknown | |

6.3

Biopharmaceuticals – Analysis of monoclonal antibodies

For several years the drug market has been changing from typical small molecule pharmaceuticals towards biopharmaceuticals such as monoclonal antibodies (mAb), fusion proteins or therapeutic proteins. Proteomic workflows are now facing the huge complexity associated with peptide mapping of these very large proteins.

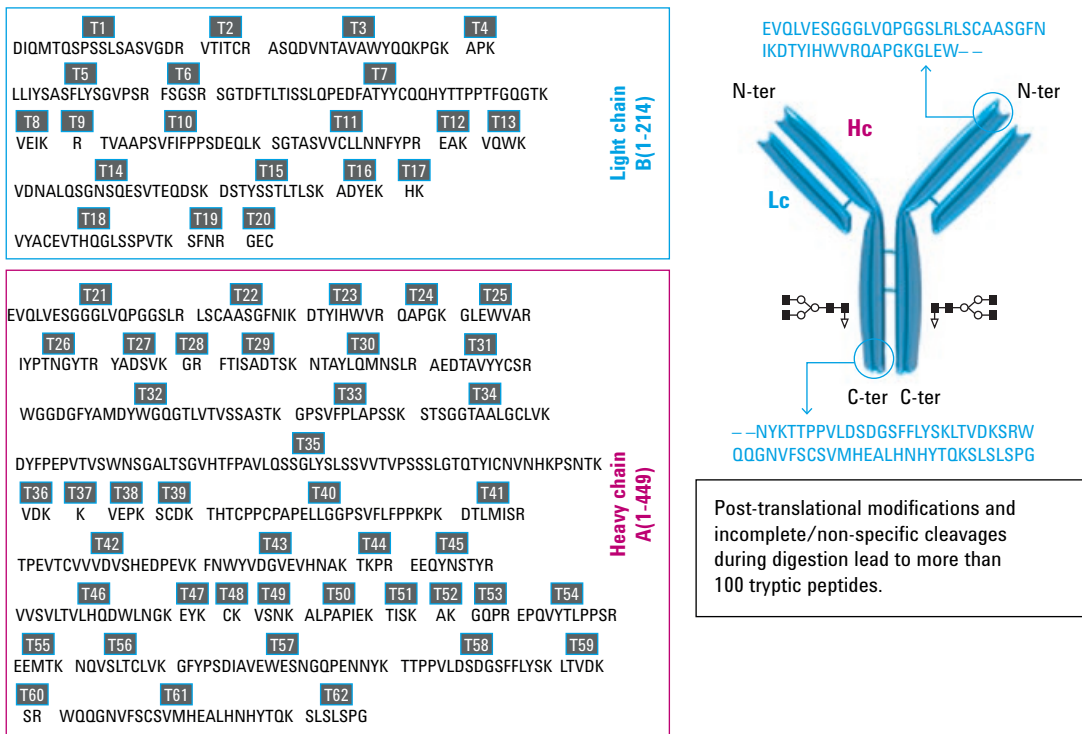


Figure 6.6 Structure and amino acid sequence of the protein Herceptin. Identity peptides are labeled T1-T62.

In this application, trastuzumab, marked as Herceptin, a 150 kDa mAb, was analyzed using comprehensive 2D-LC after tryptic digestion. The best orthogonality for more than 100 peptides was achieved by applying the combination of strong cation exchange and reversed-phase chromatography (SXCxRP). DAD detection was used for standard analysis, and quantification and identification of the peptides was performed with QTOF MS. In addition to SXCxRP, a combination of HILIC and RP was applied to gain complimentary data, especially to separate deamidated

peptides from their native forms. Comprehensive HILICxRP couples two really orthogonal techniques, but often results in high acetonitrile concentrations in the modulation valve. This can cause a loss of separation power and a breakthrough of early eluting peptides in the second dimension due to the high eluting power of acetonitrile in RP chromatography. Therefore the ¹D flow rate was reduced to 50 µL/min, the ²D flow rate was increased to 4 mL/min, and an additional dilution tee was added to dilute the effluent from the first dimension with water.

The method was used for the determination of stress-related changes to peptides as shown in Figure 6.7. Even low levels of oxidative or pH stress can be determined with this analytical setup.

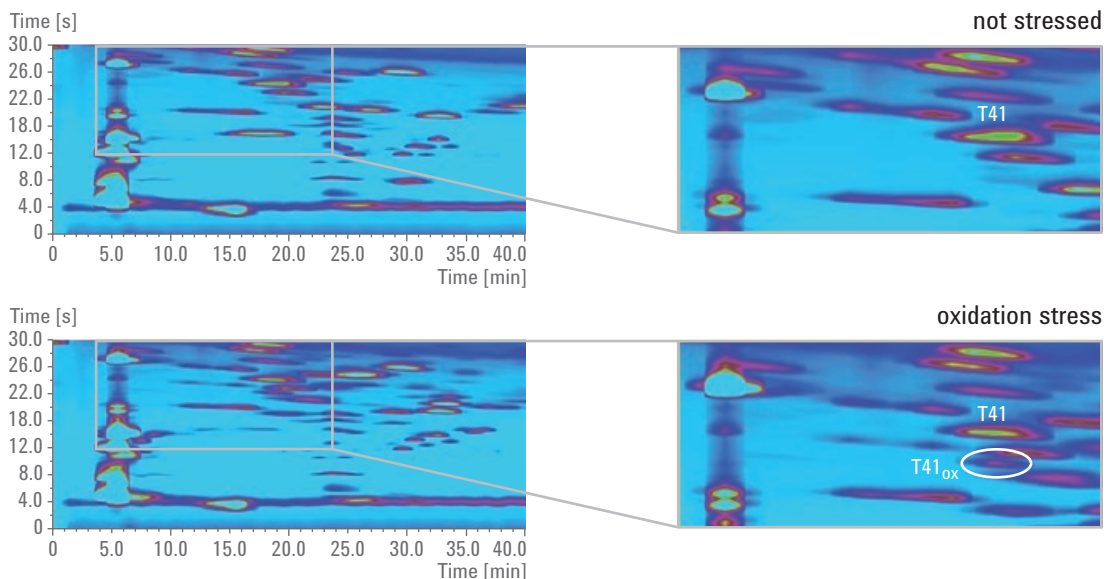


Figure 6.7 LCxLC contour plot for the analysis of a tryptic digest of non-stressed and oxidatively stressed Herceptin.

In addition to the coupling of a SCX with an RP phase, the combination of a hydrophilic interaction liquid chromatography (HILIC) with RP phase delivered very good orthogonality. The advantage of HILICxRP over SCXxRP is that the HILIC separation involves less salt than the SCX separation, thus the coupling of the two dimensions is easier and a desalting step is not needed. The setup of the 2D-LC-DAD-QTOF system is shown in Figure 6.8.

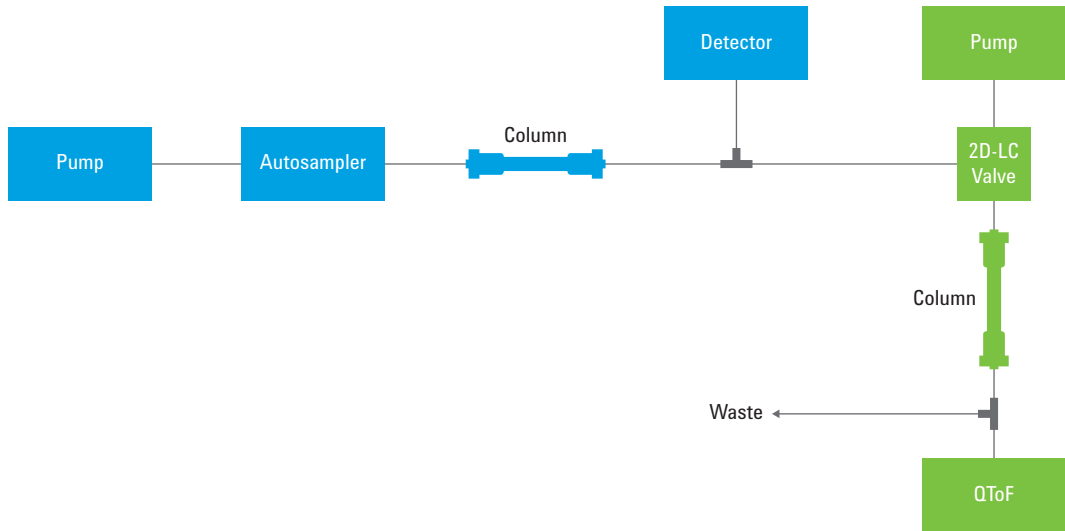


Figure 6.8 Schematic of 2D-LC system with diode array detector and QToF MS.

The chief difficulty with combining HILIC and RP concerns the mismatch between the eluents used in the two separations. The retention mechanisms in the two cases are very different, and HILIC separations tend to involve acetonitrile-rich eluents, whereas RP separations involve water-rich ones. This mismatch is handled by reducing the flow rate of the first dimension to 50 µL/min and splitting the flow into the second dimension. Even though the setup is more complex with the split, the analytical advantages outweigh the disadvantage of slightly higher complexity.

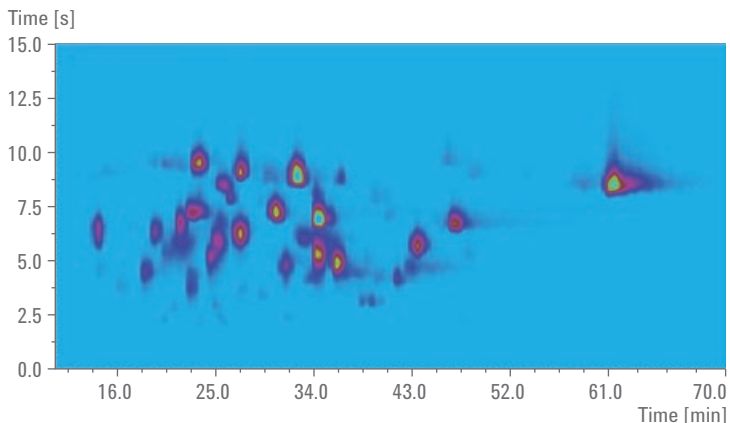


Figure 6.9 LCxLC chromatogram obtained from a HILICxRP separation of mAb tryptic peptides.

In both the SCXxRP and HILICxRP separations promising results were obtained for the analysis of monoclonal antibodies. To be sure, 2D-LC will gain more and more importance for the identification, quantitative analysis and purity control of biopharmaceuticals, and for peptide mapping in general.

6.4 Chemicals – Determination of homolog technical detergents

The chemical class of fatty alcohol ethoxylates are nonionic surfactants, which are widely used in many personal healthcare products (PHCP). Besides the different chain lengths from C12 to C18, the degree of ethoxylation and the combination of differently ethoxylated compounds are the important factors that indicate the product quality and product identity.

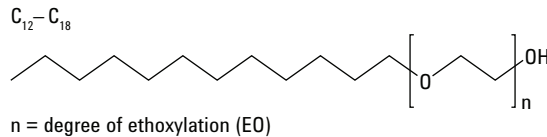


Figure 6.10 Structural formula of fatty alcohol ethoxylate compounds

The combination of HILIC and RP is an ideal match for this demanding separation. While in the first dimension (HILIC) the compounds are separated by their degree of ethoxylation, they are separated in the second dimension (RP) by the length of the hydrophobic tail. As illustrated in Figure 6.11 the two separations show almost perfect orthogonality.

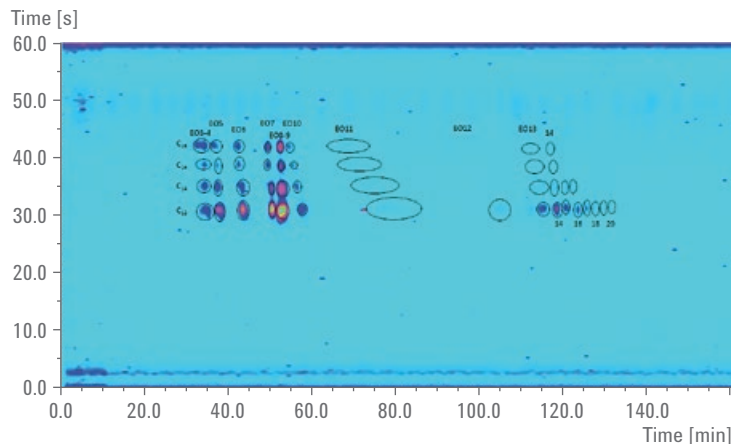


Figure 6.11 2D separation of a technical mixture of fatty alcohol ethoxylates of fatty alcohols C12 to C18 with a degree of ethoxylation of 3 to 20.

Detection of the technical detergents was performed using an ELSD as most of the analytes do not exhibit absorption of UV light. Due to the high sensitivity and data rate this detection is also a very useful tool for the whole analysis. Further, detection using mass spectrometry can enhance the detection sensitivity.

6.5 Pharmaceuticals – Determination of impurities

One of the most important tasks in pharmaceutical analysis is the determination of impurities. Impurities usually resemble the main compound or active pharmaceutical ingredient (API), but are only allowed up to certain concentration levels in the drug product. It is important to clearly distinguish between the different analytes, especially as they are often very chemically similar. Therefore it is a clear goal to separate the API from its impurities to ensure the best possible quality control.

In this application the detection of an additional impurity using heart-cutting 2D-LC is shown. In the original profiling analysis six impurities were determined as shown in Figure 6.12.

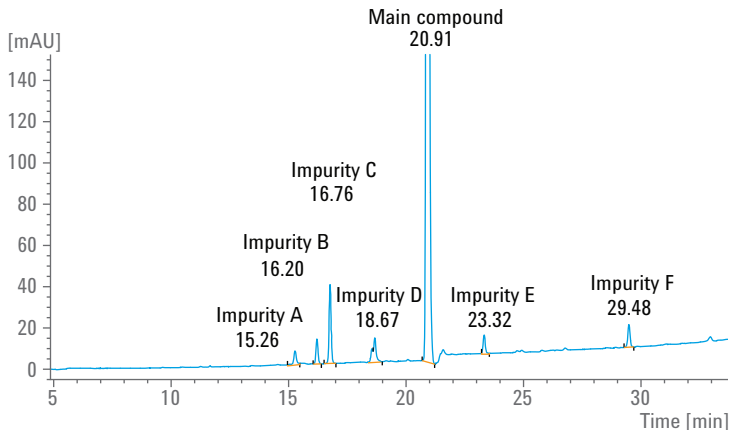


Figure 6.12 Original 1D-LC Impurity Profiling.

The interesting question is now whether additional impurities coelute with the peak of the main compound. A heart-cut of the main compound was taken and analyzed on the second dimension, leading to two additional impurities, which were found as shown in Figure 6.13. Impurity H could be confirmed by addition of a standard of this compound.

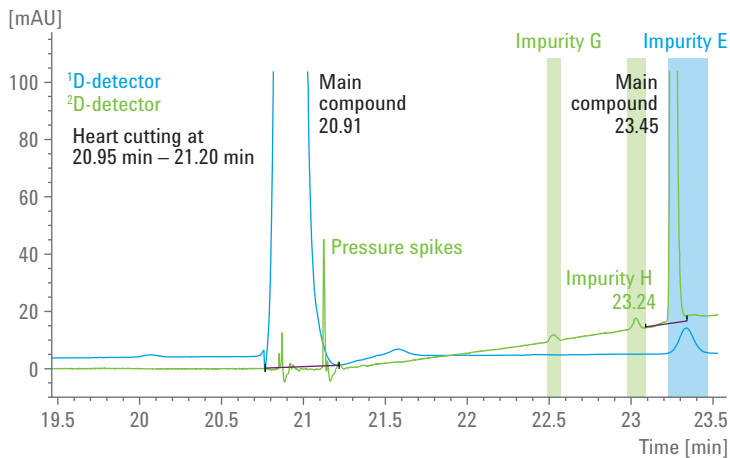


Figure 6.13 Main chromatogram (blue) and chromatogram of heart cut (green). Heart cut from the main peak between 20.75 to 21.00 minutes. Pressure spikes caused by valve switching at start and end of sampling. Delay caused by delay volume plus column volume.

6.6 Food testing – Polyphenols in beverages

Polyphenols are well known as natural antioxidants, occurring in many fruits that are used for juices, wine or other beverages such as beer or lemonades. Due to their antioxidant capacities polyphenols are free radical scavengers with positive effects against cancer. The matrix is always highly complex and therefore beverage samples like beer, wine or juices are *ideal candidates* for analysis by 2D-LC.

In the following application polyphenols are determined in fruit juices and in red wine. The qualitative and quantitative analysis is performed by comprehensive 2D-LC coupling two different reversed phase separations. After syringe filtering the samples, they were directly injected. Figure 6.14 shows a 3D plot of a standard mixture, illustrating the different separation performance of the two stationary phases.

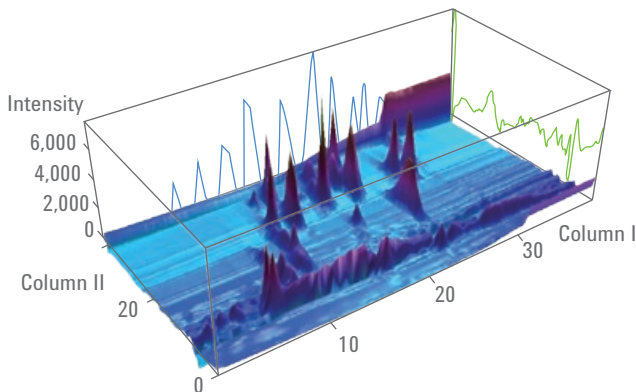


Figure 6.14 Chromatogram for the LCxLC separation of a standard mixture of polyphenols.

26 antioxidant compounds were in the standard mixture, delivering highly reproducible retention times for both dimensions (RSD typically better than 0.5 percent in the second dimension). Due to the precise and accurate retention times in both dimensions it was possible to identify many compounds in real-life samples. Further, the identified compounds could be confirmed by their DAD spectra, as illustrated in Figure 6.15.

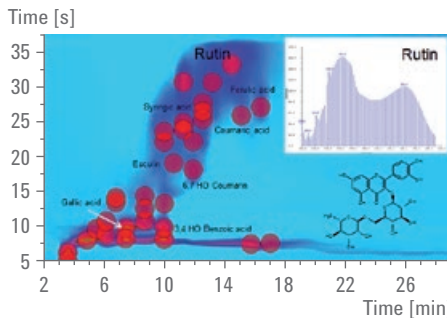


Figure 6.15 Separation of a mixed antioxidant juice containing red and green grape, apple, black current, cherry, cranberry, pomegranate and bilberry.

6.7

Food testing – Quality control of virgin olive oil

Phenolic compounds in olive oil play important roles, both presenting antioxidant value and in contributing to the flavor profile. Therefore good separation and determination of these often very similar substances in the very lipophilic matrix is not easy to achieve and comprehensive 2D-LC is the method of choice.

A complete method including QTOF detection enables characterization and differentiation of olive oils from different sources. Besides phenolic substances, which can be identified by comparison to authentic standards, many additional substances are separated in the method, so that they can be identified in subsequent analyses.

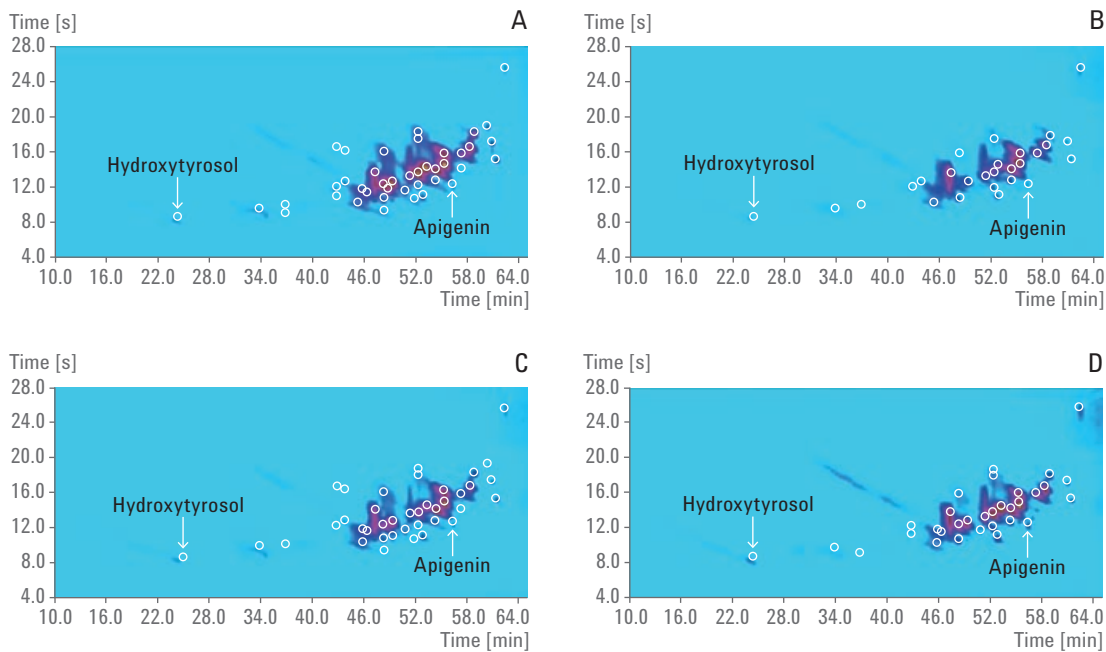


Figure 6.16 LCxLC chromatograms obtained from the separations of olive oils A-D with MS detection.

The method used a characteristic gradient shift for the ^2D gradient. This reflects the special chemical character of the analytes and the lipophilic profile of the matrix.

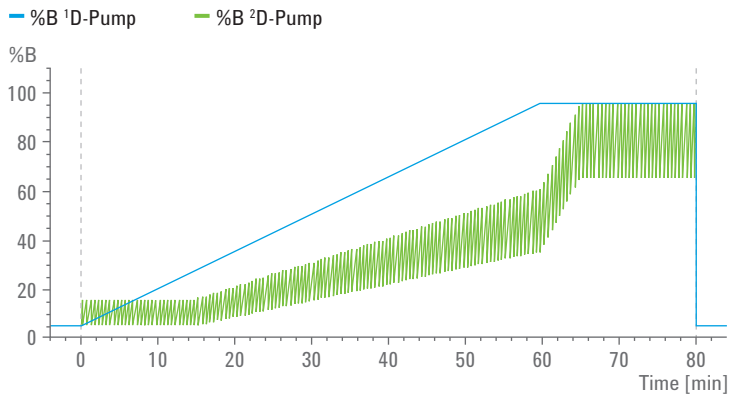


Figure 6.17 ^2D gradients with characteristic shift.

Based on the different concentration of phenols, the four olive oils can be characterized and compared.

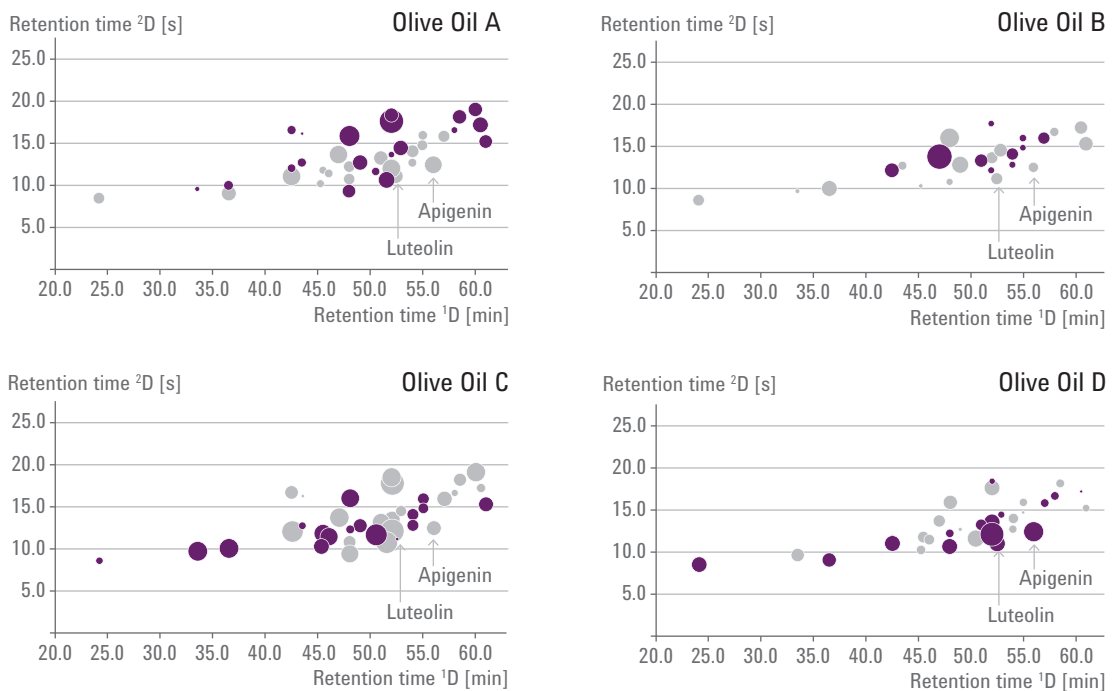


Figure 6.18 Differences between peak detection in each olive oil and an average of the olive oils analyzed (purple circles indicate peaks with a higher percent response than the average percent response of that substance; grey circles indicate peaks with a lower percent response than the average; the area of each circle indicates the magnitude of the difference between the sample and the average).

6.8

Food testing – Analysis of beer

Due to high variability during production, different beers are characterized by many different compound classes and therefore by wide variability in their chemical compositions. To address the separation of the different compounds and the separation of the different classes, polyphenols can be separated well using RP columns, while other large but very polar compounds such as carbohydrates can be better separated by SEC or IEX.

Three different combinations of columns have been tested in this work, as shown in Figure 6.19. These combinations produce peak patterns in the 2D chromatograms that look totally different. These results help inform the choice of the 'best' set of columns, depending on the needs of a particular analysis and the characteristics of the sample.

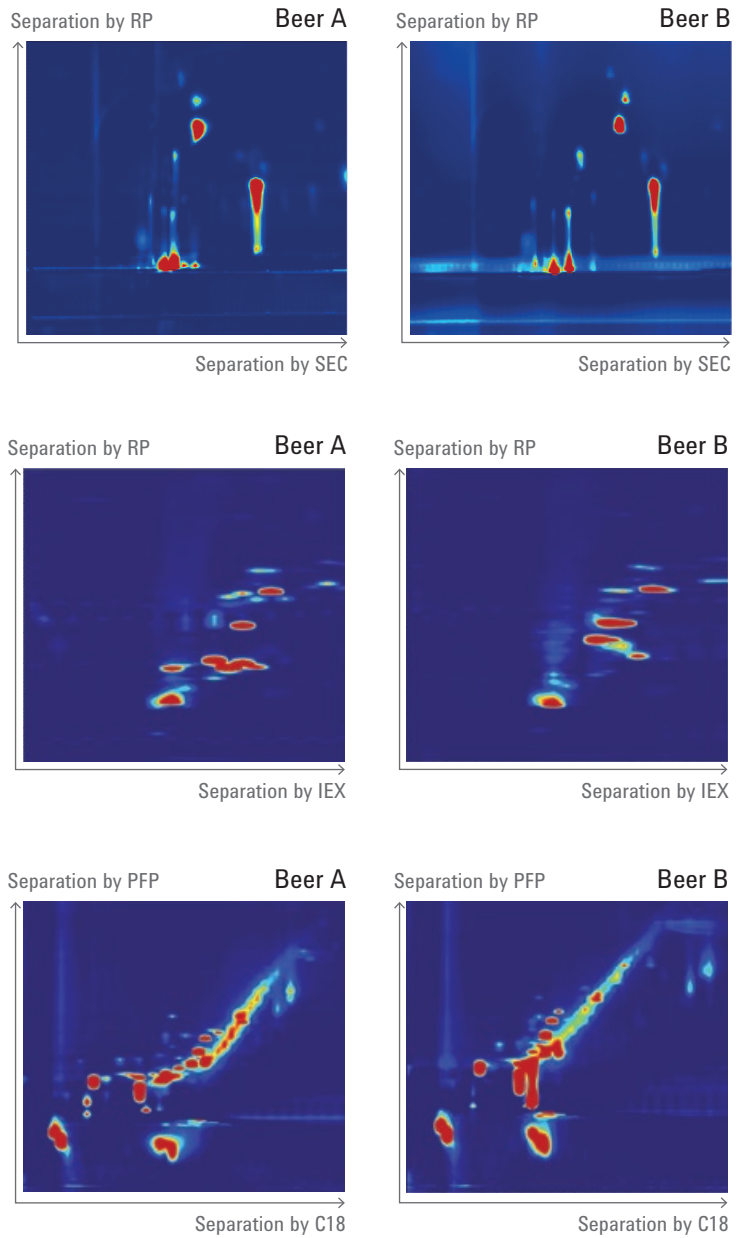


Figure 6.19 LCxLC chromatograms obtained from the comparison of two different beer samples (A and B) using three different columns combinations:
A) SECxRP, B) IEXxRP, and C) RPxRP.

6.9

Summary of application methodologies

The applications presented in this Primer only hint at the numerous potential applications of 2D-LC. Whether it is the analysis of natural products, food, fingerprinting complex mixtures, or the wide range of pharmaceutical and biopharmaceutical applications, 2D-LC will grow in importance in the analytical landscape. In order to make this happen, it is crucial to lower the threshold to use this technique as much as possible. This will enable also inexperienced users to start with 2D-LC.

More applications are expected to come; including the complex analysis of polymers, or authentication of beverages such as beer. One area that holds much potential is the large field of different metabolomics and lipidomics workflows with complex analyte profiles.

The following tables summarize the chromatographic conditions used in the applications presented above and illustrate the tremendous variety of chromatographic combinations used in these applications.

Natural products and herbal extracts – Analysis of taxanes	
First-dimension column	Agilent ZORBAX Eclipse Plus C18, 2.1 x 100 mm, 3.5 µm (p/n 959793-902)
Solvent A	Water
Solvent B	Methanol
Flow rate	60 µL/min
Gradient	30 %B at 0 minutes 55 %B at 1.5 minutes 85 %B at 36 minutes 100 %B at 37 minutes 100 %B at 45 minutes 30 %B 5 minutes posttime
Column temperature	30 °C
Second-dimension column	
Solvent A	Water + 0.008 % formic acid
Solvent B	Acetonitrile + 0.004 % formic acid
Flow rate	4 mL/min
Idle flow rate	0.4 mL/min
Initial gradient	20 %B at 0 minutes 33 %B at 0.3 minutes 20 %B at 0.31 minutes
Gradient modulation/shifting	Lower limit: 20 %B at 0 minutes 55 %B at 37 m minutes in 85 %B at 42 minutes Upper limit: 33 %B at 0.3 minutes 85 %B at 37 mi minutes n
Modulation range	9 to 37 minutes
Column temperature	40 °C
Modulation time	0.4 min (60 % loop filling)
Loop Setup	Two 40 µL loops, cocurrent configuration
Injection Volume	5 µL (injection program, mixed with 10 µL water plug)
Needle Wash	5 seconds flush port (methanol)
Sample temperature	12 °C
2D DAD Detection	Signal 228/8 nm, reference 370/60 nm 80 Hz
MS Detection	Single quadrupole with APCI Drying gas flow 5 L/min Drying gas temperature 320 °C Nebulizer pressure 50 psi Vaporizer temperature 380 °C Capillary voltage 3,000 V (pos. and neg. mode) Corona current 4 µA (pos. mode), 15 µA (neg. mode) Fast scan 250 to 1,000 m/z Fragmentor 120 V

Natural product profiling – Analysis of citrus oil extracts

First-dimension column	Agilent ZORBAX RX-SIL, 1.0 x 150 mm, 3.5 µm (custom packed)
Solvent A	Hexane/Ethyl acetate 95/5 (v/v)
Solvent B	Ethyl acetate
Flow rate	35 µL/min
Gradient	0 %B at 0 minutes 40 %B at 35 minutes 70 %B at 36 minutes 90 %B at 60 minutes 0 %B 10 minutes posttime
Column temperature	25 °C

Second-dimension column	Agilent ZORBAX RRHD Eclipse Plus C18, 3.0 x 50 mm, 1.8 µm (p/n 959757-302)
Solvent A	Water
Solvent B	Acetonitrile
Flow rate	2.2 mL/min
Idle flow rate	0.3 mL/min
Initial gradient	0 %B at 0 minutes 100 %B at 0.38 minutes 0 %B at 0.39 minutes
Gradient modulation/shifting	No shifted gradients
Modulation range	2.5 to 52 minutes
Column temperature	40 °C
Modulation time	0.5 minutes
Loop setup	Two 20-µL loops, cocurrent configuration
Injection volume	Pure oil: 0.4 µL Oil mix: 0.8 µL
Needle wash	6 seconds flush port (ethyl acetate/isopropanol/acetone)
Sample temperature	15 °C
2D DAD detection	Signal 315/4 nm, reference 500/50 nm 80 Hz
MS detection	Single quadrupole with APCI Drying gas flow 7 L/min Drying gas temperature 340 °C Nebulizer pressure 55 psi Vaporizer temperature 410 °C Capillary voltage 3,000 V (pos. and neg. mode) Corona current 4 µA (pos. mode), 15 µA (neg. mode) Fast scan 150 to 700 m/z Fragmentor 90 V

Biopharmaceuticals – Analysis of monoclonal antibodies I

First-dimension column	MIC-15-Polysulfoethyl-Asp, 1.0 x 150 mm, 5 µm (PolyLC Inc.)
Solvent A	5 mM phosphate pH 3 in 5 % acetonitrile
Solvent B	5 mM phosphate pH 3 in 5 % acetonitrile + 400 mM NaCl
Flow rate	60 µL/min
Gradient	3 %B at 0 minutes 25 %B at 30 minutes 45 %B at 50 minutes 100 %B at 55 minutes 100 %B at 58 minutes 3 %B 13 minutes posttime
Column temperature	25 °C
Second-dimension column	Agilent ZORBAX Eclipse Plus C18, 4.6 x 50 mm, 3.5 µm (p/n 959943-902)
Solvent A	Water + 0.1 % phosphoric acid
Solvent B	Acetonitrile
Flow rate	3.5 mL/min
Idle flow rate	0.5 mL/min
Initial gradient	2 %B at 0 minutes 35 %B at 0.43 minutes
Gradient modulation/shifting	Gradient modulation 35 % B at 0.43 minutes to 65 % B at 50 minutes to 100 % B at 51 minutes
Modulation range	1 to 53 minutes
Column temperature	55 °C
Modulation time	0.5 minutes
Loop setup	Two 40-µL loops, cocurrent configuration
Injection volume	20 µL
Needle wash	6 seconds flushport (5 mM phosphate pH 3 in 5 % acetonitrile)
Sample temperature	4 °C
2D DAD detection	Signal 214/4 nm, reference 360/100 nm 80 Hz

Biopharmaceuticals – Analysis of monoclonal antibodies II

First-dimension column	Agilent ZORBAX RRHD 300-HILIC, 2.1 x 100 mm, 1.8 µm (p/n 858750-901)
Solvent A	Water, 50mM ammonium formate, pH 4.5
Solvent B	90% ACN + 10 % solvent A
Flow rate	50 µL/min
Gradient	90 %B at 0 minutes 45 %B at 75 minutes 0 %B at 80 minutes 0 %B at 85 minutes 90 %B 20 minutes posttime
Column temperature	30°C
Second-dimension column	Agilent ZORBAX Eclipse Plus C18, 4.6 x 50 mm, 3.5 µm (p/n 959943-902)
Solvent A	Water + 0.1% formic acid
Solvent B	Acetonitrile
Flow rate	4 mL/min
Idle flow rate	0.25 mL/min
Initial gradient	0 %B at 0 minutes 60 %B at 0.35 minutes
Gradient modulation/shifting	
Modulation range	12 to 69 minutes
TCC	30 °C
Modulation time	0.45 minutes
Loop setup	Two 40-µL loops, cocurrent configuration
Injection volume	3 µL
Needle Wash	5 seconds flush port (water/acetonitrile 25/75)
Sample temperature	4°C
1D DAD detection	Signal 280/4 nm, reference 400/100 nm 10 Hz
MS Detection	Jet Stream, ESI+ Drying gas flow 10 L/min Drying gas temperature 340 °C Nebulizer pressure 45 psi Vaporizer temperature 400 °C Capillary voltage 3,500 V Nozzle voltage 1,000 V Fragmentor 175 V Centroid data at 8 spectra/s Extended dynamic range 2 GHz Resolution 10,000 for m/z 1,000

Chemicals – Determination of homolog technical detergents

First-dimension column	SeQuant, Sweden, ZIC-HILIC, 2.1 x 250 mm, 5 µm
Solvent A	Water, 50 mM ammonium acetate
Solvent B	Acetonitrile
Flow rate	25 µL/min
Gradient	97 %B at 0 minutes 97 %B at 10 minutes 85 %B at 60 minutes 85 %B at 100 minutes in 70 %B at 120 minutes 70 %B at 140 minutes 97 %B at 160 minutes 97 %B 20 minutes posttime
Column temperature	25 °C
Second-dimension column	Reprospher C8-Aqua, 4.6 x 30 mm, 5 µm, (Dr. Maisch GmbH)
Solvent A	Water + 10 mM ammonium acetate
Solvent B	Methanol
Flow rate	3 mL/min
Idle flow rate	
Initial gradient	50 %B at 0 minutes 70 %B at 0.1 minutes 95 %B at 0.65 minutes 95 %B at 0.75 minutes 50 %B at 0.80 minutes 50 %B at 1.00 minutes
Gradient modulation/shifting	No gradient shift
Modulation range	Full range
Column temperature	50 °C
Modulation time	1 minute
Loop setup	Two 40-µL loops, cocurrent configuration
Injection volume	5 µL
Needle wash	6 seconds in methanol
Sample temperature	8 °C
ELSD detection	Evaporator temperature 80 °C Nebulizer temperature 70 °C Data rate 40 Hz Gas flow 1.3 SLM

Pharmaceuticals – Determination of impurities

First-dimension column	Agilent ZORBAX RRHD Eclipse Plus C18, 2.1 x 150 mm, 1.8 µm (p/n 959759-902)
Solvent A	Water + 0.1% formic acid
Solvent B	Acetonitrile + 0.1% formic acid
Flow rate	200 µL/min
Gradient	5 %B at 0 minutes 95 %B at 30 minutes 95 %B at 35 minutes 5 %B 15 minutes posttime
Column temperature	25°C
Second-dimension column	Agilent ZORBAX RRHD Eclipse Plus Phenyl-Hexyl, 3.0 x 50 mm, 1.8 µm (p/n 959757-312)
Solvent A	Water + 0.1% formic acid
Solvent B	Methanol + 0.1% formic acid
Flow rate	3 mL/min
Idle flow rate	N/A
Initial gradient	Full gradient: 5 %B at 0 minutes 15 %B at 10 minutes
Gradient modulation/shifting	Not applicable for heart-cutting 2D-LC
Modulation range	Not applicable
Column temperature	60 °C
Modulation time	Not applicable
Loop setup	One 80-µL loop and a short cut capillary
Injection volume	3 µL
Needle wash	6 seconds in methanol
Sample temperature	8 °C
1D DAD detection	Signal 254/4 nm, reference 360/16 nm 20 Hz, 10-mm Max-Light flow cell
2D DAD detection	Signal 254/4 nm, reference 360/16 nm 20 Hz, 60-mm Max-Light flow cell

Food testing – Polyphenols in beverages

Column	Agilent ZORBAX RRHD Eclipse Plus, C18, 2.1 x 150 mm, 1.8 µm
Solvent A	Water + 0.1% formic acid
Solvent B	Acetonitrile + 0.1% formic acid
Flow rate	100 µL/min
Gradient	5 %B at 0 minutes 95 %B at 30 minutes 95 %B at 40 minutes 5 %B 15 minutes posttime
Column temperature	25 °C
Second-dimension column	Agilent ZORBAX RRHD Eclipse Plus Phenyl-Hexyl, 3.0 x 50 mm, 1.8 µm
Solvent A	Water + 0.1% formic acid
Solvent B	Acetonitrile + 0.1% formic acid
Flow rate	3 mL/min
Idle flow rate	Not applicable
Initial gradient	0 %B at 0 minutes 60 %B at 0.5 minutes 0 %B at 0.51 minutes 0 %B at 0.65 minutes
Gradient modulation/shifting	5 %B at 0 minutes to 50 %B at 30 minutes 15 %B at 0.5 minutes to 95 %B at 30 minutes 5 %B at 0.51 minutes to 50 %B at 30 minutes 5 %B at 0.65 minutes to 50 %B at 30 minutes
Modulation range	Full range
Column temperature	60 °C
Modulation time	0.65 minutes
Loop setup	Two 80-µL loops
Injection volume	5 µL
Needle wash	6 seconds in methanol
Sample temperature	8 °C
2D DAD detection	Signal 260 nm/4 nm, reference off 80 Hz, 60-mm Max-Light flow cell

Food testing – Quality control of virgin olive oil

First-dimension column	Agilent ZORBAX RRHD Eclipse Plus Phenyl-Hexyl, 2.1 x 150 mm, 1.8 µm (p/n 959759-912)
Solvent A	Water + 0.1% formic acid
Solvent B	Methanol + 0.1% formic acid
Flow rate	50 µL/min
Gradient	5 %B at 0 minutes 95 %B at 60 minutes 95 %B at 80 minutes 5 %B 30 minutes posttime
Column temperature	25 °C
Second-dimension column	Agilent ZORBAX RRHD Eclipse Plus, C18, 3.0 x 50 mm, 1.8 µm (p/n 959757-302)
Solvent A	Water + 0.1% formic acid
Solvent B	Acetonitrile + 0.1% formic acid
Flow rate	3 mL/min
Idle flow rate	Not applicable
Initial gradient	5 %B at 0 minutes 15 %B at 0.35 minutes 5 %B at 0.36 minutes 5 %B at 0.5 minutes 5 %B 30 minutes posttime
Gradient modulation/shifting	Not applicable
Modulation range	Full range
Column temperature	60 °C
Modulation time	0.5 minutes
Loop setup	Two 60-µL, cocurrent configuration
Injection volume	20 µL
Needle wash	6 seconds in methanol
Sample temperature	6 °C
2D DAD detection	1:1 split between DAD and MS Signal 260 nm/4 nm, reference 360 nm/100 nm Signal 280 nm/4 nm, reference 360 nm/100 nm 80 Hz
MS Detection	ESI- Gas flow 9 L/min Gas temperature 300 °C Nebulizer pressure 60 psi Sheath gas flow 12 L/min Sheath gas temperature 350 °C Capillary voltage -4,500 V Nozzle voltage -300V Acquisition rate 10 spectra/s

Food testing – Analysis of beer I

First-dimension column	TOSOH TSKgel Super Oligo PW, 6.0 x 150 mm
Solvent A	20 % methanol in water + 50 mM ammonium acetate
Solvent B	Methanol
Flow rate	100 µL/min
Gradient	0 %B at 0 minutes 0 %B at 60 minutes 20 %B at 65 minutes 20 %B at 70 minutes
Column temperature	40 °C
Second-dimension column	Agilent ZORBAX RRHT SB-Aq , 3.0 x 50mm, 1.8 µm (p/n 827975-314)
Solvent A	Water
Solvent B	Acetonitrile
Flow rate	2 mL/min
Idle flow rate	Not applicable
Initial gradient	0 %B at 0 minutes 20 %B at 0.5 minutes 0 %B at 0.51 m minutes in 0 %B at 0.65 minutes
Gradient modulation/shifting	Not applicable
Modulation range	Full range
Column temperature	50 °C
Modulation time	0.65 minutes
Loop setup	Two 40-µL loops
Injection volume	5 µL
Needle wash	Not applicable
Sample temperature	Not applicable
2D DAD detection	Signal 210 nm/4 nm, reference off Signal 254 nm/4 nm, reference off

Food testing – Analysis of beer II

First-dimension column	Agilent ZORBAX 300-SCX, 2.1 x 150 mm, 5 µm (p/n 883700-714)
Solvent A	Water + 10 mM ammonium acetate (isocratic)
Solvent B	Not applicable
Flow rate	80 µL/min
Gradient	Total run time 25 min
Column temperature	40 °C

Second-dimension column Agilent ZORBAX RRHT SB-Aq, 3.0 x 50 mm, 1.8 µm (p/n 827975-314)

Solvent A	Water
Solvent B	Acetonitrile
Flow rate	2 mL/min
Idle flow rate	Not applicable
Initial gradient	0 %B at 0 minutes 20 %B at 0.5 minutes 0 %B at 0.51 minutes 0 %B at 0.65 minutes
Gradient modulation/shifting	Not applicable
Modulation range	Full range
Column temperature	50 °C
Modulation time	0.65 minutes
Loop setup	Two 40-µL loops
Injection volume	5 µL
Needle wash	Not applicable
Sample temperature	Not applicable
2D DAD detection	Signal 210 nm/4 nm, reference off Signal 254 nm/4 nm, reference off

Food testing – Analysis of beer III

First-dimension column	Agilent ZORBAX Poroshell 120 SB-C18, , 2.1 x 150 mm, 2.7 µm (p/n 683775-902)
Solvent A	Water
Solvent B	Acetonitrile
Flow rate	100 µL/min
Gradient	0 %B at 0 minutes 50 %B at 20 minutes 50 %B at 30 minutes
Column temperature	40 °C
Second-dimension column	Agilent ZORBAX RRHD SB-Phenyl, 3.0 x 50 mm, 1.8 µm (p/n 857700-312)
Solvent A	Water
Solvent B	Acetonitrile
Flow rate	2.5 mL/min
Idle flow rate	N/A
Initial gradient	0 %B at 0 minutes 20 %B at 0.5 minutes 0 %B at 0.51 minutes 0 %B at 0.65 minutes
Gradient modulation/shifting	Not applicable
Modulation range	Full range
Column temperature	50 °C
Modulation time	0.65 minutes
Loop setup	Two 40-µL loops
Injection volume	5 µL
Needle wash	Not applicable
Sample temperature	Not applicable
2D DAD detection	Signal 210 nm/4 nm, reference off, Signal 254 nm/4 nm, reference off

7.1

The future

"It's tough to make predictions, especially about the future."

Yogi Berra

It has been clear for a number of years that for the analysis of very complex samples (for example, more than 100 to 200 constituents), the performance of 2D-LC outstrips that of the highest performing 1D-LC, albeit at the price of substantially longer analysis times (up to tens of hours, see Figure 7.1). There are important applications (for example, metabolomics and proteomics) that involve the non-targeted analysis of complex samples where historically 2D methods have dominated 1D methods. However, it must be admitted that the vast majority of all liquid chromatography is concerned with the separation of moderately complex samples containing perhaps only 10 to 30 constituents. If 2D-LC, in some form, proves to be competitive with 1D-LC for the analysis of samples containing 10 to 100 constituents, then 2D-LC might even displace some 1D-LC methods. Our view of the roles of 1D- and 2D-LC in a historical sense is depicted in Figure 7.1, emphasizing recent trends in the field.

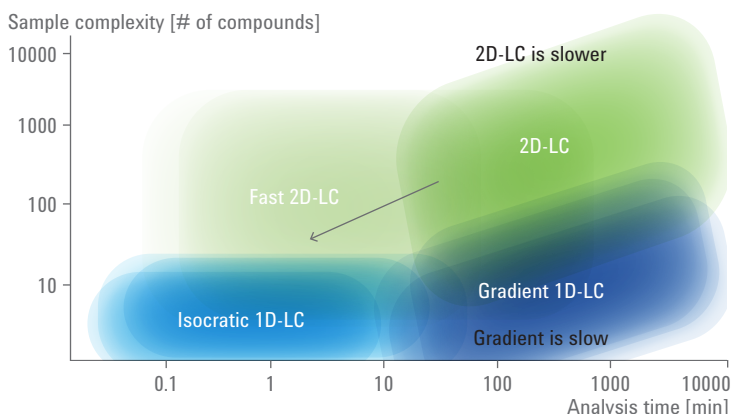


Figure 7.1 The resolving power of various LC methodologies in terms of sample complexity and requisite analysis time. Adapted from Reference 82.

When we think about analytical chemistry in broad terms we come up with the following three types of venues where 2D-LC is already playing an important role, or may play a much bigger role in the future.

A. *Discovery (or untargeted analysis)* – Proteomics and metabolomics research projects are representative of this type of problem. Here the entire dataset (comprised of all the peaks and all the multivariate signals) is mined to find a few indicators of health/disease (bio-markers), impact of treatment (state of nutrition, drug administration), and so on. These are all essentially large scale research projects involving many different samples, treatments, and time points. The hallmark characteristics of such methods are that they involve complex samples and the identities of the key analytes are not necessarily known at the start of the project. Here the need for high peak capacities and shorter analysis time is clear. Online, comprehensive 2D-LC is probably the best choice but stop-and-go methods like MudPIT may be a better compromise in some situations.

B. *Targeted analysis* – Here the identity of the analyte(s) of interest is known. Generally they are present at relatively low levels in complex matrices having many constituents and thus many potential interferences. This is the sort of problem where heart cutting 2D-LC or sLCxLC is best used. Analyses of samples of biological, environmental, and forensic origin are representative of this type of problem.

C. *Analytical engines* – The idea here involves a separation device so powerful that *it requires almost no method development to handle a variety of relatively simple samples* containing only a small number of components (e.g. less than 20). It would still have to have a very high peak capacity to overcome the statistical problems discussed in Section 2.2 “Peak capacity and related concepts” and be based on types of stationary phases and separation modes that are compatible with a wide variety of sample materials. Almost certainly this would entail using RP_xRP with different sets of columns paired with fixed gradients and pHs to limit the amount of method development. It might well have to be the case that some generalized set of highly automated pre-separation step would be part of the system and it might also involve more than two separation dimensions to increase peak capacity. Again the best approach might be sLCxLC. An example of such would be a device that could analyze the impurities in a variety of drugs during a stability study with a *minimal amount of method development*.

It should be obvious that with problems that fall in class A above we have no choice but to use multidimensional separations. However, for problems in class B you must bear in mind that method development with 2D-LC is going to be more complex in view of the larger number of interacting variables and especially the need to make two different kinds of chromatography to work together. Thus we anticipate that in general method development will take a more time. On the other hand, there is also the potential to develop a higher absolute peak capacity in 2D-LC, so this benefit may be a good return on the initial investment of method development time. In order for the advantages of the more powerful methodology to pay back the time involved to develop them there must be a sufficient volume of work to pay back the method development cost. There are a number of aspects of the optimization and implementation of 2D-LC that have been studied, to a greater or lesser extent, but are nowhere near being fully resolved. There is still a lot of work that remains to be done before we can develop 2D-LC methods with the same efficiency and effectiveness that we have seen in 1D-LC in recent years.

In our view there are two ways of making a head-to-head comparison of 1D- and 2D-LC. One is highly theoretical in nature, and provides answers to questions including: which technique provides a given peak capacity or number of observed peaks in the shortest time? The second perspective is more practical in nature, and gives insight into practical questions including: which technique provides the lowest cost per analysis? which technique/method is more robust? which technique provides the shortest method development time? In the following sections we discuss these perspectives in a bit more detail.

7.2

Theoretical factors influencing the comparison of 1D and 2D-LC

In Section 2.5 “Comparison of 1D gradient elution and online LCxLC” we showed that with an analysis time of between 5 and 10 minutes the effective peak capacity of an online LCxLC separation of maize seed extract exceeded that of a highly optimized 1D gradient separation. In a recent theoretical study⁸³ it was shown that when the first dimension is seriously undersampled, as it almost always is in practice especially when the first dimension is optimized, the *crossover time* (τ) is well approximated as in Equation 7.1:

$$\tau \approx \frac{1.83 \cdot {}^2t_c}{{}^2n_c \cdot f_{cov} \cdot {}^1\lambda} \cdot n_{c,1D}(t_{g,1D})$$

Equation 7.1 Calculation of crossover time.

The crossover time is the total analysis time in both 1D and 2D chromatography at which the effective 2D peak capacity becomes equal to the 1D peak capacity. The total analysis time in 2D chromatography is related to the 1D gradient time through the 1D efficiency factor (λ_1) defined as in Equation 7.2.

$$\lambda_1 \equiv \frac{t_g}{t_g + t_{re-eq}} = \frac{t_g}{t_{2D, anal}}$$

Equation 7.2 Calculation of 1D efficiency factor.

Similarly the 1D efficiency factor is related to the 1D analysis time as in Equation 7.3.

$$\lambda_{1D} \equiv \frac{t_{g,1D}}{t_{g,1D} + t_{1D,re-eq}} = \frac{t_{g,1D}}{t_{1D, anal}}$$

Equation 7.3 Relationship of 1D efficiency factor to 1D analysis time.

All the terms in Equation 7.1 have been defined elsewhere (see Symbols and Abbreviations). We can now approximate the 1D peak capacity with an equation of the form on the right hand side of Equation 2.11 as in Equation 7.4.

$$n_{c,1D} \approx \frac{a \cdot t_{g,1D}}{b + t_{g,1D}} = \frac{a \cdot \lambda_{1D} \cdot t_{1D, anal}}{b + \lambda_{1D} \cdot t_{1D, anal}}$$

Equation 7.4 Approximating the 1D peak capacity.

Substitution of Equation 7.4 for $n_{c,1D}$ in Equation 7.1 and solving for τ gives the simple result in Equation 7.5.

$$\tau = 1.83 \frac{^2t_c \cdot a}{^2n_c \cdot \lambda_1 \cdot f_{cov}} - \frac{b}{\lambda_{1D}}$$

Equation 7.5 Calculating the crossover time by substitution.

These equations tell us that the time at which the 2D method becomes superior can be minimized by minimizing ${}^2t_c/{}^2n_c$ and λ_{1D} and by maximizing f_{cov} and ${}^1\lambda$. Obviously the larger is a , which represents the maximum 1D peak capacity (see Equation 2.11 and Equation 2.13), the longer will be the crossover time. Clearly the dependence on f_{cov} means that crossover time will be sample dependent. Thus we must strive to do the 2D separation as fast as possible while achieving the highest possible peak capacity. Frankly we do not see that it will be possible to make *major* gains in the productivity of the second dimension. It is likely that speeds of somewhat more than 2 units of 2D peak capacity per second will be about the best one can hope for in the foreseeable future. Based on this the values in Table 7.1 were computed from Equation 7.5.

f_{cov}	${}^1\lambda$	λ_{1D}	a	b	τ [min]	$\% \Delta^{**}$
0.6	0.7	0.9	100	50	2.7	
0.8	0.7	0.9	100	50	1.8	-34
0.6	0.85	0.9	100	50	2.1	-24
0.6	0.7	0.95	100	50	2.8	2
0.6	0.7	0.9	200	50	6.3	134
0.6	0.7	0.9	100	100	1.8	-34

Table 7.1 Effect of system parameters on crossover time assuming ${}^2n_c/{}^2t_c = 2$ peaks/second. The parameter varied is shown in bold. ** This is the percent change in crossover time from the time given in the first row of results.

The first row represents reasonable values of each of the parameters. Then the parameters are changed, one at a time, to an ambitious but not excessively larger value. The last column is the percent change in the crossover time from the first row and the penultimate column is the estimated crossover time in minutes. It is quite evident that for analyses on the timescale of a few seconds to perhaps two to three minutes 1D-LC is the clear winner. If you can afford longer analysis times you should give serious consideration to doing 2D-LC.

Techniques such as shifting gradients (see Section 4.3 "Optimizing performance through use of separation space or shifted gradients") do offer some hope of making f_{cov} closer to 1.0, perhaps increasing it from current typical values of about 0.4 to 0.6 to more like 0.8 to 0.9; however, this will only decrease τ by 30 to 50 percent or conversely increase effective 2D peak capacities by 30 to 50 percent at fixed τ .

The most interesting thing about Equation 7.1 is that there is no dependence of the 1D peak capacity but there is a strong dependence on the 1D peak capacity ($n_{c,1D}$). This occurs because under conditions of significant undersampling the 1D peak capacity does not have any influence of the effective 2D peak capacity (see Section 2.4 “Fundamentals of peak capacity in LCxLC”). What this means is that if the peak capacity of 1D technology is improved e.g. by the use of even smaller particles and higher pressures, elevated temperatures or optimized eluent velocity the crossover time will increase thereby making the comprehensive 2D approach less attractive compared to 1D-LC. However, given a long enough analysis time 2D-LC will always offer more resolving power than 1D-LC and thus it will always dominate 1D-LC in the realm of very complex discovery type problems.

7.3 Practical factors influencing the comparison of 1D and 2D-LC

If we look back only ten or so years we see that the majority of LC separations were carried out under isocratic conditions. This was the case for several reasons.

- The instrumentation for gradient elution was not as reliable as it is now, and much larger volume gradient mixers were used.
- Gradient elution theory and practical method development guidelines had not been developed¹⁸.
- Perhaps most importantly gradient elution was much slower than isocratic in large part because columns took a long time to re-equilibrate. It was advised that the column be flushed with 10 to 20 column volumes of initial eluent but now, at least in the case of RPLC, two to three column volumes often suffices to get reproducible results⁸⁴⁻⁸⁶.

The last reason was probably the greatest impediment to the *routine* use of gradient elution. However, the demands of separating more complex samples and the greater power of gradient elution to do so have greatly increased the use of gradient elution so that now the vast majority of all LC instruments sold are gradient instruments. This historical trend is shown schematically in Figure 7.1 and extended to incorporate the likely trend with 2D-LC.

Analogous advances need to be made in 2D-LC to lower the barriers to more widespread and routine use of the technique. The required instrumentation for 2D-LC has become more robust and is now available from several mainstream instrument manufacturers. However, the establishment of more thorough, precise, and easy-to-use method development guidelines is still in its infancy. It is likely some of the widely held perceptions of the current limitations of 2D-LC will be overturned just as they were in the case of gradient elution 1D-LC.

7.4

Progress in instrumentation for 2D-LC

Tremendous progress has been made in the last decade in the design and implementation of both hardware and software developed specifically for application in 2D-LC. Foremost among the changes in hardware have been improvements in the capabilities of analytical-scale pumping systems that now exhibit pressure limits reaching 1300 bar (20,000 psi), gradient delay volumes under 100 μ L, and unprecedented precision under ultrafast (for example, < 15 seconds) elution conditions. Additionally use of volumetrically based LC pumping systems will allow maximization of flow rates in the 2 D of 2D-LC, while maintaining constant pressure, thereby lessening the stresses associated with pressure fluctuations that limit column lifetimes. These performance characteristics are critically important for 2D-LC to be competitive with 1D-LC, particularly at intermediate analysis times in the range of 10 to 60 minutes. Nevertheless, the ultrafast 2 D separations that are important to fast 2D-LC are currently only semicompatible with mass spectrometry as they still require a split of the analytical flow before entering the MS interface.

7.5

Other challenges and opportunities for 2D-LC

There are many opportunities for improving the performance of 2D-LC relative to 1D-LC and also a great deal of development that must be done before 2D-LC can be used more routinely.

7.5.1

Data structure advantages of 2D separation methods

Two-dimensional chromatography implemented with a univariate (e.g., single wavelength UV) detector provides opportunities for mathematical resolution of chromatographically unresolved peaks in a way that is similar to the situation with one-dimensional chromatography coupled to multivariate (e.g., DAD, or MS) detection. Namely you can use the data structure to implement some form of curve resolution.

Consider 1D-LC with a DAD detector. Imagine that two components produce absolutely overlapped peaks (same retention time and same peak shape/width) but the two components have absorption spectra that

differentiate them. In principle you can still resolve the chromatographic peak into two components by a number of mathematical approaches. Of course, the more different are the spectra the better will be the quantitative precision and accuracy and similarly the greater is the chromatographic resolution of the two peaks the smaller the difference in spectra that is required to obtain acceptable results. Now consider a 2D chromatogram acquired using a single wavelength detector. Even if the two components overlap completely on the ^1D column we can still analyze them if they don't overlap completely in the second dimension.

At this juncture it is worthwhile pointing out that there are many different mathematical ways to use the additional information provided by the second separation dimension (or the multivariate detector) to perform the curve resolution. The bilinear structure of these data sets allows two powerful chemometric methods namely *parallel factor analysis* (PARAFAC) and *generalized rank annihilation method or generalized rank annihilation factor analysis* (GRAM) to be used. These techniques have a number of very important advantages over methods not based on factor analytic methods.

- The fact that both GRAM and PARAFAC allow the baseline to be modeled so the baseline need not be estimated by doing a blank analysis.
- Both are highly immune to the presence of detector noise.
- Accurate and precise quantitative results can be obtained even when unknown interferences are present.

Let us turn now to where we believe the future of 2D chromatography with a multivariate detector lies. Such data inherently has *trilinear* not bilinear structure. A 2D hyphenated method such as LC \times LC-DAD has a huge putative advantage over a hyphenated 1D chromatographic technique. This is the so-called *trilinear advantage*. The PARAFAC and GRAM methods when applied to a dataset with a *known number* of components produce an absolutely unique answer. That is, no other answer will have a smaller set of residual differences between the experimental and modeled data. But it is essential to know the number of components that contribute to the signal on the scale of subsections of the data that are analyzed piecewise by these techniques. This is the main difficulty in doing the actual data analysis. By *answer* we mean the result of *decomposing* the data structure into a set of ^1D and ^2D chromatographic peaks (retention times, profiles) and spectral profiles where each factor represents a single chemical constituent or background signal component.

In order for the factor analytic methods to work we must assume absolute linearity of the data. Thus there can be no chromatographic overload and no nonlinear detector responses. Further, there can be no variation in chromatographic peak shape or retention time in the second dimension in the case of a single 2D chromatogram and if a series of analyses of different samples are included in the data set then there can be no shifting in retention or peak shape in either dimension. In fact changes in retention of only a few tenths of the peaks σ value have disastrous consequences when using the PARAFAC and GRAM algorithms. Clearly these are very stringent requirements. When they can be met the trilinear advantage is very powerful and there is potentially an extremely large increase in resolving power that arises from the mathematical treatment of the data, and adds to the physical resolution of the sample by the actual 2D-LC separation⁸⁷. These advantages are dramatically illustrated in Figure 7.2. In this case we see that PARAFAC was able to find three components that for all intents were totally overlapped in both the ¹D and ²D separations.

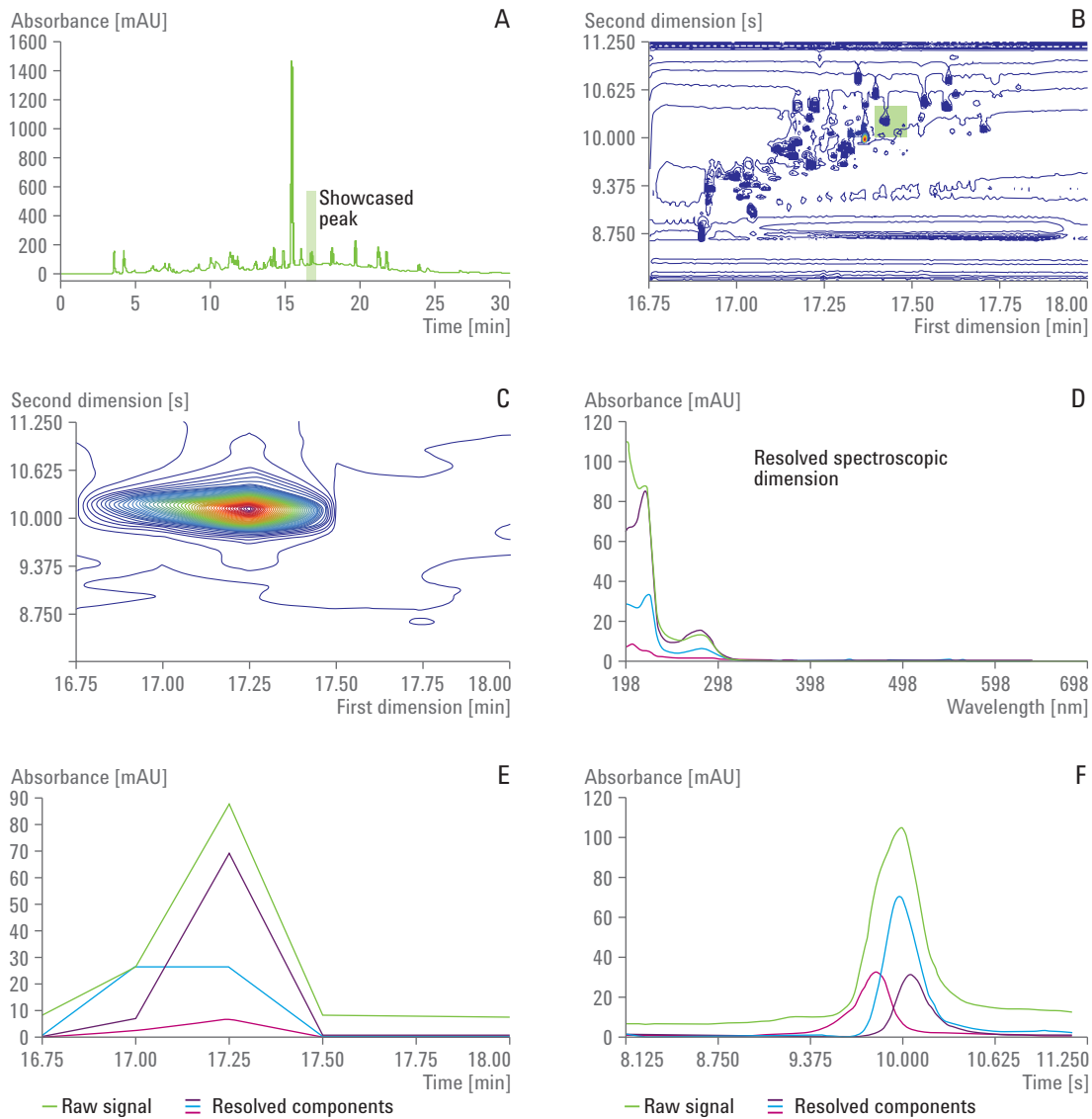


Figure 7.2 Application of the PARAFAC algorithm to analysis of 2D-LC-DAD data.
Figure courtesy of Dr. Robert Allen.

Panel A: First-dimension chromatogram where the region bracketed in green shows a peak subjected to subsequent mathematical treatment.

Panel B: Two-dimensional contour plot defining the region of space of interest.

Panel C: Zoomed-in view of the region in panel B showing that only a single peak maximum is observed.

Panel D: Absorption spectra of components found by PARAFAC in the region shown in panel C.

Panel E: Severely overlapped 1D chromatographic peak profiles determined by PARAFAC. The green plot is what is observed by the detector at 220 nm, the red, blue and purple peaks were resolved by PARAFAC.

Panel F: Severely overlapped 2D peak profiles resolved by PARAFAC. The green plot is the peak observed by the detector at 220 nm, the red, blue and purple peaks were resolved by PARAFAC.

REFERENCES

- 1.** Filgueira, M.R., Huang, Y., Witt, K., Castells, C., Carr, P.W., Improving peak capacity in fast online comprehensive two-dimensional liquid chromatography with post-first-dimension flow splitting, *Anal. Chem.*, **2011**, *83*, 9531 – 9539, doi:10.1021/ac202317m
- 2.** Stoll, D., Cohen, J., Carr, P., Fast, comprehensive online two-dimensional high performance liquid chromatography through the use of high temperature ultra-fast gradient elution reversed-phase liquid chromatography, *J. Chromatogr. A.*, **2006**, *1122*, doi:10.1016/j.chroma.2006.04.058
- 3.** Marriott, P.J., Schoenmakers, P.J., Wu, Y., Nomenclature and conventions in comprehensive multidimensional chromatography - an update, *LC-GC Eur.*, **2012**, *266*, 268, 270, 272 – 275
- 4.** Synge, R., Applications of partition chromatography, *Nobel Lecture*, **1952**
- 5.** Dent, C.E., Stepka, W., Steward, F.C., Detection of the free amino-acids of plant cells by partition chromatography, *Nature*, **1947**, *160*, 682 – 683. doi:10.1038/160682a0
- 6.** Erni, F., Frei, R.W., Two-dimensional column liquid chromatographic technique for resolution of complex mixtures, *J. Chromatogr. A.*, **1978**, *149*, 561 – 569, doi:10.1016/S0021-9673(00)81011-0
- 7.** Bushey, M.M., Jorgenson, J.W., Automated instrumentation for comprehensive two-dimensional high-performance liquid chromatography of proteins, *Anal. Chem.*, **1990**, *62*, 161 – 167, doi:10.1021/ac00201a015
- 8.** Hyötyläinen, T., Riekkola, M.-L., On-line coupled liquid chromatography – gas chromatography, *J. Chromatogr. A.*, **2003**, *1000*, 357 – 384, doi:10.1016/S0021-9673(03)00181-X

- 9.** Cortes, H.J., Campbell, R.M., Himes, R.P., Pfeiffer, C.D., On-line coupled liquid chromatography and capillary supercritical fluid chromatography: Large-volume injection system for capillary SFC, *Journal of Microcolumn Separations*, **1992**, *4*, 239 – 244, doi:10.1002/mcs.1220040310
- 10.** Chambers, A.G., Mellors, J.S., Henley, W.H., Ramsey, J.M., Monolithic integration of two-dimensional liquid chromatography – Capillary electrophoresis and electrospray ionization on a microfluidic device, *Anal. Chem.*, **2011**, *83*, 842 – 849, doi:10.1021/ac102437z
- 11.** Guiochon, G., Marchetti, N., Mriziq, K., Shalliker, R., Implementations of two-dimensional liquid chromatography, *J. Chromatogr. A.*, **2008**, *1189*, 109 – 168, doi:10.1016/j.chroma.2008.01.086
- 12.** Zhang, K., Li, Y., Tsang, M., Chetwyn, N.P., Analysis of pharmaceutical impurities using multi-heartcutting 2D LC coupled with UV-charged aerosol MS detection: Liquid Chromatography, *Journal of Separation Science*, **2013**, *36*, 2986 – 2992, doi:10.1002/jssc.201300493
- 13.** Wolters, D.A., Washburn, M.P., Yates, J.R., An automated multidimensional protein identification technology for shotgun proteomics, *Anal. Chem.*, **2001**, *73*, 5683 – 5690, doi:10.1021/ac010617e
- 14.** Bedani, F., Kok, W.T., Janssen, H.-G., A theoretical basis for parameter selection and instrument design in comprehensive size-exclusion chromatography x liquid chromatography, *J. Chromatogr. A.*, **2006**, *1133*, 126 – 134, doi:10.1016/j.chroma.2006.08.048
- 15.** Adahchour, M., Beens, J., Vreuls, R.J.J., Brinkman U.A.T., Recent developments in comprehensive two-dimensional gas chromatography (GCxGC) - Introduction and Instrumental Setup, *Trends Analyt. Chem.*, **2006**, *25*, 438 – 454, doi:10.1016/j.trac.2006.03.002
- 16.** Davis, J.M., Giddings, J.C., Statistical theory of component overlap in multicomponent chromatograms, *Anal. Chem.*, **1983**, *55*, 418 – 424, doi:10.1021/ac00254a003
- 17.** Martin, M., Herman, D.P., Guiochon, G., Probability distributions of the number of chromatographically resolved peaks and resolvable components in mixtures, *Anal. Chem.*, **1986**, *58*, 2200 – 2207, doi:10.1021/ac00124a019

- 18.** Snyder, L.R., High-performance gradient elution: the practical application of the linear-solvent-strength model, *John Wiley, Hoboken, NJ*, **2007**
- 19.** Huang, Y., Gu, H., Filgueira, M., Carr, P.W., An experimental study of sampling time effects on the resolving power of on-line two-dimensional high performance liquid chromatography, *J. Chromatogr. A.*, **2011**, 1218, 2984 – 2994, doi:10.1016/j.chroma.2011.03.032
- 20.** Snyder, L.R., Introduction to modern liquid chromatography, 3rd ed., *Wiley, Hoboken, NJ*, **2010**
- 21.** Poppe, H., Some reflections on speed and efficiency of modern chromatographic methods, *J. Chromatogr. A.*, **1997**, 778, 3 – 21, doi:10.1016/S0021-9673(97)00376-2
- 22.** Wang, X., Stoll, D.R., Carr, P.W., Schoenmakers P.J., A graphical method for understanding the kinetics of peak capacity production in gradient elution liquid chromatography, *J. Chromatogr. A.*, **2006**, 1125, 177 – 181, doi:10.1016/j.chroma.2006.05.048
- 23.** Carr, P.W., Wang, X., Stoll, D.R., Effect of pressure, particle size, and time on optimizing performance in liquid chromatography, *Anal. Chem.*, **2009**, 81, 5342-5353, doi:10.1021/ac9001244
- 24.** Hsu, S.-H., Raglione, T., Tomellini, S.A., Floyd, T.R., Sagliano, N. Jr., Hartwick, R.A., Zone compression effects in high-performance liquid chromatography, *J. Chromatogr. A.*, **1986**, 367, 293 – 300, doi:10.1016/S0021-9673(00)94850-7
- 25.** Schure, M.R., Limit of detection, dilution factors, and technique compatibility in multidimensional separations utilizing chromatography, capillary electrophoresis, and field-flow fractionation, *Anal. Chem.*, **1999**, 71, 1645 – 1657, doi:10.1021/ac981128q
- 26.** Vivó-Truyols, G., van der Wal, S., Schoenmakers P.J., Comprehensive study on the optimization of online two-dimensional liquid chromatographic systems considering losses in theoretical peak capacity in first- and second-dimensions: A pareto-optimality approach, *Anal. Chem.*, **2010**, 82, 8525 – 8536, doi:10.1021/ac101420f

- 27.** Giddings, J. in Multidimensional Chromatography: Techniques and Applications; *Cortes, H. Ed.; Marcel Dekker: New York*, **1990**.
- 28.** Giddings, J.C., Sample dimensionality: A predictor of order-disorder in component peak distribution in multidimensional separation, *J. Chromatogr. A.*, **1995**, 703, 3–15, doi:10.1016/0021-9673(95)00249-M
- 29.** This is a term used facetiously by Peter Schoenmakers to describe the clusters made by groups of different kinds of polymers having a range in molecular sizes and some other distinctive chemical property
- 30.** Carr, P., Davis, J., Rutan, S., Stoll, D. in Advances in Chromatography; Grushka, E., Grinberg, N. Eds.; *CRC Press: Boca Raton, FL*, **2012**; pp 140–222.
- 31.** Stoll, D.R., Wang, X., Carr, P.W., Comparison of the Practical Resolving Power of One- and Two-Dimensional High-Performance Liquid Chromatography Analysis of Metabolomic Samples, *Anal. Chem.*, **2008**, 80, 268–278, doi:10.1021/ac701676b
- 32.** Gilar, M., Olivova, P., Daly, A.E., Gebler, J.C., Orthogonality of Separation in Two-Dimensional Liquid Chromatography, *Anal. Chem.*, **2005**, 77, 6426–6434, doi:10.1021/ac050923i
- 33.** Rutan, S.C., Davis, J.M., Carr, P.W., Fractional coverage metrics based on ecological home range for calculation of the effective peak capacity in comprehensive two-dimensional separations, *J. Chromatogr. A.*, **2012**, 1255, 267–276, doi:10.1016/j.chroma.2011.12.061
- 34.** Gilar, M., Fridrich, J., Schure, M.R., Jaworski, A., Comparison of Orthogonality Estimation Methods for the Two-Dimensional Separations of Peptides, *Anal. Chem.*, **2012**, 84, 8722–8732, doi:10.1021/ac3020214
- 35.** Murphy, R.E., Schure, M.R., Foley, J.P., Effect of Sampling Rate on Resolution in Comprehensive Two-Dimensional Liquid Chromatography, *Anal. Chem.*, **1998**, 70, 1585–1594, doi:10.1021/ac971184b
- 36.** Davis, J.M., Stoll, D.R., Carr, P.W., Effect of First-Dimension Undersampling on Effective Peak Capacity in Comprehensive Two-Dimensional Separations, *Anal. Chem.*, **2008**, 80, 461–473, doi:10.1021/ac071504j

- 37.** Bedani, F., Schoenmakers P.J., Janssen, H.-G., Theories to support method development in comprehensive two-dimensional liquid chromatography - A review: Liquid Chromatography, *Journal of Separation Science*, **2012**, 35, 1697 – 1711, doi:10.1002/jssc.201200070
- 38.** Murphy, R., Schure, M. in Multidimensional Liquid Chromatography: Theory and Applications in Industrial Chemistry and the Life Sciences; Cohen, S., Schure, M., Eds; Wiley: Hoboken, NJ, **2008**; pp 127 – 146.
- 39.** van der Horst, A., Schoenmakers P.J., Comprehensive two-dimensional liquid chromatography of polymers, *J. Chromatogr. A.*, **2003**, 1000, 693 – 709, doi:10.1016/S0021-9673(03)00495-3
- 40.** Stoll, D.R., Li, X., Wang, X., Carr, P.W., Porter, S.E.G., Rutan, S.C., Fast, comprehensive two-dimensional liquid chromatography, *J. Chromatogr. A.*, **2007**, 1168, 3 – 43, doi:10.1016/j.chroma.2007.08.054
- 41.** Verstraeten, M., Pursch, M., Eckerle, P., Luong, J., Desmet, G., Thermal Modulation for Multidimensional Liquid Chromatography Separations Using Low-Thermal-Mass Liquid Chromatography (LC), *Anal. Chem.*, **2011**, 83, 7053 – 7060, doi:10.1021/ac201207t
- 42.** Wilson, S.R., Jankowski, M., Pepaj, M., Mihailova, A., Boix, F., Vivo Truyols, G., et al., 2D LC Separation and Determination of Bradykinin in Rat Muscle Tissue Dialysate with On-Line SPE-HILIC-SPE-RP-MS, *Chromatographia*', **2007**, 66, 469 – 474, doi:10.1365/s10337-007-0341-4
- 43.** Liang, Z., Li, K., Wang, X., Ke, Y., Jin, Y., Liang, X., Combination of off-line two-dimensional hydrophilic interaction liquid chromatography for polar fraction and two-dimensional hydrophilic interaction liquid chromatography x reversed-phase liquid chromatography for medium-polar fraction in a traditional Chinese medicine, *J. Chromatogr. A.*, **2012**, 1224, 61 – 69, doi:10.1016/j.chroma.2011.12.046
- 44.** Giddings, J.C., Two-dimensional separations: concept and promise, *Anal. Chem.*, **1984**, 56, 1258A – 1270A, doi:10.1021/ac00276a003
- 45.** Stoll, D.R., Carr, P.W., Fast, Comprehensive Two-Dimensional HPLC Separation of Tryptic Peptides Based on High-Temperature HPLC, *J. Am. Chem. Soc.*, **2005**, 127, 5034 – 5035, doi:10.1021/ja050145b

- 46.** Opiteck, G.J., Jorgenson, J.W., Moseley, M.A., Anderegg, R.J., Two-dimensional microcolumn HPLC coupled to a single-quadrupole mass spectrometer for the elucidation of sequence tags and peptide mapping,, *J. Microcol. Sep.*, **1998**, *10*, 365 – 375, doi:10.1002/(SICI)1520-667X(1998)10:4<365::AID-MCS6>3.0.CO;2-E
- 47.** Dugo, P., Kumm, T., Crupi, M., Cotroneo, A., Mondello, L., Comprehensive two-dimensional liquid chromatography combined with mass spectrometric detection in the analyses of triacylglycerols in natural lipidic matrixes, *J. Chromatogr. A.*, **2006**, *1112*, 269 – 275, doi:10.1016/j.chroma.2005.10.070
- 48.** Elsner, V., Laun, S., Melchior, D., Köhler, M., Schmitz, O.J., Analysis of fatty alcohol derivatives with comprehensive two-dimensional liquid chromatography coupled with mass spectrometry, *J. Chromatogr. A.*, **2012**, *1268*, 22 – 28, doi:10.1016/j.chroma.2012.09.072
- 49.** Mondello, L., Tranchida, P.Q., Stanek, V., Jandera, P., Dugo, G., Dugo, P., Silver-ion reversed-phase comprehensive two-dimensional liquid chromatography combined with mass spectrometric detection in lipidic food analysis, *J. Chromatogr. A.*, **2005**, *1086*, 91 – 98, doi:10.1016/j.chroma.2005.06.017
- 50.** Jiang, X., van der Horst, A., Lima, V., Schoenmakers, P.J., Comprehensive two-dimensional liquid chromatography for the characterization of functional acrylate polymers, *J. Chromatogr. A.*, **2005**, *1076*, 51 – 61, doi:10.1016/j.chroma.2005.03.135
- 51.** Adrian, J., Two-dimensional chromatography of complex polymers Part 1. Analysis of a graft copolymer by two-dimensional chromatography with on-line FTIR detection, *Polymer*, **2000**, *41*, 2439 – 2449, doi:10.1016/S0032-3861(99)00402-4
- 52.** USP Column Equivalency Application
- 53.** Németh, T., Haghedooren, E., Noszál, B., Hoogmartens, J., Adams, E., Three methods to characterize reversed phase liquid chromatographic columns applied to pharmaceutical separations, *Journal of Chemometrics*, **2008**, *22*, 178 – 185, doi:10.1002/cem.1108
- 54.** Snyder, L.R., Dolan, J.W., Carr, P.W., A new look at the selectivity of RPC columns, *Anal. Chem.*, **2007**, *79*, 3254 – 3262, doi:10.1021/ac071905z

- 55.** Wilson, N.S., Nelson, M.D., Dolan, J.W., Snyder, L.R., Wolcott, R.G., Carr, P.W., Column selectivity in reversed-phase liquid chromatography. I. A general quantitative relationship, *J. Chromatogr. A.*, **2002**, *961*, 171 – 193, doi:10.1016/S0021-9673(02)00659-3
- 56.** <http://hplccolumns.org/index.php>, accessed November 1, **2014**
- 57.** <http://www.usp.org/usp-nf/compendial-tools/pqri-approach-column-equiv-tool>, accessed November 1, **2014**
- 58.** Zhang, Y., Carr, P.W., A visual approach to stationary phase selectivity classification based on the Snyder – Dolan Hydrophobic-Subtraction Model, *J. Chromatogr. A.*, **2009**, *1216*, 6685 – 6694, doi:10.1016/j.chroma.2009.06.048
- 59.** Alexander, A.J., Ma, L., Comprehensive two-dimensional liquid chromatography separations of pharmaceutical samples using dual Fused-Core columns in the 2nd dimension, *J. Chromatogr. A.*, **2009**, *1216*, 1338 – 1345, doi:10.1016/j.chroma.2008.12.063
- 60.** Li, D., Schmitz, O.J., Use of shift gradient in the second dimension to improve the separation space in comprehensive two-dimensional liquid chromatography, *Anal. Bioanal. Chem.*, **2013**, doi:10.1007/s00216-013-7089-5
- 61.** Dugo, P., Škeříková, V., Kumm, T., Trozzi, A., Jandera, P., Mondello, L., Elucidation of Carotenoid Patterns in Citrus Products by Means of Comprehensive Normal-Phase x Reversed-Phase Liquid Chromatography, *Anal. Chem.*, **2006**, *78*, 7743 – 7750, doi:10.1021/ac061290q
- 62.** Francois, I., Devilliers, A., Tienpont, B., David, F., Sandra, P., Comprehensive two-dimensional liquid chromatography applying two parallel columns in the second dimension, *J. Chromatogr. A.*, **2008**, *1178*, 33 – 42, doi:10.1016/j.chroma.2007.11.032
- 63.** Uliyanenko, E., Cools, P.J.C.H., van der Wal, S., Schoenmakers P.J., Comprehensive Two-Dimensional Ultrahigh-Pressure Liquid Chromatography for Separations of Polymers, *Anal. Chem.*, **2012**, *84*, 7802 – 7809, doi:10.1021/ac3011582

- 64.** Bedani, F., Kok, W.T., Janssen, H.-G., Optimal gradient operation in comprehensive liquid chromatography x liquid chromatography systems with limited orthogonality, *Anal. Chim. Acta.*, **2009**, 654, 77 – 84, doi:10.1016/j.aca.2009.06.042
- 65.** Stevenson, P.G., Mnatsakanyan, M., Guiochon, G., Shalliker, R.A., Peak picking and the assessment of separation performance in two-dimensional high performance liquid chromatography, *The Analyst*, **2010**, 135, 1541, doi:10.1039/b922759h
- 66.** Peters, S., Vivó-Truyols, G., Marriott P.J., Schoenmakers P.J., Development of an algorithm for peak detection in comprehensive two-dimensional chromatography, *J. Chromatogr. A.*, **2007**, 1156, 14 – 24, doi:10.1016/j.chroma.2006.10.066
- 67.** Reichenbach, S.E., Tian, X., Cordero, C., Tao, Q., Features for non-targeted cross-sample analysis with comprehensive two-dimensional chromatography, *J. Chromatogr. A.*, **2012**, 1226, 140 – 148, doi:10.1016/j.chroma.2011.07.046
- 68.** Reichenbach, S.E., Ni, M., Zhang, D., Ledford, E.B., Image background removal in comprehensive two-dimensional gas chromatography, *J. Chromatogr. A.*, **2003**, 985, 47 – 56, doi:10.1016/S0021-9673(02)01498-X
- 69.** Reichenbach, S.E., Ni, M., Kottapalli, V., Visvanathan, A., Information technologies for comprehensive two-dimensional gas chromatography, *Chemometr. Intell. Lab.*, 2004, 71, 107 – 120, doi:10.1016/j.chemolab.2003.12.009
- 70.** Skov, T., Hoggard J.C., Bro, R., Synovec R.E., Handling within run retention time shifts in two-dimensional chromatography data using shift correction and modeling, *J. Chromatogr. A.*, **2009**, 1216, 4020 – 4029, doi:10.1016/j.chroma.2009.02.049
- 71.** Hoggard, J.C., Synovec, R.E., Parallel Factor Analysis (PARAFAC) of Target Analytes in GC x GC-TOFMS Data: Automated Selection of a Model with an Appropriate Number of Factors, *Anal. Chem.*, **2007**, 79, 1611 – 1619, doi:10.1021/ac061710b
- 72.** Hoggard, J.C., Synovec, R.E., Automated Resolution of Nontarget Analyte Signals in GC x GC-TOFMS Data Using Parallel Factor Analysis, *Anal. Chem.*, **2008**, 80, 6677 – 6688, doi:10.1021/ac800624e

- 73.** Bailey, H.P., Rutan, S.C., Carr, P.W., Factors that affect quantification of diode array data in comprehensive two-dimensional liquid chromatography using chemometric data analysis, *J. Chromatogr. A.*, **2011**, *1218*, 8411 – 8422, doi:10.1016/j.chroma.2011.09.057
- 74.** Porter, S.E.G., Stoll, D.R., Rutan, S.C., Carr, P.W., Cohen, J.D., Analysis of Four-Way Two-Dimensional Liquid Chromatography-Diode Array Data: Application to Metabolomics, *Anal. Chem.*, **2006**, *78*, 5559 – 5569, doi:10.1021/ac0606195
- 75.** Mazet, V., Carteret, C., Brie, D., Idier, J., Humbert, B., Background removal from spectra by designing and minimising a non-quadratic cost function, *Chemometr. Intell. Lab.*, **2005**, *76*, 121 – 133, doi:10.1016/j.chemolab.2004.10.003
- 76.** Moore, A.W., Jorgenson, J.W., Median filtering for removal of low-frequency background drift, *Anal. Chem.*, **1993**, *65*, 188 – 191, doi:10.1021/ac00050a018
- 77.** Filgueira M.R., Castells, C.B., Carr, P.W., A Simple, Robust Orthogonal Background Correction Method for Two-Dimensional Liquid Chromatography, *Anal. Chem.*, **2012**, *84*, 6747 – 6752, doi:10.1021/ac301248h
- 78.** Latha, I., Reichenbach, S.E., Tao, Q., Comparative analysis of peak-detection techniques for comprehensive two-dimensional chromatography, *J. Chromatogr. A.*, **2011**, *1218*, 6792 – 6798, doi:10.1016/j.chroma.2011.07.052
- 79.** Thekkudan, D.F., Rutan, S.C., Carr, P.W., A study of the precision and accuracy of peak quantification in comprehensive two-dimensional liquid chromatography in time, *J. Chromatogr. A.*, **2010**, *1217*, 4313 – 4327, doi:10.1016/j.chroma.2010.04.039
- 80.** Seeley, J., Theoretical study of incomplete sampling of the first dimension in comprehensive two-dimensional chromatography, *J. Chromatogr. A.*, **2002**, *962*, 21 – 27, doi:10.1016/S0021-9673(02)00461-2
- 81.** Adcock, J.L., Adams, M., Mitrevski, B.S., Marriott, P.J., Peak Modeling Approach to Accurate Assignment of First-Dimension Retention Times in Comprehensive Two-Dimensional Chromatography, *Anal. Chem.*, **2009**, *81*, 6797 – 6804, doi:10.1021/ac900960n

- 82.** Stoll, D.R., Fast, comprehensive two-dimensional liquid chromatography, *Ph.D. Dissertation, University of Minnesota, 2007*
- 83.** Potts, L.W., Carr, P.W., Analysis of the temporal performance of one versus on-line comprehensive two-dimensional liquid chromatography, *J. Chromatogr. A.*, **2013**, 1310, 37 – 44,
doi:10.1016/j.chroma.2013.07.102
- 84.** Schellinger, A.P., Stoll, D.R., Carr, P.W., High speed gradient elution reversed-phase liquid chromatography, *J. Chromatogr. A.*, **2005**, 1064, 143 – 156, doi:10.1016/j.chroma.2004.12.017
- 85.** Schellinger, A.P., Stoll, D.R., Carr, P.W., High speed gradient elution reversed phase liquid chromatography of bases in buffered eluents, *J. Chromatogr. A.*, **2008**, 1192, 54 – 61,
doi:10.1016/j.chroma.2008.02.049
- 86.** Schellinger, A.P., Stoll, D.R., Carr, P.W., High-speed gradient elution reversed-phase liquid chromatography of bases in buffered eluents, *J. Chromatogr. A.*, **2008**, 1192, 41 – 53,
doi:10.1016/j.chroma.2008.01.062
- 87.** Davis, J.M., Rutan, S.C., Carr, P.W., Relationship between selectivity and average resolution in comprehensive two-dimensional separations with spectroscopic detection, *J. Chromatogr. A.*, **2011**, 1218, 5819 – 5828, doi:10.1016/j.chroma.2011.06.086
- 88.** Elsner, V., Analyse fettchemischer Produkte mittels
comprehensiver zweidimensionaler Flüssigchromatographie
gekoppelt mit der Massenspektrometrie (LC_xLC-MS), unv.
Diss., der Bergischen Universität Wuppertal, September 2013.
(urn:nbn:de:hbz:468-20140113-115443-6)

www.agilent.com/chem/2d-lc

This information is subject to change without notice.

© Agilent Technologies, Inc., 2015

Printed in Germany, May 15, 2015

5991-2359EN



Agilent Technologies